UNIVERSITÀ DI PARMA

UNIVERSITÀ DEGLI STUDI DI PARMA

DOTTORATO DI RICERCA IN
" NEUROSCIENZE"

CICLO XXXVII

Memory-driven coding of objects in monkey parieto-frontal grasping network

Coordinatore:
Chiar.mo Prof. Luca Bonini

Tutore:
Chiar.mo Prof. Luca Bonini

Dottoranda: Anna Mitola

Anni Accademici 2021/2022 – 2023/2024

INDEX

ABSTRACT

Every goal-directed action begins with a computational challenge: translating what is seen into how to move. Yet kinematically precise movements can be generated in complete darkness, as in grasping familiar or just-seen objects relying on memory-based mechanisms that bridge perception and action. How does the brain transform object information into appropriate motor plans in the absence of vision? To address this question, we recorded single-unit activity (n = 551) from key parietal and frontal nodes of the macaque extended grasping network (AIP, F2, F5, F6) during both visually- and memory-guided grasping. Area AIP stands out as a central hub for memory-driven actions, with neurons exhibiting temporally stable, object-specific tuning from object presentation through grasp execution in darkness, indicating a parietal substrate that maintains object representation during memory-driven grasping. In contrast, premotor regions showed transient, phase-locked, context-dependent activity, consistent with flexible transformation of parietal information into motor output rather than its maintenance. At the cellular level, object stability in AIP was strongest among broad-spiking (excitatory-like) units, consistent with local recurrent dynamics able to stabilize the code and support its redistribution across the parieto-frontal network. Together, these findings outline a distributed parieto-frontal organization in which parietal stability and frontal flexibility jointly keep perception and action aligned, even when sensory input is unavailable.

ABSTRACT IN ITALIAN

Ogni azione finalizzata inizia con una sfida computazionale: tradurre ciò che si vede in un movimento efficace. Eppure movimenti cinematicamente precisi possono essere generati anche nel buio completo, come nell'afferrare oggetti familiari o appena visti, affidandosi a meccanismi basati sulla memoria che raccordano percezione e azione. In assenza di visione, come trasforma il cervello le informazioni sull'oggetto in piani motori appropriati? Per rispondere a questa domanda, abbiamo registrato l'attività a singola unità (n = 551) nei principali nodi della rete estesa della prensione del macaco (AIP, F2, F5, F6) durante compiti di prensione guidata dalla visione e dalla memoria. L'area AIP emerge come snodo centrale per le azioni guidate dalla memoria, con neuroni che mostrano una selettività specifica per l'oggetto, stabile nel tempo, dalla presentazione fino all'esecuzione della prensione al buio, indicando un substrato parietale che mantiene la rappresentazione dell'oggetto durante la prensione basata sulla memoria. Al contrario, le regioni premotorie hanno mostrato un'attività transiente, ancorata alle fasi del compito e dipendente dal contesto, coerente con una trasformazione flessibile delle informazioni parietali in output motorio più che con il loro mantenimento. A livello cellulare, la stabilità della rappresentazione in AIP risultava più marcata nelle unità broad-spiking (putativamente eccitatorie), in linea con dinamiche ricorrenti locali in grado di stabilizzare il codice e sostenerne la ridistribuzione attraverso la rete parieto-frontale. Nel complesso, questi risultati delineano un'organizzazione parieto-frontale distribuita in cui la stabilità parietale e la flessibilità frontale mantengono allineate percezione e azione, anche quando l'input sensoriale non è disponibile.

1 INTRODUCTION

1.1 NEURAL BASIS OF GOAL-DIRECTED ACTION

“Movement is not produced by muscles, but by the brain solving a problem”.

(Nikolai Bernstein)

1.1.1 From perception to action: the sensorimotor continuum

The classical view of the brain–behavior relationship, originating in the 19th century and dominating much of 20th-century neuroscience, was built upon a modular and hierarchical model of neural processing. The foundational work of Fritsch and Hitzig (1870), who demonstrated that electrical stimulation of the anterior cerebral cortex in dogs elicited motor responses, laid the groundwork for the idea that specific brain regions are specialized for discrete functions: “*a part of the brain is motor, another is not*” (Fritsch & Hitzig, 1870). This early dichotomy between motor and non-motor areas, later reinforced by Brodmann’s cytoarchitectonic maps, lesion studies, and classical neurophysiology (Sherrington, 1906), supported the notion of an anatomical and functional separation between sensory, associative, and motor cortices.

In this framework, posterior sensory areas (e.g., occipital and temporal lobes) were seen as responsible for extracting information about the external world. These inputs would then be relayed to association cortices, primarily within the parietal lobe, where information would be integrated and transformed into internal representations of potential motor plans, finally turned into voluntary behavior through frontal premotor and motor areas (Kandel et al., 2013). This serial and unidirectional model implied that cognition mediates between perception and action, which are otherwise functionally distinct.

Such a feedforward “perception → cognition → action” architecture remained dominant until the 1970s. Indeed, with the advent of neurophysiological, neuroimaging, and computational approaches, this strict compartmentalization began to dissolve. A growing body of evidence began to show that perception and action are not processed in discrete, sequential stages, but rather as dynamically interdependent processes that share overlapping neural substrates and temporal profiles (Jeannerod, 1997; Mountcastle, 1997; Cisek & Kalaska, 2010; Pezzulo & Cisek, 2016; Balasubramaniam et al., 2021). This shift

in perspective began with a reconceptualization of the motor system itself. While early approaches aimed to localize functions at finer anatomical scales, down to individual cortical columns or even neurons (Hubel & Wiesel, 1968), this reductionism overlooked the distributed and population-based nature of neural coding. Assigning a specific cognitive or perceptual function to an individual cell ignores the emergent properties of large-scale sensorimotor networks (Churchland et al., 2012; Shenoy et al., 2013).

The idea that perceptual and motor functions could be co-localized within the same brain regions, especially within so-called "motor" areas, was significantly shaped by ecological and embodied theories of cognition, which emphasized the intrinsic link between sensory experience and motor behavior. As early as the 1950s, James J. Gibson (1950, 1979) challenged the notion of passive visual perception. With his theory of *affordances*, Gibson argued that the visual environment "invites" specific motor actions: perception is therefore structured by the possibilities for action it reveals. This framework implies that space itself is not an abstract geometric entity but a *behavioral space*, defined in terms of the motor capacities of the agent interacting with it. In this view, objects are not merely recognized: they are grasped, reached for, manipulated, and avoided. The encoding of space, then, becomes inherently egocentric and action-oriented.

Neurophysiological studies in the following decades provided strong support for this integrative view. Research in non-human primates demonstrated that neurons in the posterior parietal cortex (PPC), traditionally considered part of the "association" cortex, respond not only to sensory stimuli but also encode movement plans, effectors, and goals (Snyder et al., 1997; Andersen & Buneo, 2002; Scherberger & Andersen, 2007; Petzschner & Krüger, 2012). Similar functional overlap was found in the premotor cortex, where activity reflects both the visual properties of objects and the type of movement they afford (Gallese et al., 1996; Rizzolatti & Luppino, 2001; Bonini et al., 2014b; Vargas-Irwin et al., 2015; Orban et al., 2021). These findings blurred the boundaries between perception and action, showing that motor and sensory processing are co-localized and integrated in time.

Moreover, contemporary theoretical frameworks such as *predictive coding* and *the free energy* principle further dissolve the separation between perception and action. In these models, perception is not the passive registration of sensory data, but an *active inference* process wherein the brain constantly generates predictions about incoming stimuli based on internal models and adjusts these models via motor behavior (Friston, 2010; Clark,

2013; Parr et al., 2022; Mazzaglia et al., 2022). Action, in this context, is not a terminal output but an intrinsic part of the perceptual process, used to reduce uncertainty and update predictions. Crucially, the integration of perception and action enables behavior to be flexible, anticipatory and context-sensitive. When sensory input is ambiguous or incomplete, motor planning and expectations fill in the gaps. This is evident in tasks that require rapid responses to uncertain stimuli, where parieto-frontal circuits encode multiple potential actions in parallel before selecting one based on evolving environmental conditions (Cisek & Kalaska, 2005; Thura & Cisek, 2017; Beste et al., 2012). The brain, in this view, does not wait for perception to be completed before acting, it *perceives in order to act* and *acts in order to perceive.*

In summary, contemporary neuroscience reframes the modular, serial view of perception and action in favor of a sensorimotor continuum, in which cognition is deeply embedded in bodily action. This integrative perspective recognizes that perception, motor control and decision-making emerge from dynamic interactions within distributed neural networks, shaped by both environmental context and internal goals. It invites a reconceptualization of brain function, one where *to perceive is already to be acting*, and *to act is already to be perceiving.*

While the perception–action continuum challenges the traditional modular view of brain organization, it also raises critical questions about how actions are selected, initiated and shaped by internal goals and external contexts. Not all perceived affordances lead to action: some are ignored, others postponed, and some require complex decisions. In natural environments, organisms must navigate an overabundance of potential actions, constrained by bodily capabilities, situational demands and evolving internal states such as intentions, motivations, and expectations.

Thus, to fully understand sensorimotor integration, it is essential to examine how voluntary control operates, namely how the brain resolves ambiguity, inhibits irrelevant actions, and flexibly adapts behavior in context-sensitive ways. The next section addresses this additional level of complexity by focusing on how voluntary action emerges from the interplay of affordances, task constraints, and internal goals.

1.1.2 Voluntary action and contextual constraints

Voluntary actions require the integration of sensory, motivational, and contextual information to generate adaptive motor behavior. Unlike reactive movements, they depend on internal decision-making processes that reflect not only the physical properties of external stimuli but also subjective goals, expectations, and learned associations (Passingham et al., 2010; Haggard, 2008; Banks & Gamblin, 2022). Central to this process is the brain's ability to encode action goals before movement initiation.

Electrophysiological and neuroimaging studies have demonstrated that parieto-frontal regions are active well before movement onset, suggesting the existence of abstract motor intentions that are shaped by internal states and external contingencies (Rizzolatti et al., 1998; Cisek & Kalaska, 2005; Shadlen & Newsome, 2001; Thoenissen et al., 2002). This preparatory activity reflects both the *what* (goal of the action) and the *when* (timing) of movement, allowing for flexible and context-sensitive behavior (Shadlen & Newsome, 2001; Thoenissen et al., 2002; Stentiford & Cerminara, 2019). Contextual constraints, including task demands, object relevance, affordances and environmental uncertainty, profoundly influence how actions are planned and executed (Figure 1). For instance, even in identical sensory contexts, the brain may generate different motor plans depending on task rules or behavioral relevance (Gallivan et al., 2011; Brosowsky & Crump, 2021; Borghi, 2021). This implies that action selection is not a fixed response to stimuli but rather a dynamic process guided by internal models of possible outcomes (Pezzulo et al., 2018).

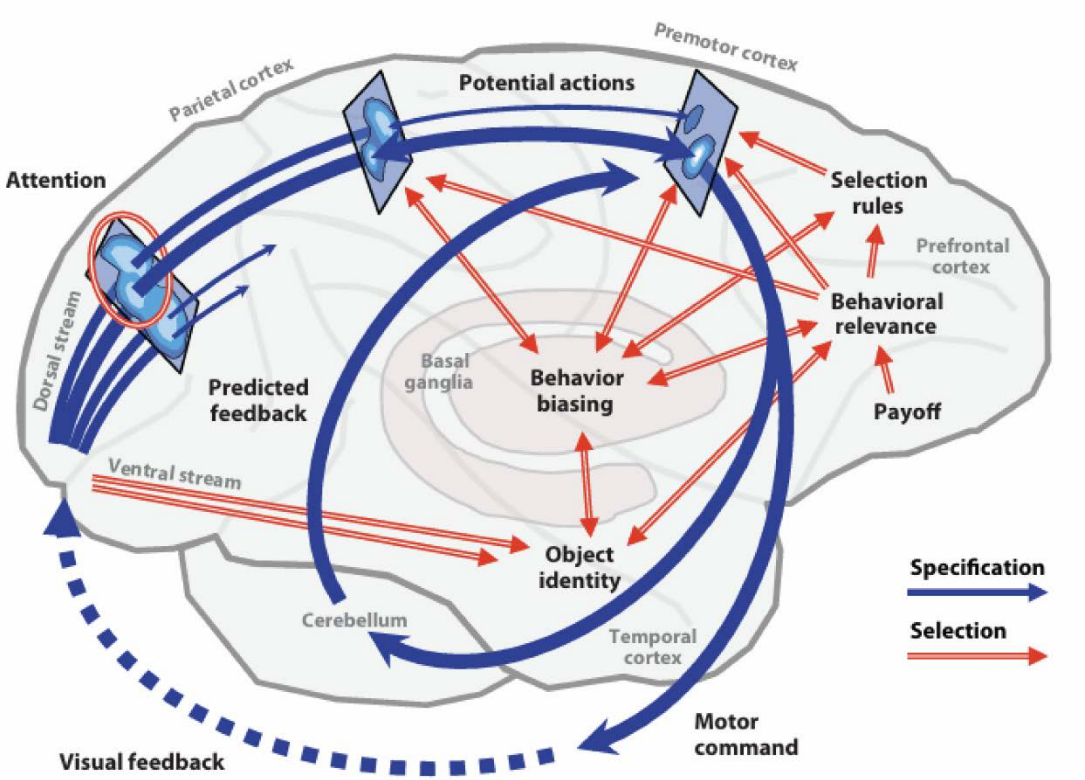

Figure 1. Schematic of the affordance competition hypothesis. The diagram illustrates how the cerebral cortex, basal ganglia, and cerebellum interact to transform sensory input into motor output, according to the affordance competition hypothesis. Visual information, initially processed in occipital areas, is progressively transformed into potential motor plans along parietal regions through processes of action specification. These evolving representations, depicted as competing neural populations with varying levels of activation, undergo selection influenced by top-down biasing signals from the prefrontal cortex and basal ganglia. Such biases modulate the competition across multiple cortical areas, integrating contextual and motivational factors into action selection. Once a motor plan is selected, it is executed, generating both external sensory feedback and internal predictive feedback via the cerebellum. This framework supports flexible, goal-directed behavior in dynamic environments. Figure from (Cisek & Kalaska, 2005).

Moreover, voluntary control involves inhibitory mechanisms that prevent premature or inappropriate actions, especially when multiple competing options are present. Structures such as the pre-supplementary motor area (pre-SMA) and right inferior frontal cortex have been implicated in the ability to suppress preplanned responses and reconfigure action plans based on evolving task demands (Nachev et al., 2008; Aron et al., 2014; Cai et al., 2014; Boen et al., 2022). These findings point toward a flexible and hierarchical motor control system where voluntary actions are continuously shaped by the interaction between internal goals and external constraints. This framework sets the stage for understanding how the brain plans movements not just reactively, but prospectively, anticipating future states of the body and the environment.

1.1.3 Brain systems for adaptive motor planning

To implement voluntary, context-sensitive action, the brain must engage a distributed set of cortical and subcortical areas capable of adaptive motor planning, the ability to prepare actions in advance, update them as needed and flexibly switch between alternatives. This capacity relies on both stable internal representations of movement goals and online sensory feedback, integrated within a dynamic neural architecture.

The parieto-frontal networks play a central role in this system design. Within this network, the PPC contributes to sensorimotor transformations by integrating multisensory input into egocentric reference frames (Andersen & Cui, 2009; Buneo & Andersen, 2006; Bernier & Grafton, 2010; Bencivenga et al., 2023). Regions such as the anterior intraparietal area (AIP), parietal reach region (PRR), and lateral intraparietal area (LIP) are involved in forming spatial and object-centered action plans, encoding both target location and motor intention (Snyder et al., 1997; Murata et al., 2000; Cui & Andersen, 2011; Orban et al., 2021). In the frontal cortex, the premotor areas (dorsal and ventral, PMd and PMv) and prefrontal cortex (PFC) are critical for selecting, maintaining and updating action plans. Premotor regions are known to encode motor goals and prepare movement parameters such as direction (Figure 2), force or grip type even before movement execution (Wise et al., 1998; Crammond & Kalaska, 2000; Moreno et al., 2025). In turn, prefrontal areas, particularly the dorsolateral prefrontal cortex (dlPFC), contribute to working memory and rule-based modulation of motor plans (Miller & Cohen, 2001; Mars & Grol, 2007). Notably, adaptive planning involves recurrent interactions among these regions. Rather than following a strict feedforward hierarchy, motor planning emerges from continuous feedback loops between parietal and frontal areas, where predictions and sensory inputs are iteratively reconciled (Cisek, 2007; Pezzulo & Cisek, 2016). This interactive dynamic allows for rapid corrections and re-planning in response to unexpected changes or errors during movement.

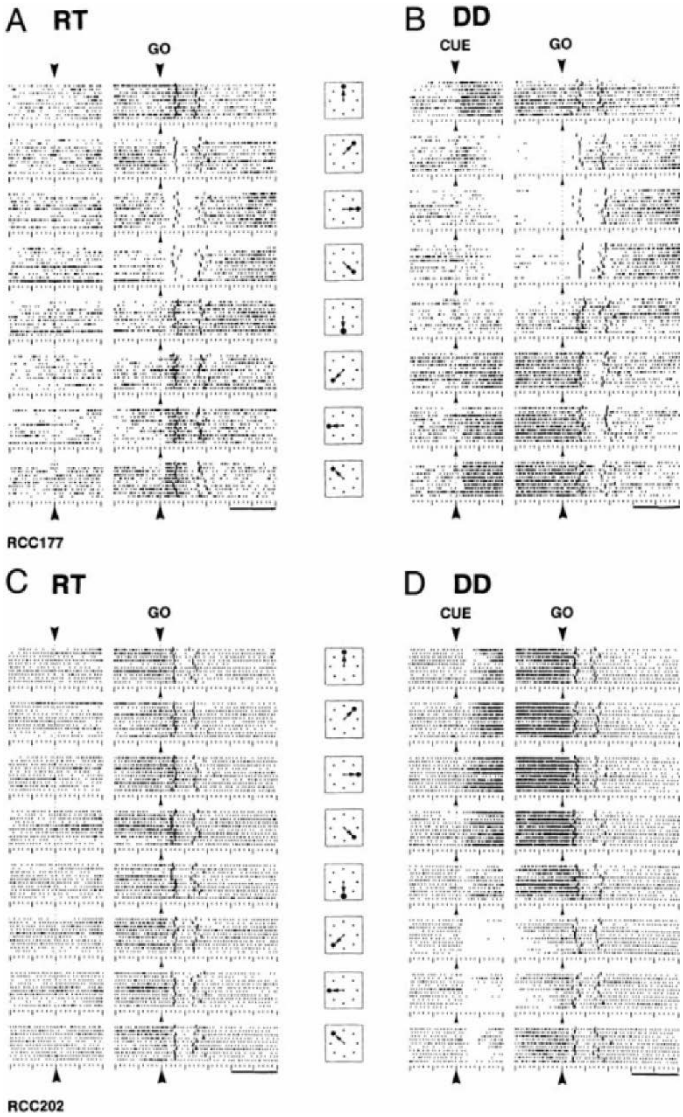

Figure 2. Directional activity of PMd neurons during reaction time (RT) and delayed decision (DD) tasks. Raster plots showing the discharge patterns of two dorsal premotor cortex (PMd) neurons during RT and DD trials across eight movement directions, as indicated by the target cartoons between raster sets. Panels A and B depict a neuron with relatively consistent directional tuning across task epochs, while panels C and D illustrate a neuron with more complex response dynamics. In panel A (RT trials), the neuron exhibits a broadly tuned, phasic burst of activity confined to the reaction time epoch (RTE), with a preferred direction of 171°. In panel B (DD trials), the same neuron shows an early burst following cue onset, followed by a ramp-like increase in discharge during the instructed delay period (IDP), with preferred directions of 149° (early IDP), 161° (late IDP), and 157° overall. The neuron was significantly tuned in all three IDP epochs. Notably, this cell generated sustained activity during the IDP despite showing only a brief phasic response in RT trials, a pattern commonly observed across the PMd sample. Vertical dotted lines mark the appearance of the CUE and GO signals; thick horizontal markers to the right of GO indicate movement onset and offset for each trial. Calibration bar: 1,000 ms. Figure from (Crammond Kalaska, 2000).

Subcortical structures also play a central role. The basal ganglia, for instance, support action selection through mechanisms of disinhibition and reinforcement learning, biasing motor plans according to expected value or reward probability (Pasquereau et al., 2007; Graybiel, 2008; Redgrave et al., 2010; Mulcahy et al., 2020; Park et al., 2020). The cerebellum, traditionally associated with fine motor control and error correction, has been increasingly recognized for its contribution to internal forward models, which support simulations of the sensory consequences of planned actions (Miall et al., 1996; Wolpert et al., 1998; Shadmehr et al., 2010; Welniarz et al., 2021; Streng et al., 2022).

Together, these systems constitute a flexible and distributed control network that adjusts motor plans in real time by combining contextual information and sensory feedback with goal-directed processes. This dynamic sensorimotor framework embodies the core premise that action is not merely a motor output, but an evolving process shaped by prediction, learning and continuous integration, forming the foundation for adaptive, goal-directed behavior in real-world contexts.

Yet, to understand how the brain orchestrates specific classes of actions, such as object grasping, which represents the focus of this study, it is necessary to move beyond general models of action selection and motor planning toward more specialized, anatomically defined circuits. Within this broader framework, among the systems outlined above, the parieto-frontal network stands out for its critical role in visually guided prehension. It represents a particularly well-studied implementation of sensorimotor principles, transforming visual object features into precisely timed motor commands for grasping.

This expression of object-directed behavior offers a rich model to examine how perceptual analysis, cognitive appraisal and fine motor execution converge in purposeful interaction with the external world. Unlike more generic forms of motor planning, successful grasping requires encoding not just *where* to act, but *how* to interact with specific object properties (e.g., shape, texture, orientation), often under constraints of uncertainty or temporal pressure. This sophisticated process, known as sensorimotor transformation, relies on a mosaic of interconnected parietal and frontal areas collectively referred to as the *extended grasping network*. Its anatomical organization, functional specialization, and inter-regional dynamics will be examined in the following section, with particular emphasis on how this circuit enables the transformation of visual input into goal-directed motor plans for effective object manipulation.

1.2 THE EXTENDED GRASPING NETWORK IN VISUOMOTOR TRANSFORMATIONS

1.2.1 Architecture and principles

Building on the principles of continuous sensorimotor integration discussed in the previous section, decades of neurophysiological, neuroimaging and lesion studies have progressively characterized the extended grasping network as a distributed and hierarchically organized system of interconnected parietal and frontal areas, particularly in primates. This network orchestrates the transformation of visual and somatosensory input into finely tuned motor output required for purposeful prehension behaviors (Rizzolatti & Luppino, 2001). Its connectivity architecture reflects a clear division between extrinsic, intrinsic, and descending projections, supporting the graded flow of sensorimotor information across cortical and subcortical regions.

Each frontal motor area is embedded in a broader network of connections (Figure 3). Intrinsic connections link neighboring motor fields (e.g., F1–F5), forming a tightly organized, somatotopically aligned system for coordinating movement execution. Extrinsic connections extend toward higher-order cortical areas, including the posterior parietal cortex, the dorsolateral and medial prefrontal cortices, and the cingulate motor areas (Luppino & Rizzolatti, 2000). Furthermore, descending projections from specific premotor and motor fields reach the spinal cord and brainstem nuclei, mediating execution-level control and posture adjustment (Dum & Strick, 1991; Kandel et al., 2013; Innocenti et al., 2019; Takakusaki et al., 2024).

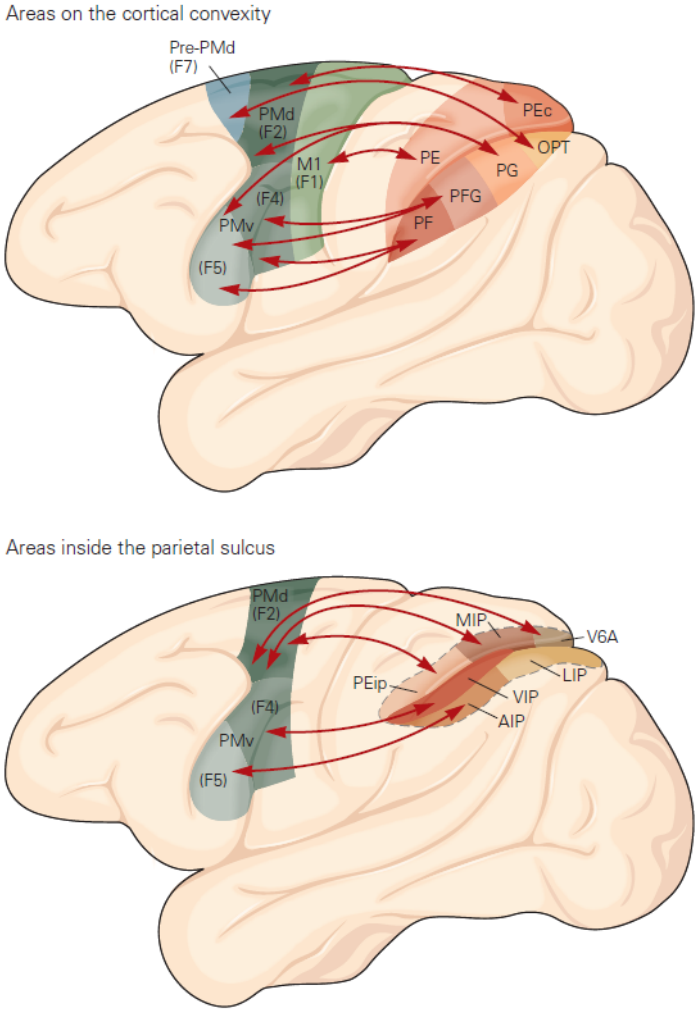

Figure 3. Sketch of parieto-frontal connections of the macaque's brain. The figure shows lateral views of a macaque brain. Motor cortex has been represented with different tones of green to highlight the cytoarchitectonic organization of this region. Similarly, cytoarchitectonic subdivisions of the parietal cortex have been indicated in tones of red. PMd, dorsal premotor; PMv, ventral premotor; MIP, medial intraparietal area; LIP, lateral intraparietal area; VIP, ventral intraparietal area; AIP, anterior intraparietal area. All the remaining acronyms defined as in (Pandya and Seltzer, 1982). Figure from (Kandel, 2013).

Notably, caudal premotor areas such as F2 and F4, together with rostral premotor regions including F5, are tightly linked to the primary motor cortex (F1), both functionally and anatomically, and follow a precise somatotopic organization that preserves the specificity of effector-related movements (Rizzolatti et al., 1998; Cerri et al., 2003; Rolls et al., 2023). In contrast, anterior areas (F6–F7) have limited or mostly indirect access to F1 or the spinal cord, projecting instead to prefrontal and limbic regions, including the basal ganglia and thalamus, and are thus more implicated in action selection, volitional

planning, and inhibitory control (Luppino et al., 1993; Picard & Strick, 2001). This anatomical hierarchy finds its counterpart in the PPC, a key region for integrating sensory inputs with motor planning processes. The PPC is topographically divided by the intraparietal sulcus (IPS) into a superior (SPL) and an inferior parietal lobule (IPL), with each subregion projecting to distinct premotor targets and participating in specialized sensorimotor computations (Caminiti et al., 2015; Borra & Luppino, 2017) (Figure 4).

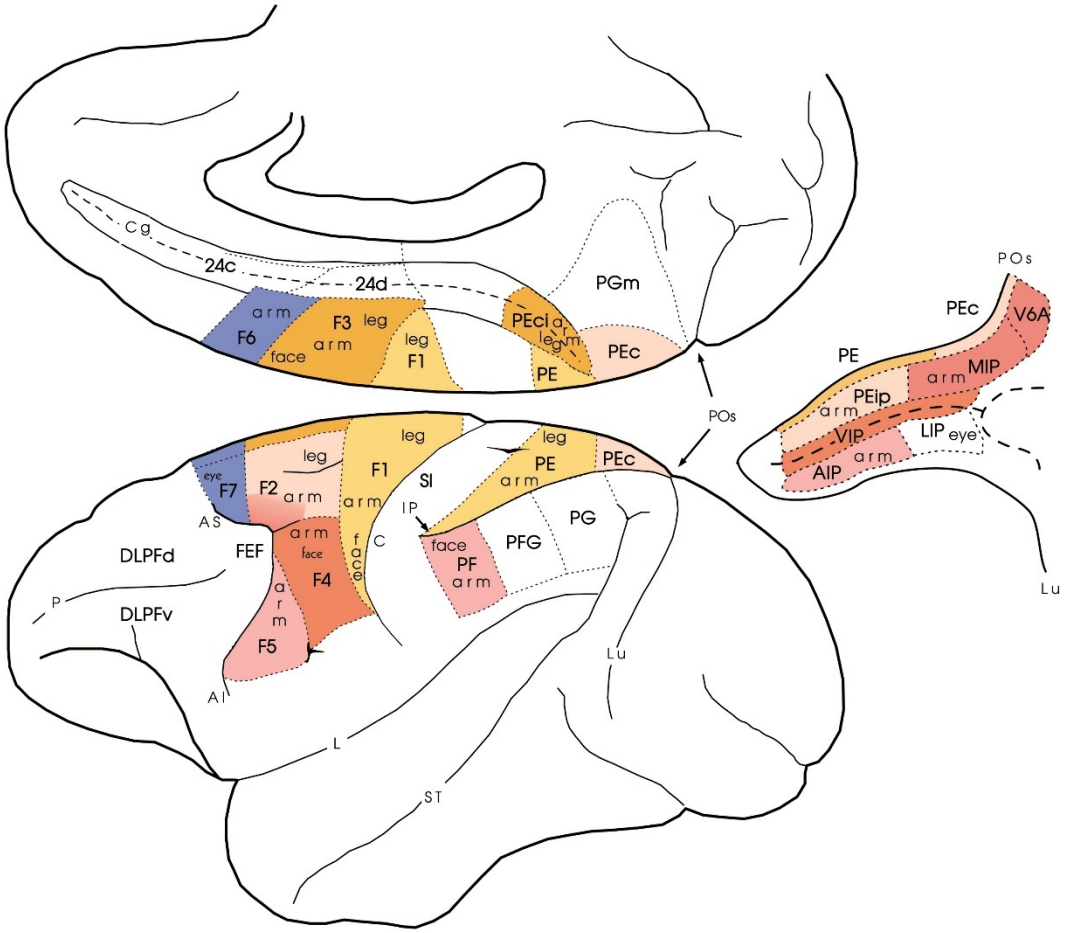

Figure 4. Mesial and Lateral Views of the Monkey Brain Showing the Parcellation of the Motor Cortex, Posterior Parietal, and Cingulate Cortices. The areas located within the intraparietal sulcus are shown in an unfolded view of the sulcus in the right part of the figure. For the nomenclature and definition of motor, posterior parietal, and cingulate areas, see Rizzolatti et al. (1998). The parieto-dependent motor areas and the parietal areas that are the source of their major cortical afferents are indicated with the same color. Prefronto-dependent areas are indicated in blue. AI, inferior arcuate sulcus; AS, superior arcuate sulcus; C, central sulcus; Cg, cingulate sulcus; DLPFd, dorsolateral prefrontal cortex, dorsal; DLPFv, dorsolateral prefrontal cortex, ventral; L, lateral fissure; Lu, lunate sulcus; P, principal sulcus; POs, parieto-occipital sulcus; ST, superior temporal sulcus. Figure from (Rizzolatti and Luppino, 2001).

For example, the AIP maintains dense, reciprocal connections with the ventral premotor area F5, forming a circuit responsible for translating object features - such as

size, shape, and orientation - into suitable configurations of the wrist and the fingers (Taira et al., 1990; Murata et al., 1997; Luppino et al., 1999; Begliomini et al., 2007; Gerbella et al., 2017). Similarly, the medial intraparietal area (MIP) connects with the dorsal premotor area F2 and supports the transport phase of reaching by integrating visual and somatic cues relevant to arm posture and trajectory (Johnson et al., 1996; Battaglia-Mayer et al., 2001; Marconi et al., 2001; Filimon et al., 2007; Nelissen et al., 2018).

Other crucial parieto-frontal loops include the VIP–F4 circuit, involved in encoding peripersonal space and coordinating defensive or target-directed hand movements. Depending on behavioral context, this circuit may support either defensive responses or goal-directed hand movements, reflecting the flexible use of shared peripersonal representations (Graziano & Cooke, 2006; Bufacchi & Iannetti, 2018), and the LIP–FEF pathway, which supports saccadic eye movements toward salient stimuli during action planning and visual exploration (Colby et al., 1996; Grefkes & Fink, 2005; Sambo et al., 2012). (Figure 5).

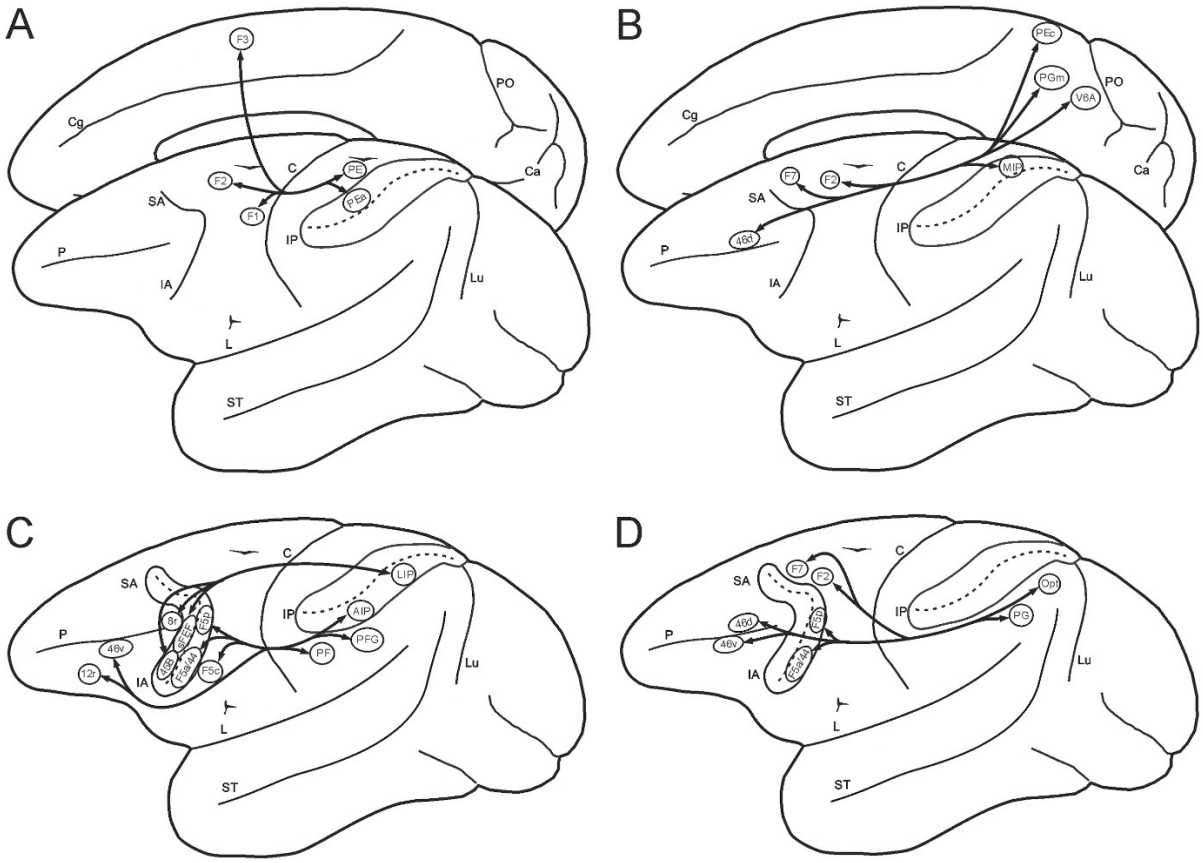

Figure 5. Summary view of the main frontal connections of the macaque PPC. A: Connections of rostral SPL areas. B: Connections of caudal SPL areas. C: Connections of rostral IPL areas. D: Connections of caudal IPL areas. Figure from (Borra and Luppino, 2017).

Importantly, these circuits are not isolated modules but operate as a functionally specific, yet dynamically integrated network, enabling the flexible coordination of reaching, grasping, eye movements, and posture control; within this framework, sensorimotor transformations are implemented in a distributed fashion, with different extended grasping network nodes encoding overlapping information in task-specific formats (Pouget & Snyder, 2000; Cisek & Kalaska, 2010; Filimon, 2010; Barany et al., 2014; Grafton, 2014; Fleming, 2017; Klein et al., 2020). Taken together, the anatomical and functional architecture of the extended grasping network supports its role as the cortical backbone of visually guided grasping and object-directed behavior, providing the substrate upon which the subsequent transformations, examined in the next sections, are built.

1.2.2 Parieto-frontal nodes: roles in sensorimotor transformation

Within the extended grasping network, several parieto-frontal regions operate as functionally specialized nodes, each contributing to different stages of the sensorimotor transformation that underlies visually guided grasping. This distributed yet topographically organized architecture enables the progressive integration of visual, somatosensory and motor information essential for object-directed actions. Among the most prominent of these nodes, explored in the present study, are AIP, the ventral premotor area F5, the dorsal premotor area F2 and the pre-supplementary motor area F6.

AIP area, together with other parietal regions involved in reach-to-grasp behavior (e.g., V6A, PE and PEc; Fattori et al., 2010; Breveglieri et al., 2016), is a critical site for the extraction of object features relevant for action planning. Neurons in AIP respond selectively to three-dimensional visual attributes such as object shape, size and orientation (Murata et al., 2000; Schaffelhofer & Scherberger, 2016; Orban et al., 2021; Maranesi et al., 2024) (Figure 6). Crucially, these representations are action-oriented: their tuning is modulated by the type of grip required, indicating that AIP encodes not abstract geometry but motor-relevant affordances. This makes AIP a prime candidate for mediating the visuo-motor interface. Anatomically, it is reciprocally connected with area F5, forming a canonical parieto-frontal loop that translates perceptual inputs into motor intentions (Borra et al., 2008; Rizzolatti et al., 1998).

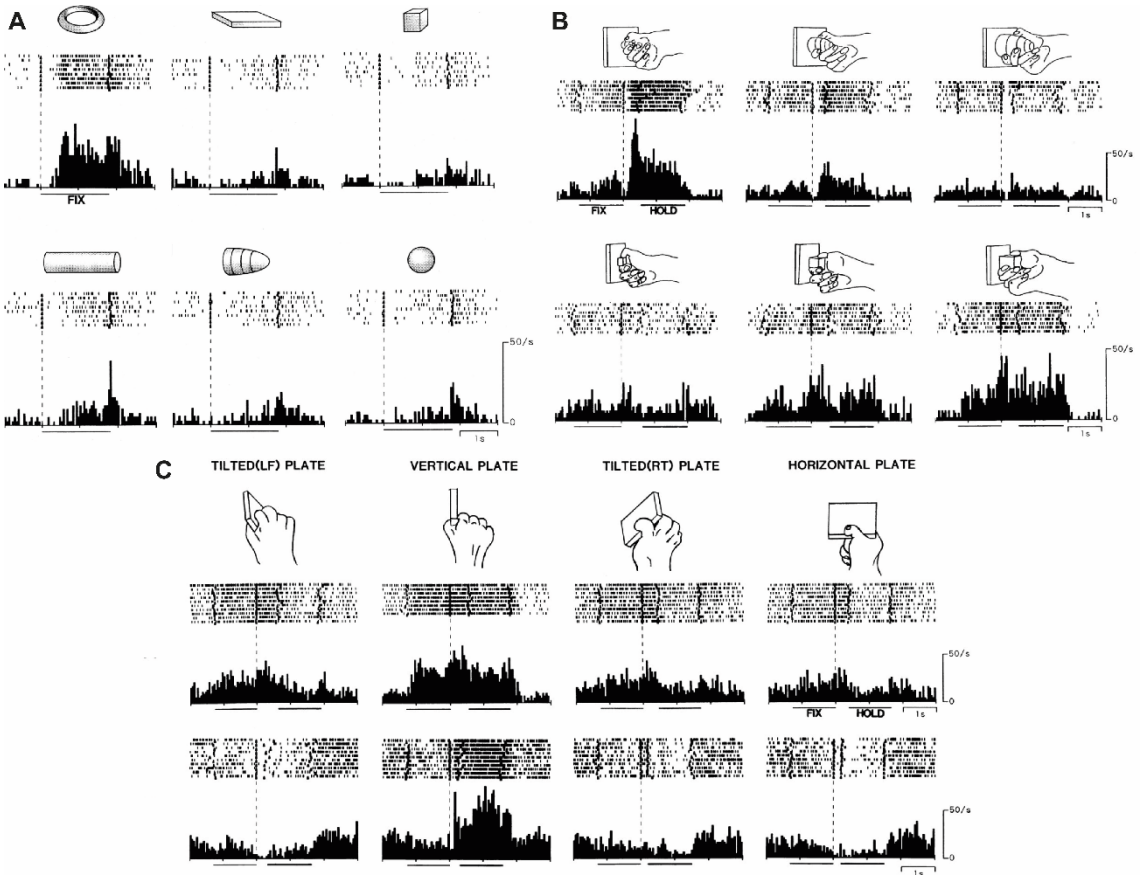

Figure 6. Neural selectivity for object shape, size, and orientation in area AIP. (A) Example of a highly selective object-type visual-dominant neuron during the object-fixation task. Raster plots and histograms show responses to six medium-sized 3D objects (horizontal ring, horizontal plate, cube, cylinder, cone, sphere). The neuron exhibited a strong preference for the horizontal ring. (B) Two examples of size-selective neurons during object manipulation. *Upper*: a motor-dominant neuron showing increased activity for small cones. *Lower*: an object-type visual-motor neuron preferring large cubes. Bar graphs indicate mean net activity across trials. (C) Orientation-selective responses to a plate presented at 45° intervals in the frontal plane. *Upper*: object-type visual-motor neuron. *Lower*: nonobject-type visual-dominant neuron recorded in a separate experiment (Miyashita et al., 1998), not included in the main dataset. Figure adapted from (Murata et al., 2000).

Within this loop, area F5 plays a pivotal role in motor encoding. Neurons here are not primarily tuned to the visual features of objects but instead respond to specific hand/finger configurations (e.g., precision grip vs. power grip) (Umiltà et al., 2007; Schaffelhofer & Scherberger, 2016; Bruni et al., 2017), with some evidence suggesting that these representations can be partially independent from the visual properties of the grasped object (Fluet et al., 2010). Some F5 neurons also exhibit anticipatory discharge, with activity increasing before the onset of the corresponding hand movement and reflecting internal goals and the expected sensory consequences of the action (Bonini et al., 2014c) (Figure 7), a phenomenon associated with higher-order motor planning and action intention (Jeannerod, 1995).

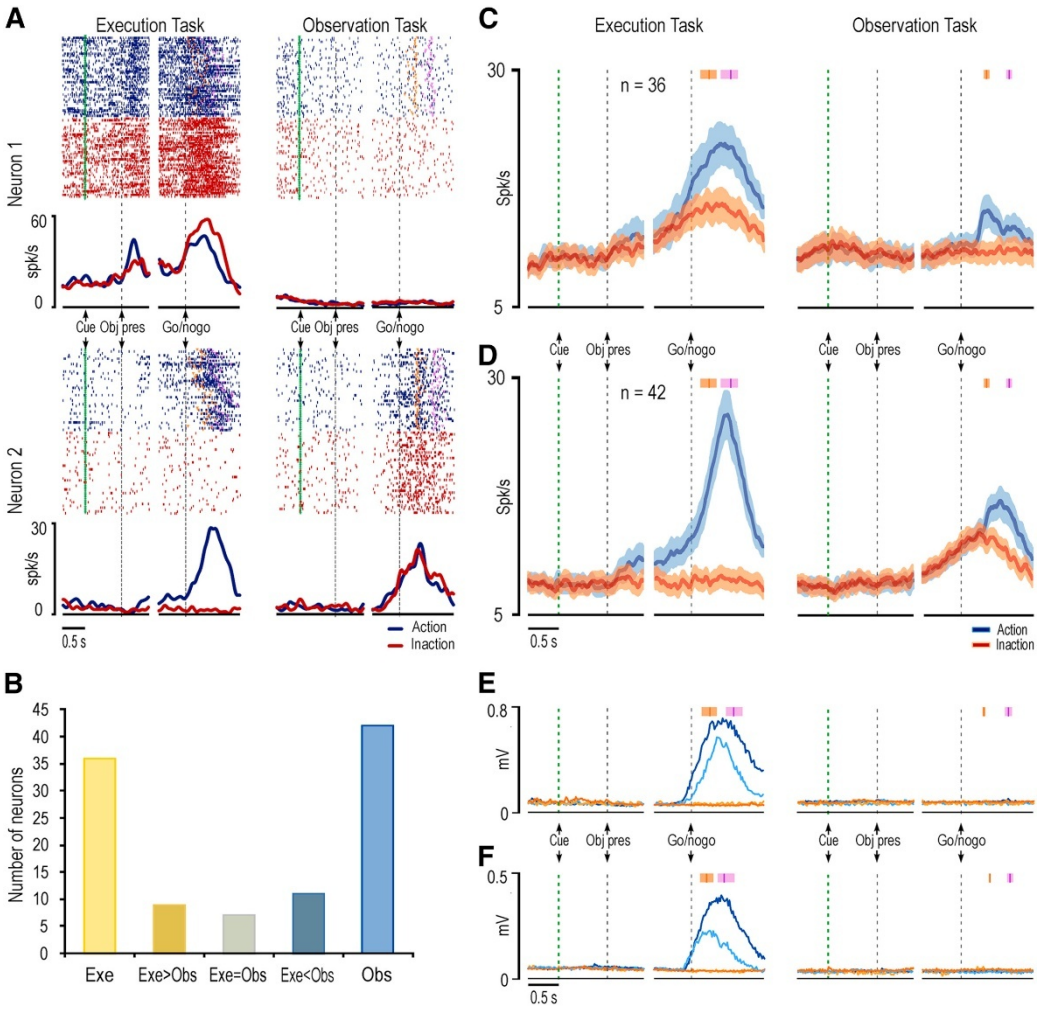

Figure 7. Neuronal activity in area F5 reflecting internal representations of action during both execution and observation. Panel A shows two example neurons that respond during both action and inaction conditions, aligned to key task events (object presentation, go/no-go cue, reaching onset, and object pulling). Notably, some neurons discharge even when the action is withheld, indicating internal goal representation. Panel B summarizes task-context selectivity across the population of inaction-responsive neurons (n = 105), while Panels C and D show population responses during execution and observation, respectively. Mirror neurons in Panel D exhibit similar modulation during observed inaction, supporting the idea that F5 encodes expected sensory consequences even in the absence of overt movement. Panels E and F confirm that muscle activity is absent during inaction and observation, ruling out covert motor execution. These findings align with predictive coding models, suggesting that F5 neurons simulate action outcomes internally. Figure adapted from (Bonini et al., 2014c).

Beyond the AIP–F5 loop, other circuits within the extended grasping network support complementary components of manual action. The dorsal premotor cortex (F2) receives input from medial parietal regions such as the MIP area (Marconi et al., 2001) and is particularly involved in the spatial guidance of reaching. F2 neurons encode movement direction, limb trajectory, and timing (Raos et al., 2004, 2006), and are preferentially active during arm transport phases of grasping, but they can also show

selectivity for both grip type and wrist orientation during grasping movements (Figure 8).

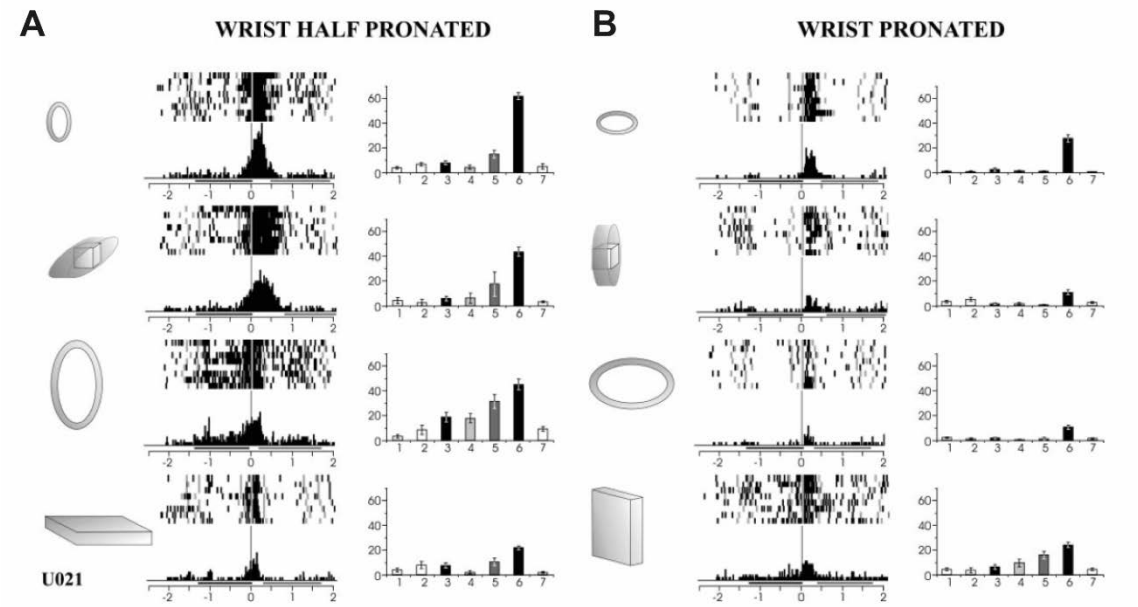

Figure 8. Activity of a purely motor neuron in area F2 selective for both grip type and wrist orientation. The figure displays raster plots and histograms of neural activity recorded during movement in light conditions. Four different objects, each presented in two orientations, were grasped using distinct wrist postures. Objects are arranged in two columns based on the wrist orientation required for grasping: (A) half-pronated wrist; (B) fully pronated wrist. Note that the arrangement reflects wrist posture rather than object axis orientation. Neural activity is aligned (vertical bar) to movement onset. The neuron exhibits combined selectivity for grip configuration and wrist orientation, independent of the spatial orientation of the object. Figure from (Raos et al., 2004).

Finally, the pre-supplementary motor area (F6), located more medially and anteriorly, contributes to the planning and sequencing of goal-directed behavior. Unlike AIP or F5, F6 activity often reflects internal decision processes and task rules rather than immediate sensorimotor contingencies (Shima & Tanji, 2000; Hoshi & Tanji, 2004) (Figure 9) . This region is particularly recruited when actions must be selected among alternatives, suppressed or reprogrammed, indicating its role in high-level volitional control.

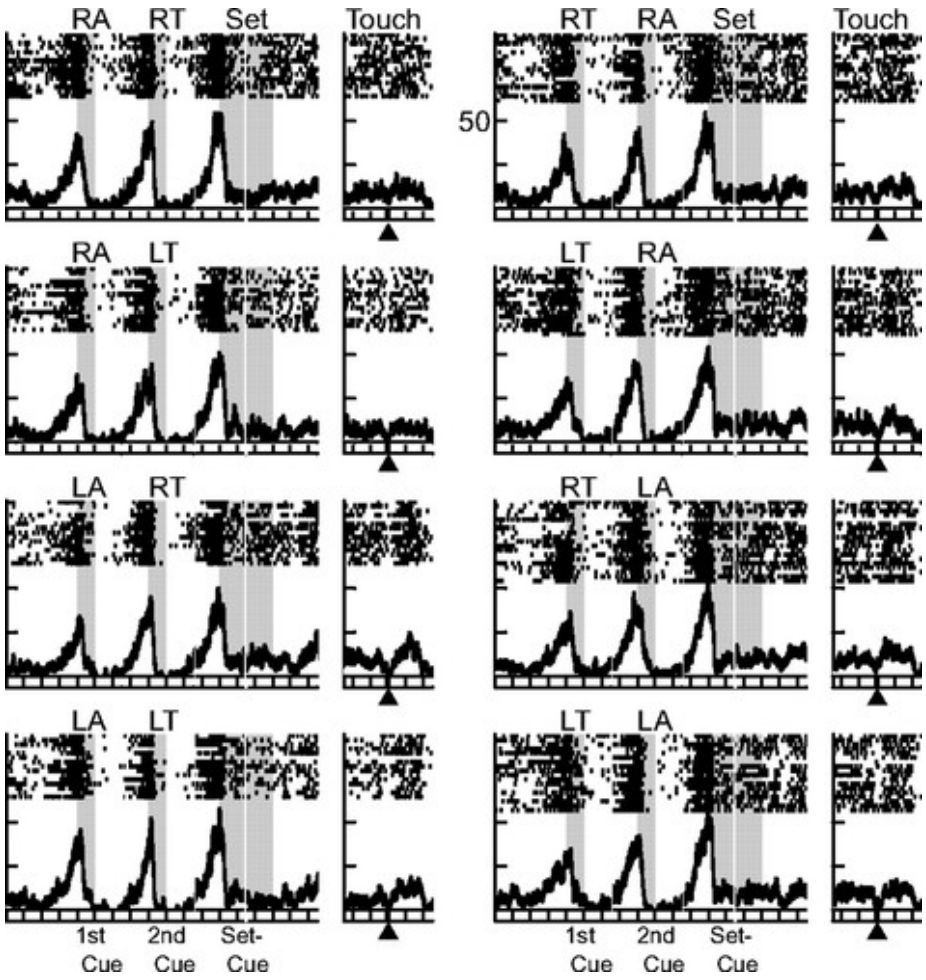

Figure 9. Anticipatory activity of a pre-SMA neuron during a delayed instruction task. Raster plots and spike density functions (SDFs; Gaussian kernel, σ = 20 ms; mean ± SE) show neuronal activity across trials sorted according to eight different instruction-cue sequences. Each row of the raster represents a trial, and each dot indicates a neuronal spike. SDFs are aligned to the onset of the 1st cue, 2nd cue, set cue, and GO signal, merged at the midpoint of the corresponding delay periods. Gray areas indicate the timing of the 1st, 2nd, and set cues. Instruction cues for arm and target are indicated above each panel (RA = right arm; LA = left arm; RT = right target; LT = left target). The panel on the right shows activity during the movement period (aligned to screen touch, ▲). This neuron exhibits anticipatory activity before the presentation of each cue, reflecting preparation and planning of the upcoming action. Figure from (Hoshi & Tanji, 2004).

Taken together, the parieto-frontal nodes of the extended grasping network support distinct yet overlapping functions, forming dynamic sub-networks specialized for object encoding, motor planning, reach guidance and cognitive modulation. Their anatomical and functional segregation underlies the partitioning of grasping into modular components (e.g., hand shaping, arm transport, grip type selection), while their interconnectivity ensures coordinated action. At its core, the balance between functional specificity and network integration supports the merging of grasp-related processes into effective behavior.

1.2.3 Functional integration across the network

Far from being reducible to anatomical connectivity alone, the interconnections described above support the network's ability to synchronize sensory processing and motor output in real time through temporally structured, bidirectional communication. This functional integration enables the convergence of the distinct response properties of each node, giving rise to a functional synergy during grasp execution. Rather than functioning as a serial hierarchy, the extended grasping network operates through reentrant loops that integrate feedforward transmission of sensory information with feedback modulation from premotor and prefrontal regions (Cisek, 2007; Verduzco-Flores & De Schutter, 2022) (Figure 10). This perspective extends beyond modular interpretations of visuomotor processing, emphasizing the continuous bidirectional exchange that links parietal and frontal populations during action planning and control. In this framework, AIP receives bottom-up visual input but its activity is also shaped by top-down influences from F5 related to ongoing motor planning and contextual constraints (Verduzco-Flores & De Schutter, 2022). This reciprocal architecture allows the system to update grasp parameters dynamically according to changes in the environment or task demands.

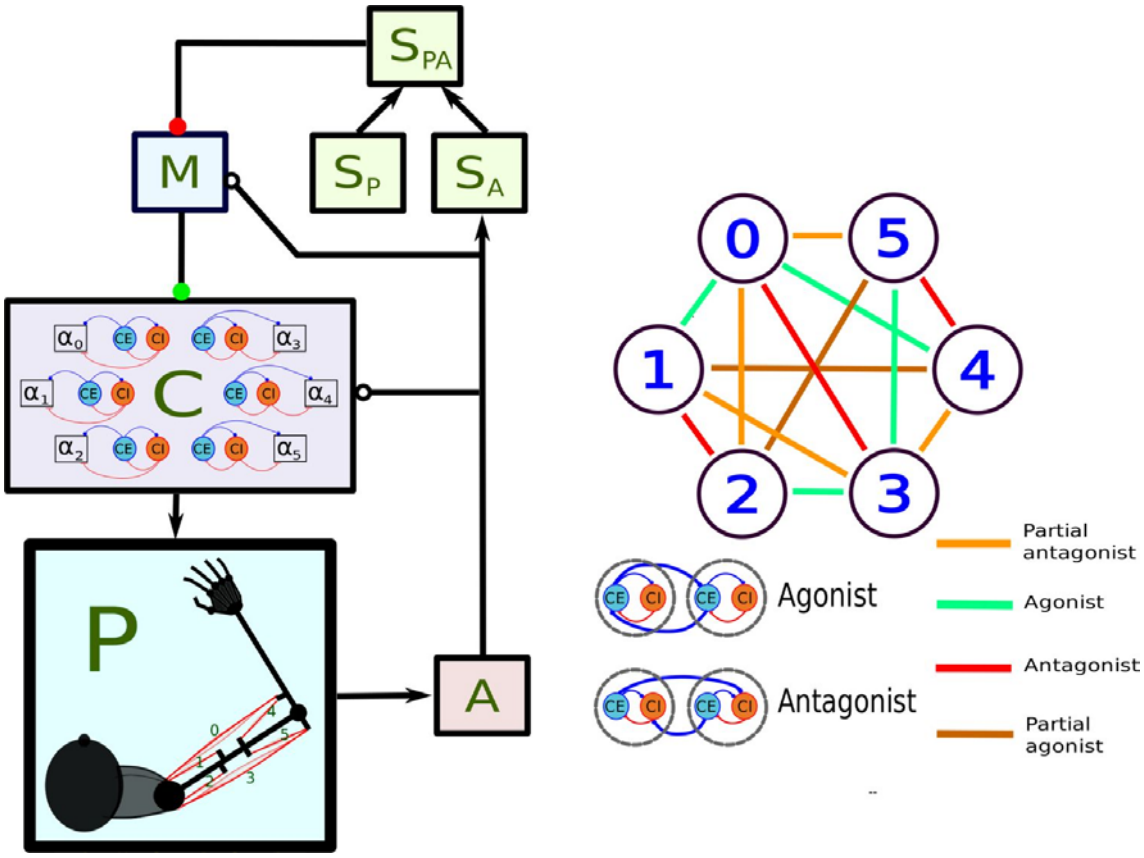

Figure 10. Reentrant organization of sensorimotor control loops. Schematic representation of the main components of the computational model proposed by Verduzco-Flores and De Schutter (2022), illustrating how adaptive sensorimotor control arises from interconnected neural populations organized in recurrent feedback loops. Each box represents a distinct population, including afferent inputs (A), somatosensory areas (SA, SP, SPA), motor cortex (M), and spinal circuitry (C). Arrows indicate feedforward and feedback connections linking cortical and spinal components, while colored circles denote sites of plastic or static synapses depending on the model variant. The right panel depicts the organization of excitatory (E) and inhibitory (I) interneurons and α-motoneurons controlling agonist–antagonist muscle pairs. Together, the model highlights how bidirectional interactions between sensory and motor circuits enable self-organizing, flexible coordination of action. Figure from (Verduzco-Flores & De Schutter, 2022).

Integration within the extended grasping network is temporally structured but not strictly sequential. Electrophysiological recordings and neuroimaging studies converge in showing that activity in parietal and premotor regions unfolds with overlapping time courses, reflecting continuous interactions rather than a unidirectional flow of information (Culham et al., 2003; Michelet et al., 2010; Gallivan et al., 2013; Lanzilotto et al., 2020). Posterior parietal areas such as AIP and PRR are typically engaged during early stages of object encoding, while premotor regions including F5, F2 and F6 exhibit sustained or context-dependent modulation as the motor plan evolves. In delayed-

response tasks, persistent activity in AIP and F5 supports the maintenance of action-related representations, whereas in fast reaction paradigms, premotor activity emerges earlier to enable anticipatory control (Michelet et al., 2010; Lanzilotto et al., 2020).

At the population level, oscillatory synchronization further supports inter-regional communication within the grasping network. Studies in humans and non-human primates have shown that beta-band desynchronization (15–30 Hz) across parieto-frontal regions accompanies motor preparation, while gamma-band synchronization (30–100 Hz) increases during object encoding and movement execution (Michelet et al., 2010; Spadone et al., 2021; Verduzco-Flores & De Schutter, 2022). These frequency-specific dynamics are thought to facilitate the integration of sensory and motor representations across distributed cortical sites. Such parieto-frontal pathways also coordinate effectors across shared spatial reference frames: for instance, connections linking VIP to F4 and LIP to the frontal eye fields (FEF) support the coordination of gaze and limb movements (Colby et al., 1996; Batista & Andersen, 2001; Marzocchi et al., 2008; Gamberini et al., 2009). Such cross-effector alignment is critical for spatial coherence, allowing coordinated eye, hand and body movements toward a common target (Pesaran et al., 2008).

Beyond the coordination of sensory and motor representations, functional coupling within the extended grasping network is also modulated by higher-order cognitive demands. Task rules, contextual contingencies and learning history can reshape the strength and timing of parieto-frontal interactions (Tunik et al., 2005; Petrides, 2005; Grol et al., 2007). Perturbation studies further demonstrate that disrupting specific nodes through transcranial magnetic stimulation over parietal (Tunik et al., 2005; Rice et al., 2006) or premotor regions (Davare et al., 2006) leads to selective impairments in grasp configuration, reach trajectory or action selection, depending on the behavioral context. Together, these findings indicate that inter-area coordination is dynamically reconfigured across time and task conditions, allowing the network to flexibly adapt its communication patterns to current goals.

Thus, the extended grasping network operates as a context-sensitive and functionally flexible system. Rather than a simple mapping between stimulus and response, action emerges from the dynamic interplay of distributed nodes whose interactions evolve in relation to internal goals, sensory conditions and environmental

contingencies. To capture these interactions, it is necessary to investigate how sensorimotor transformations unfold within neuronal populations, linking local computations to large-scale network coordination.

1.2.4 Electrophysiological signatures of object-to-action transformation

At the neuronal level, the transformation from object perception to action execution emerges through coordinated activity patterns. In posterior parietal regions such as AIP, object-selective responses appear within approximately 100–150 ms after stimulus onset, though timing varies with task and stimulus complexity (Sakata et al., 1999; Murata et al., 2000; Baumann et al., 2009; Intveld et al., 2018). These neurons are tuned to grasp-relevant object features, such as shape, size and orientation, which directly constrain possible hand configurations. Their tuning remains stable across moderate changes in viewing angle, suggesting a partially viewpoint-invariant encoding of object geometry (Baumann et al., 2009; Intveld et al., 2018). Notably, in delayed grasping tasks, many AIP neurons preserve this selectivity during the memory period, indicating that object-related information can be maintained to guide actions in the absence of visual input (Sakata et al., 1999; Townsend et al., 2011; Schaffelhofer & Scherberger, 2016). The same visual features that guide grasp planning when the object is visible can therefore be internally represented to support action under memory-driven conditions.

Activity in ventral premotor cortex, particularly in area F5, reflects a complementary stage of this transformation. Neural selectivity here shifts from visual to motor variables, encoding grip configuration and hand orientation that link the perceived object to a specific motor plan (Raos et al., 2004; Schaffelhofer & Scherberger, 2016). These motor representations are modulated by contextual factors such as task rules, movement timing and behavioral goals (Rizzolatti et al., 1998). In addition, many F5 neurons exhibit anticipatory activity that precedes movement onset, consistent with the preparation of forthcoming actions within an internal motor representation (Jeannerod, 1995).

At the population level, simultaneous recordings reveal that neural ensembles in AIP and F5 evolve along smooth, low dimensional trajectories that bridge perceptual and motor states, supporting a dynamical systems view of sensorimotor control (Churchland et al., 2012; Michaels et al., 2016) (Figure 11).

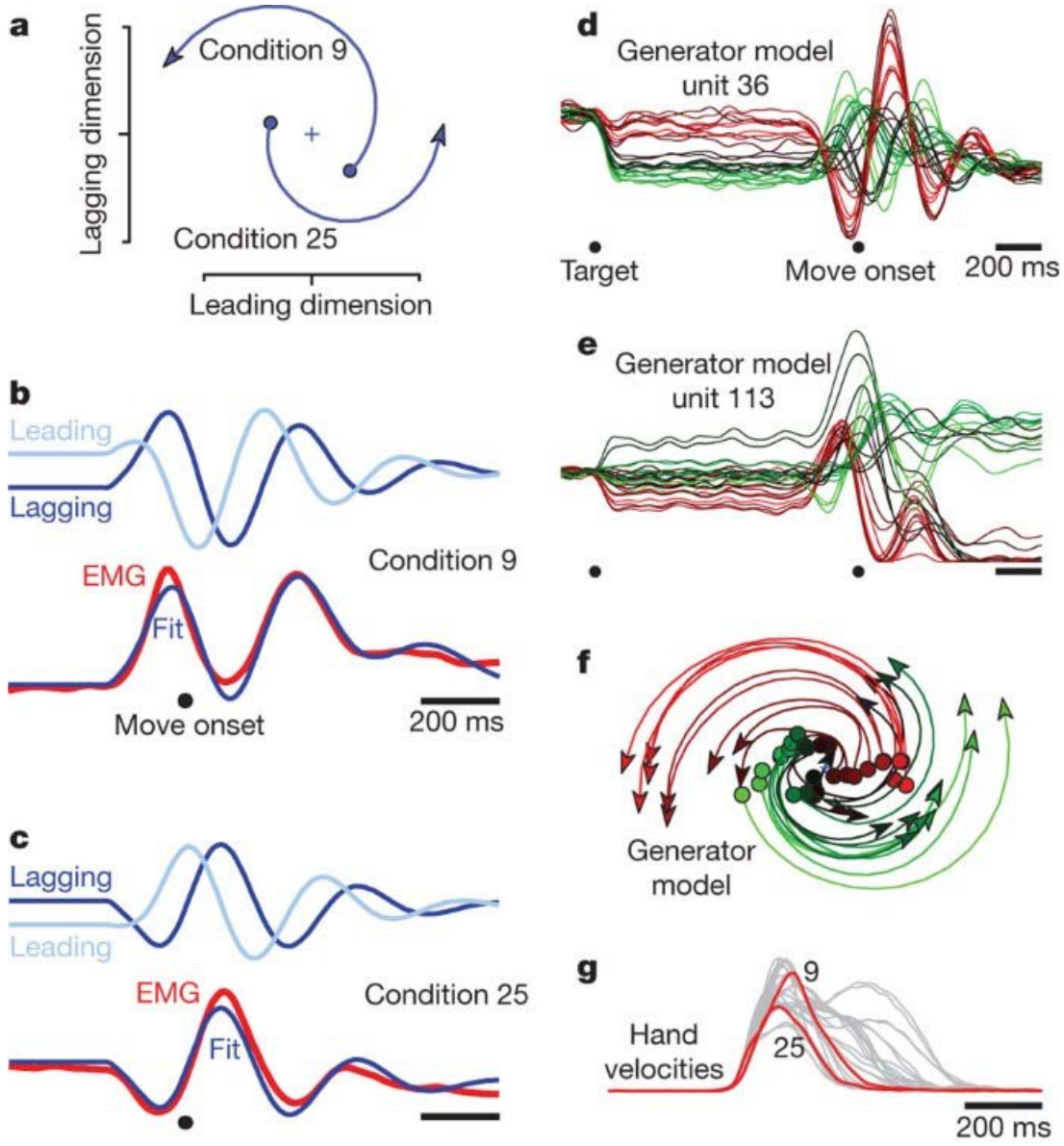

Figure 11. Low-dimensional rotational dynamics of neural population activity in motor cortical areas during reaching movements. Panel (A) shows the higher-frequency rotation at 2.8 Hz for two reach conditions (9 and 25), depicting the first 200 ms of evolution away from the preparatory state (filled circles). The preparatory state determines both the amplitude and phase of the rotation. One state dimension ('leading', x-axis) is always 90° ahead of the other ('lagging', y-axis). Panels (B) and (C) show projections onto the leading and lagging dimensions over time (light and dark blue) for conditions 9 and 25, respectively. The summed lagging components from this 2.8 Hz rotation (shown) and a lower frequency rotation (0.3 Hz, not shown) fit the electromyographic (EMG) data. The 2.8 Hz rotation in panel C is approximately 180° out of phase with that in panel B. Panels (D) and (E) show simulated responses of two individual units from the computational generator model (Methods), presented similarly to Fig. 2 in the original paper. Panel (F) displays the jPCA projection of the simulated population activity, which can be compared directly with the neural data in Fig. 3c of the original study. Panel (G) illustrates hand velocities across the 27 experimental conditions used in panels D–F, with red traces highlighting conditions 9 and 25**.** Figure from (Churchland et al., 2012).

Oscillatory activity provides a complementary, mesoscale view of this transformation. Beta band desynchronization between 15 and 30 Hz accompanies the release of motor inhibition, whereas gamma band synchronization between 30 and 100 Hz increases during the integration of sensory and motor information during movement preparation and execution (Pfurtscheller & Lopes da Silva, 1999; Cheyne et al., 2008; Khanna & Carmena, 2017; Spadone et al., 2021). The timing and amplitude of these oscillations vary with task demands: increased delays or uncertainty shift both the onset and strength of beta and gamma modulations (Gallivan et al., 2016). At the level of neuronal populations, decoding analyses further reveal how these transformations are expressed in representational space. Neural ensembles in AIP and F5 contain sufficient information to predict upcoming grip type or target location before movement initiation, indicating that motor plans are explicitly represented well in advance of execution. These population codes generalize across time and, to some extent, across effector configurations, suggesting that grasp-related representations are both stable and flexible across task contexts (Gallivan et al., 2011; Schaffelhofer & Scherberger, 2016).

In summary, electrophysiological studies reveal a progressive and interactive transformation within the extended grasping network: early encoding of object geometry in parietal cortex, sustained maintenance of grasp-relevant information, and anticipatory motor activity in premotor regions. Together, these findings describe a distributed system that continuously links perception and action, maintaining functional stability and goal-directed control even when visual input is transient or absent.

1.3 MEMORY-DRIVEN GRASPING

When perceptual input is no longer available, purposeful action must rely on internally maintained representations. Grasping without visual feedback, whether due to temporal delays or occlusions, offers an effective model for studying how the brain links previous sensory information to upcoming motor output. Rather than reflecting a secondary control strategy, memory-driven grasping underscores the ability of the extended grasping network to maintain and update action-related representations across time, integrating stored object features with ongoing motor planning. Examining grasp execution under these conditions allows us to identify how parietal and frontal regions encode, sustain, and transform internal representations to guide behavior. This approach provides a direct means to investigate how perception and action remain coordinated in the absence of real-

time sensory input.

1.3.1 Grasping in the dark: behavioral and neurophysiological evidence

Grasping actions can be executed with remarkable precision even in the absence of visual input at the time of movement, a phenomenon extensively investigated through delayed grasping paradigms in both humans and non-human primates. Behavioral studies have shown that, following a brief visual presentation of an object, subjects are able to initiate and complete accurate grasping movements even after several seconds of delay, during which the object is no longer visible (Goodale et al., 1994; Hu et al., 1999; Westwood & Goodale, 2003; Hesse & Franz, 2009) (Figure 12). Although performance gradually deteriorates as the delay lengthens, core kinematic parameters such as grip aperture scaling remain largely preserved. This preservation suggests that object-related information is actively maintained within the sensorimotor system rather than being stored as a purely visual trace, allowing accurate movement execution even in the absence of online visual feedback.

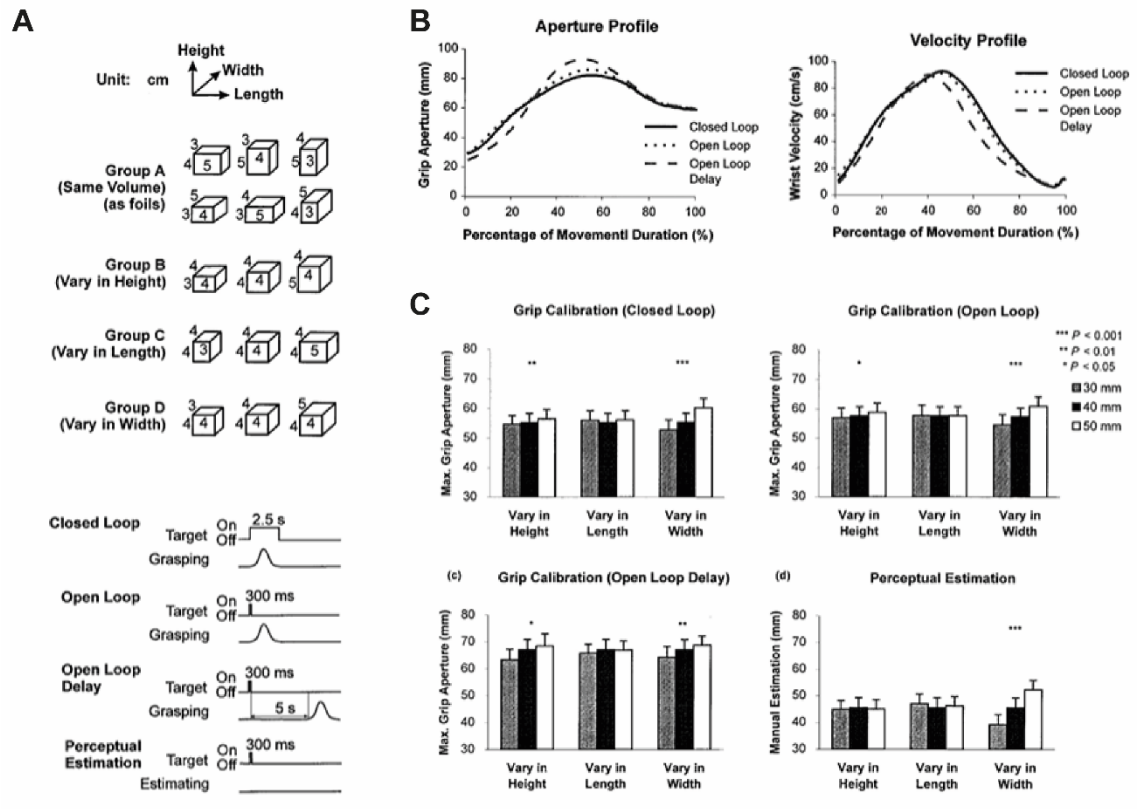

Figure 12. Kinematic parameters during delayed grasping. This panel illustrates an experimental paradigm used to investigate the precision of grasping actions executed without visual input at the time of movement. (A) Top: examples of the target objects used in the study. Bottom: schematic representation of the four experimental conditions: Closed Loop: the object remained visible throughout the movement, allowing full visual guidance. Open Loop: the object was visible for only 300 ms; the grasp was executed without visual feedback. Open-Loop Delay: after a 300 ms viewing period, a 5-second delay was introduced before movement initiation, with no visual access to the object or hand. Perceptual Estimation: participants viewed the object for 300 ms and then estimated its width by opening their fingers accordingly, without performing a reach. (B) Averaged kinematic profiles across trials for the three grasping conditions. Left: grip aperture over time; right: velocity profile. Movements were normalized for duration. (C) Mean values of maximum grip aperture and manual estimation as a function of object size. Top left: calibration in the Closed-Loop condition; top right: Open Loop; bottom left: Open-Loop Delay; bottom right: Perceptual Estimation. Error bars represent standard error. Figure adapted from (Hu et al., 1999).

At the neural level, available evidence suggests that memory-guided actions engage a distributed set of cortical regions within the extended grasping network. In macaques, studies employing delayed grasping paradigms without continuous visual feedback have reported persistent activity in both AIP and F5 during the memory delay (Sakata et al., 1999; Murata et al., 2000). This delay activity has been interpreted as reflecting the temporary retention of object- and action-related information that supports the maintenance of grasp parameters over time.

Complementary evidence from functional neuroimaging in humans, particularly using multivariate pattern analysis, shows that both parietal and premotor areas retain decodable grasp-related information during delay periods (Monaco et al., 2014; Gallivan et al., 2016) (Figure 13). This sustained activity appears to reflect an action-oriented form of working memory, in which representations are biased toward upcoming motor parameters rather than passive visual features, supporting the idea of a prospective sensorimotor memory.

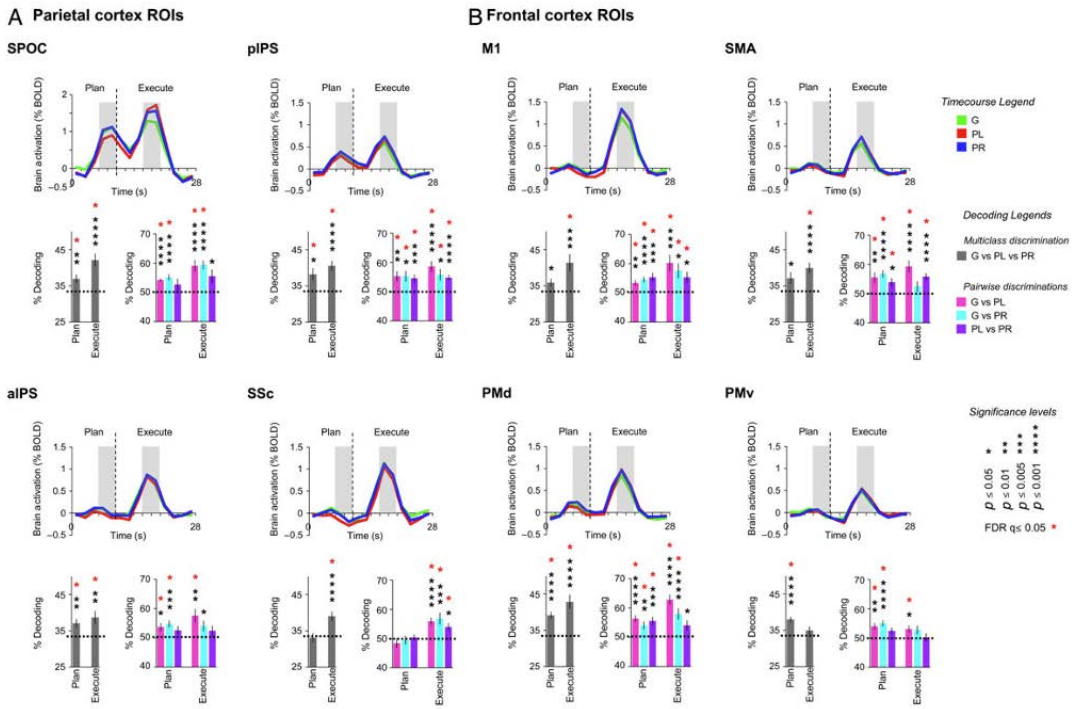

Figure 13. Decoding Object-Directed Action Sequences from Pre-Movement Signals in Frontoparietal ROIs. (A) Time-course plots showing percent signal change in BOLD activity for the three action conditions: G (Grasp-to-Hold), PL (Grasp-to-Place-Left), and PR (Grasp-to-Place-Right). Data are averaged across all voxels within each ROI and across participants. Due to jittering in the delay period, only trials with 5-volume (10 s) delays are shown. The vertical dashed line marks the onset of the Execute epoch. Gray shaded bars indicate the 4-second windows used for decoding analysis. (B) Multiclass decoding accuracies for G, PL, and PR, shown for the Plan and Execute epochs. Classification was performed using all three trial types and a leave-one-run-out cross-validation procedure. Dashed horizontal lines indicate chance level (33.3%). Black asterisks denote statistical significance based on two-tailed t-tests across participants; red asterisks indicate significance after FDR correction ($q \leqslant 0.05$). Note that decoding performance reflects voxel-wise pattern differences rather than overall signal amplitude, as time-courses in Panel A are largely overlapping during the Plan epoch. Pairwise decoding results are also shown alongside multiclass decoding, using the same procedure. Chance level for pairwise classification is 50%. These results demonstrate that frontoparietal ROIs retain grasp-relevant, action-specific information during the delay period, supporting the idea of a prospective, embodied sensorimotor memory. Figure from (Gallivan et al., 2016).

Taken together, these studies highlight the capacity of the extended grasping network to support object-directed actions in conditions of sensory uncertainty by relying on internal models. However, while these findings establish that internal object representations can guide action in the absence of immediate sensory input, they leave open crucial questions about how such representations are sustained and adapted over time, particularly with respect to their neural format, their temporal evolution and their integration within a broader network architecture.

1.3.2 Delay activity, working memory and motor planning

Building on this behavioral and neurophysiological evidence, one of the most consistently observed neural signatures of memory-guided grasping is the presence of delay-period activity, a sustained elevation of neuronal firing during the interval between stimulus presentation and action execution. This activity has been documented in several nodes of the extended grasping network, including AIP, F5 and PMd, and is thought to reflect the temporary maintenance of task-relevant information (Romo et al., 2004; Michaels et al., 2018; Maranesi et al., 2024). Within the broader framework of sensorimotor processing, this delay activity has frequently been interpreted as a neural correlate of working memory, particularly sensorimotor working memory. While sustained firing remains a central feature in this interpretation, recent models suggest that it may not be the only underlying mechanism. Instead, so-called “activity-silent” working memory may rely on transient synaptic changes that preserve information without continuous spiking (Stokes, 2015; Barbosa et al., 2020).

Electrophysiological studies in non-human primates have provided important observations on the temporal dynamics of sustained responses, even in the absence of visual feedback (Fluet et al., 2010; Berger et al., 2021; Buchwald & Scherberger, 2021) (Figure 14). Recent evidence further suggests that this activity can include both visual and action-related components, reflecting a pragmatic rather than purely sensory representation of the object (Maranesi et al., 2024). However, the specific organization of this coding within parietal and premotor regions, and its contribution to the maintenance and transformation of action-related information without visual feedback, remains to be fully clarified.

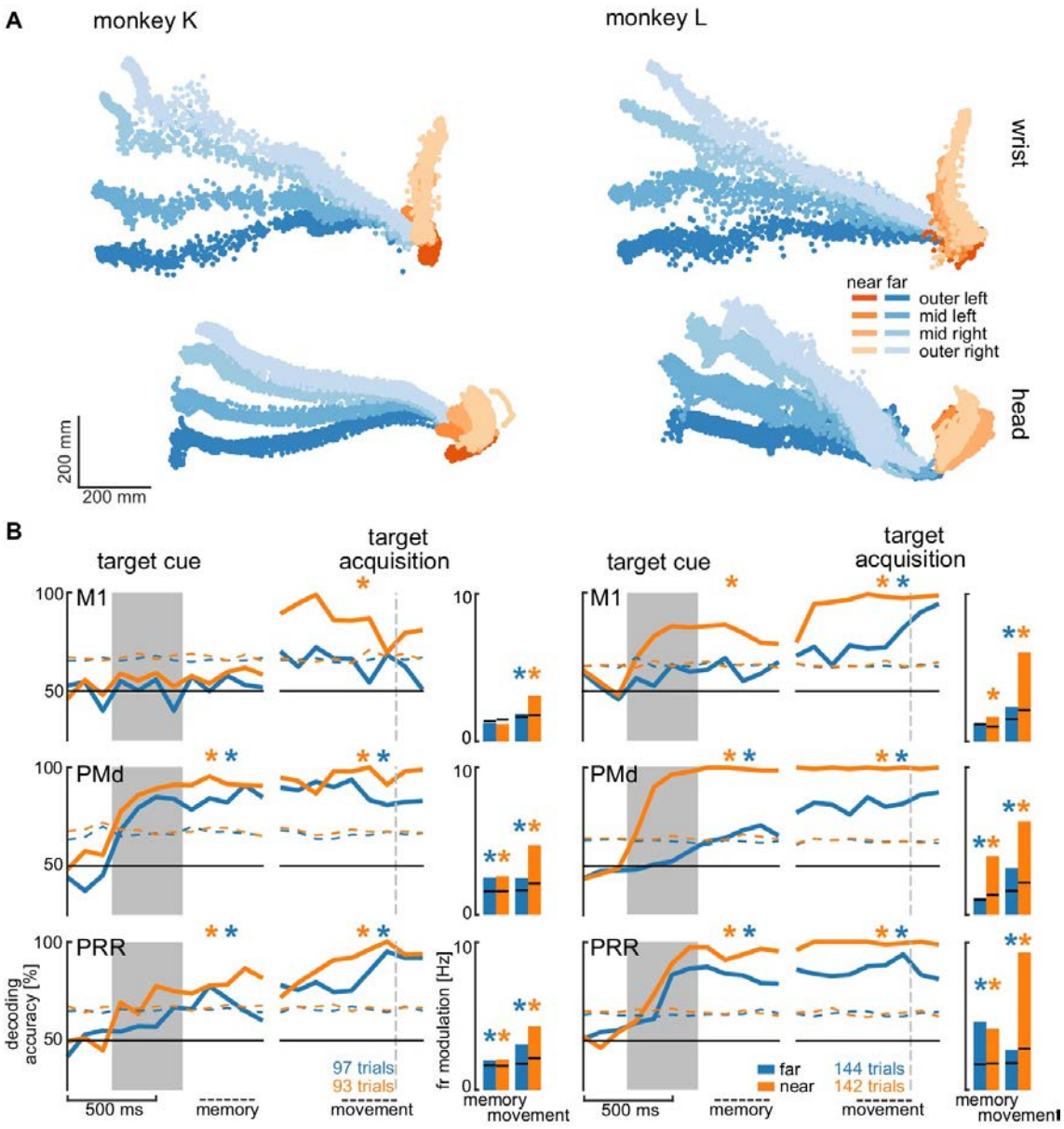

Figure 14. Direction decoding in the walk-and-reach task. (A) Top-view projection of wrist and head positions during reach (orange) and walk-and-reach (blue) movements toward eight spatial targets. (B) Decoding accuracy of target direction (left vs. right) using a linear SVM applied to neuronal activity in premotor, parietal, and motor cortex. Significant decoding was observed in premotor and parietal areas even during the memory period (100–400 ms after cue), indicating sustained neural representations of motor goals in the absence of visual feedback. Asterisks denote statistical significance after Bonferroni correction**.** Figure from (Berger et al., 2021).

Intriguingly, temporal analyses of single-neuron responses reveal that neural codes are not static across the delay interval. Rather, there appears to be a dynamic evolution from early stimulus-related coding, such as object location or identity, toward later activity patterns that may anticipate the motor response (Curtis & D'Esposito, 2003; Lara & Wallis, 2015; Hogendoorn & Burkitt, 2019). These findings support models in which

delay-period activity reflects a gradual transformation of perceptual inputs into motor plans, although comparisons spanning multiple regions and task phases have yet to be comprehensively explored.

Additionally, delay activity seems to be modulated by various cognitive factors, including attentional load (Andersen et al., 1997; Snyder et al., 1997), rule complexity (Sakai & Passingham, 2006), and expectations regarding movement timing (Maimon & Assad, 2006). Such modulation suggests that top-down influences shape how internal representations are conveyed and utilized, further complicating the identification of regional functional specificities. Yet, much of this evidence remains constrained to analyses within isolated regions, offering limited insight into how delay-period signals are coordinated across the network to support integrated sensorimotor planning. Building on this gap, the question of how temporally sustained, action-relevant representations may be distributed and dynamically reconfigured across the extended grasping network will be discussed in the following section.

1.3.3 Object representation stability across time and areas

For memory-guided grasping to succeed, object-related information must be preserved across temporal gaps and remain accessible for motor planning. As previously discussed, electrophysiological studies in macaques suggest that memory-guided grasping relies on a distributed encoding process but also indicate that this encoding may be temporally dynamic, with different regions of the extended grasping network contributing at distinct task epochs. Indeed, during the initial sensory phase, parietal areas such as AIP exhibit pronounced tuning to object features like shape and orientation, whereas premotor regions including F5 and PMd tend to become more engaged as the movement execution approach (Snyder et al., 2000; Fuster, 2008; Schaffelhofer & Scherberger, 2016; Intveld et al., 2018). These shifts have been interpreted as evidence for a transformation from sensory-based to action-oriented representations.

In humans, fMRI studies using multivariate pattern analysis provide complementary insights. Grasp-specific neural patterns observed during the initial stimulus period can persist into the delay phase and even predict parameters of the upcoming action (Gallivan et al., 2011; Gallivan et al., 2013). These representations appear to withstand both temporal decay and intervening distractors, suggesting a degree of functional stability. MEG data further reveal that such object-specific representations can be reactivated

shortly before movement onset, hinting at a potential retrieval mechanism (Boettcher et al., 2020; Boettcher et al., 2021) (Figure 15).

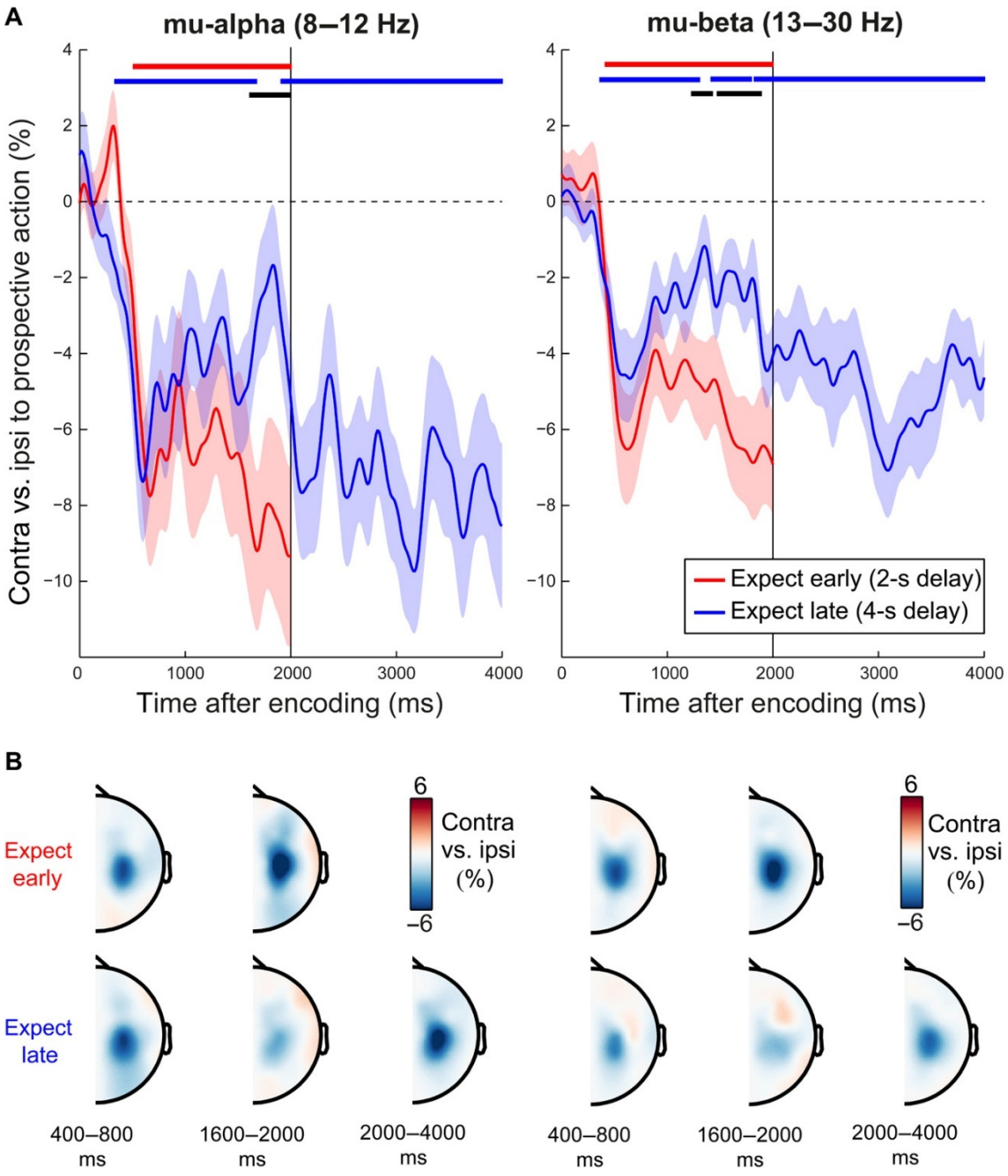

Figure 15. Temporal dynamics of anticipatory motor preparation as a function of expected memory utilization. This figure illustrates how effector-specific motor preparation unfolds over time depending on when visual working memory is expected to be used. (A) Time courses of lateralized EEG activity in canonical motor electrodes (C3/C4) are shown for the mu-alpha (left) and mu-beta (right) frequency bands, separated by condition: early vs late expected memory utilization (2 s vs 4 s). Black horizontal lines indicate statistically significant clusters ($P < 0.05$) between conditions, and shaded areas represent ±1 SEM across 25 participants. (B) Scalp topographies at representative time windows from panel (A) reveal effector-specific motor activation patterns, consistent with gradual action planning. Figure from (Boettcher et al., 2021).

While these findings underscore the robustness of object-specific representations across time and conditions, they also expose unresolved questions about their functional format and cross-regional dynamics. It remains unclear whether the encoded information is best characterized as visual, motoric or integrative, and how such representations are routed and transformed across the network to support action preparation. In particular, the extent to which object features are maintained in parallel across areas, relayed sequentially or flexibly redistributed depending on task context is still debated. Addressing these questions, prior evidence suggests a particular role for AIP in the neural computations underlying memory-guided actions, making it a useful entry point for exploring how local activity may reflect, or even mediate, broader circuit-level representational dynamics.

1.3.4 From local processing to distributed mechanisms: AIP in memory-driven grasping

Among the regions of the parieto-frontal grasping network, AIP provides a strategic site for examining how object information can be sustained and re-engaged for action when visual input is unavailable, consistent with evidence from other parietal areas involved in memory-guided reach-to-grasp behavior (Fattori et al., 2010; Galletti et al., 2022). Neurons in AIP encode grasp-relevant features such as shape, size, and orientation, and their activity can persist beyond the disappearance of the visual stimulus in delayed grasping paradigms (Murata et al., 2000). Perturbation studies in humans show that disruption of the anterior intraparietal sulcus selectively impairs grasp correction under conditions without visual feedback, providing causal evidence for a parietal contribution to maintaining internal action representations (Tunik et al., 2005; Rice et al., 2006; Davare et al., 2007) (Figure 16). Taken together, these findings suggest that AIP may play a distinctive role within the network, supporting the transformation of object-related signals into representations that remain behaviorally relevant across perceptual contexts.

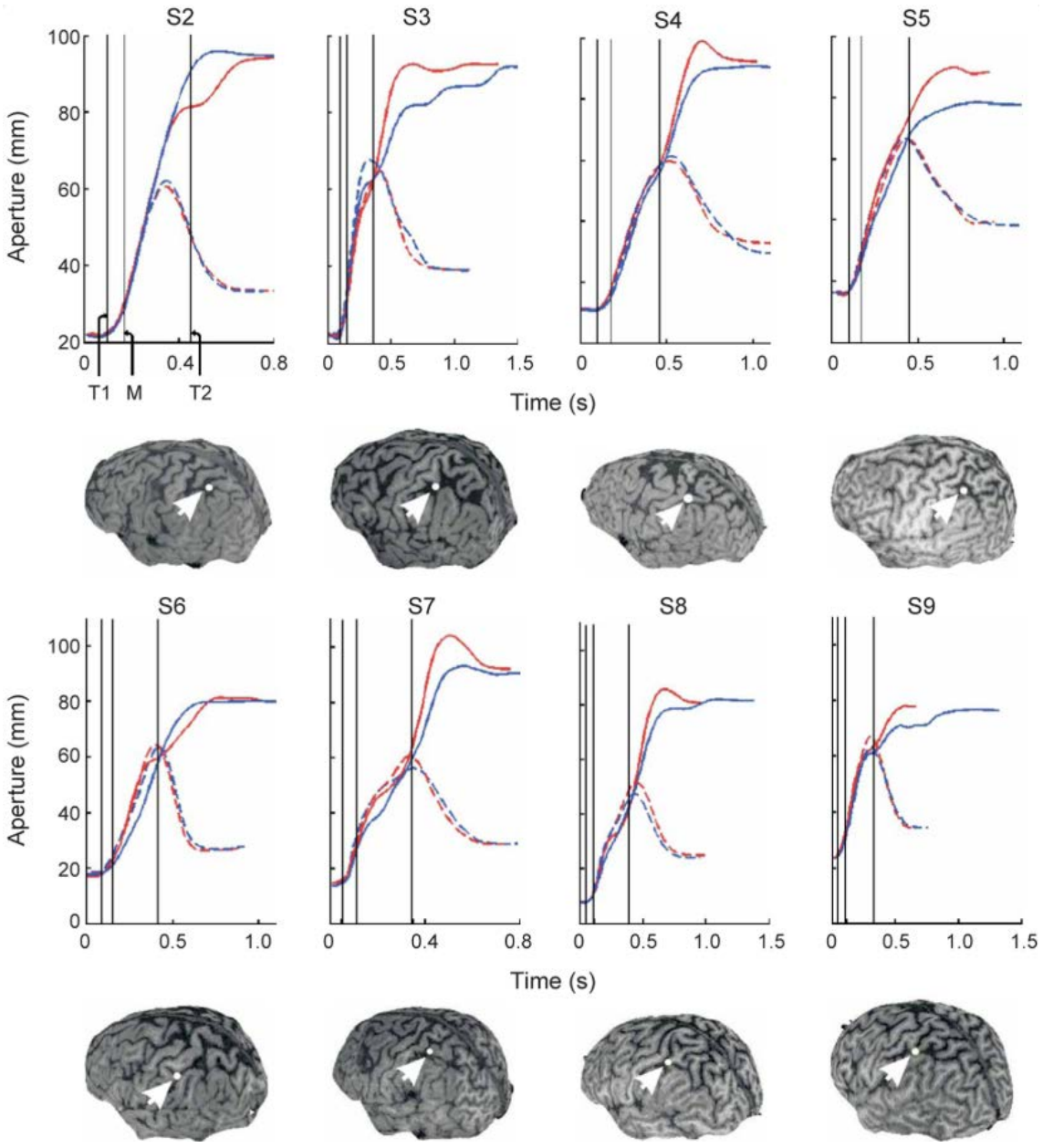

Figure 16. Disruption of aIPS via TMS selectively impairs grasp adjustment during memory-guided object perturbation. Mean aperture profiles for eight participants following transcranial magnetic stimulation (TMS) over the anterior intraparietal sulcus (aIPS), adapted from Tunik et al. (2005). The figure illustrates hand aperture trajectories during a precision grasping task under perturbed (solid lines) and unperturbed (hatched lines) conditions. TMS was applied either early (blue lines) or late (red lines) relative to the onset of object perturbation. Vertical markers indicate the timing of early stimulation (T1), late stimulation (T2), and motor rotation onset (M). Insets show each subject's reconstructed 3D brain image with the targeted stimulation site (white dot) over aIPS. The results demonstrate that early TMS over aIPS selectively disrupts grasp adjustment in response to unexpected object changes, without affecting reach kinematics. This provides causal evidence for the role of aIPS in memory-guided, goal-dependent grasp shaping. (Tunik et al., 2005).

Beyond the persistence of single-neuron firing, population-level analyses reveal that AIP activity is not homogeneous across time or cells. Temporal dynamics within the delay period indicate a gradual evolution from stimulus-related to action-related encoding (Michaels et al., 2016), while functional diversity across the neuronal ensemble points to partially specialized subpopulations, some preferentially representing object identity, others modulated by contextual or preparatory variables (Maranesi et al., 2024). This internal heterogeneity may reflect a differential engagement of neural populations within AIP, where distinct circuits operate over different temporal scales to preserve and transform grasp-relevant information. Such organization could provide the flexibility required to link perceptual and motor representations as task demands evolve.

From a mechanistic perspective, computational and physiological models propose that recurrent interactions among excitatory and inhibitory neurons can sustain neural activity in parietal circuits even in the absence of external input (Compte et al., 2000; Wang, 2001). More recent models emphasize the importance of network microarchitecture, specifically, the presence of highly connected excitatory “hub” neurons, in shaping the persistence and stability of delay-period activity (Yu et al., 2024) (Figure 17). In AIP, such cellular and synaptic heterogeneity may provide the local substrate through which distributed influences are selectively integrated, allowing specific functional units to couple transiently with different nodes of the grasping network (Caminiti et al., 2017).

.

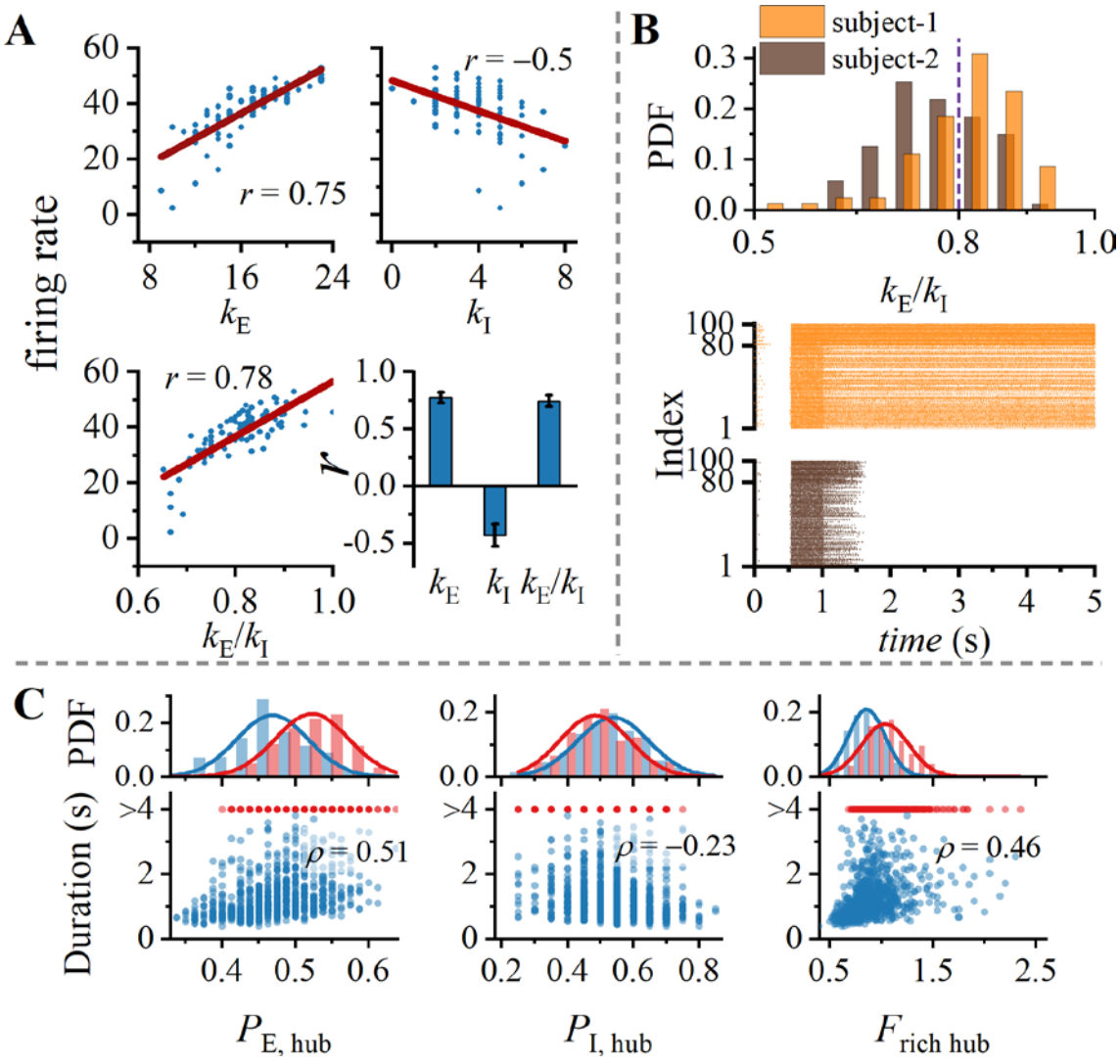

Figure 17. Rich hub connectivity regulates the duration of working memory activity during the delay period. This figure illustrates how the structural properties of local neural networks, specifically the presence of highly connected excitatory neurons (rich hubs), modulate the persistence of neural activity during the delay period in a working memory (WM) task. (A) shows that neurons with a higher ratio of excitatory to inhibitory inputs (E/I ratio) exhibit stronger and longer-lasting firing rates during the delay. This suggests that local input balance influences delay-period activity at the single-neuron level. (B) compares two networks with different E/I input distributions. The spike raster plots reveal that networks with stronger excitatory hubs maintain more sustained activity during the delay. (C) quantifies the relationship between WM duration and hub strength, showing significant correlations between delay-period persistence and the presence of rich excitatory hubs. Figure from (Yu et al., 2024).

Collectively, the evidence suggests that AIP's role in memory-guided grasping extends beyond any uniform or purely local computation. Its contribution seems to emerge from the interplay of evolving neural dynamics, partially specialized representations, and flexible inter-regional interactions, features that challenge region-

centric models and call for a broader systems-level perspective. Clarifying how local and distributed processes interact will be crucial for defining the mechanisms that sustain stable yet adaptable goal-directed behavior across variable sensory contexts, and for understanding how the grasping network supports the flexibility of natural sensorimotor control in complex real-world environments, challenges it has evolved to overcome.

2 AIMS OF THE STUDY

Building on current evidence of the parieto-frontal contribution to visuomotor transformations, we hypothesize that memory-guided grasping engages internal mechanisms within the extended grasping network that also support visually guided actions. As discussed, previous studies have particularly highlighted AIP's involvement in grasp execution without concurrent sensory feedback, suggesting its role as a hub for integrating object-related information across perceptual contexts. However, the specific contribution of AIP and its functional interplay with premotor regions lacks systematic characterization, particularly with respect to the temporal coding mechanisms and inter-area dynamics that support action-related representations in the absence of visual input.

Clarifying the neural mechanisms underlying sensorimotor transformations under conditions of perceptual variability is therefore a critical goal for ongoing research. Such knowledge has important implications for both basic neuroscience and translational applications, including the design of neural prosthetics and rehabilitation strategies. Addressing this challenge requires a fine-grained, comparative approach that links temporal coding dynamics, cell-type specific contributions and inter-area coordination within the extended grasping network.

Within this framework, the present study aims to systematically characterize how key regions of the extended grasping network (AIP, F5, F2, and F6) encode object features and motor plans during both visually guided and memory-guided grasping. To this end, we recorded single-unit activity in macaques performing a randomized delayed grasping task under both conditions. This design allows us to identify shared and divergent coding strategies across areas and contexts, and specifically to:

- Determine how parieto-frontal areas encode object information across sensory- and memory-driven contexts throughout different phases of the grasping action.

- Assess the relative contributions of parietal and frontal regions to the neural processes underlying memory- and visually guided transformations.

- Examine whether memory-guided grasping depends on functionally distinct neuronal subpopulations (e.g., cell-type specificity) or instead reflects a distributed reorganization of activity within each area.

By combining single-neuron resolution with a comparative analysis across cortical regions, this study aims to identify the functional properties that enable sensorimotor transformations during memory-guided manual actions. These findings will provide new insight into how the extended grasping network supports goal-directed behavior in the absence of visual input, and will lay the groundwork for integrative models of distributed sensorimotor coordination.

3 MATERIALS AND METHODS

3.1 SUBJECTS AND SURGERIES

Three socially housed adult macaques participated in the experimental procedures: Mk1 (*Macaca nemestrina*, male, 9 kg), Mk2 (*Macaca mulatta*, male, 7 kg), and Mk3 (*Macaca mulatta*, female, 4 kg). Prior to data acquisition, all animals underwent a habituation phase, during which they were progressively trained to sit in a primate chair and interact with human experimenters. Using positive reinforcement protocols, the animals were trained to perform a visuomotor task (VMT) with the hand contralateral to the hemisphere from which recordings were obtained, following procedures described in previous work (Bonini et al., 2014b; Lanzilotto et al., 2016, 2019).

Once behavioral training was completed, a custom-designed head fixation system and a plastic recording chamber were surgically implanted. Depending on the recording approach, chronic multielectrode arrays were permanently implanted in targeted cortical areas, or acute multielectrode probes were inserted through the chamber during recording sessions. Surgical interventions were performed under general anesthesia, using intramuscular injections of ketamine hydrochloride (5 mg/kg) and medetomidine hydrochloride (0.1 mg/kg), and were followed by appropriate postoperative care, including analgesic administration. Surgical techniques followed protocols described in previous works (Bonini et al., 2014a; Barz et al., 2017; Ferroni et al., 2017).

All experimental procedures were conducted in accordance with the European Directive 2010/63/EU and Italian legislation (D.lgs. 26/2014) on the protection of animals used for scientific purposes. The protocols received approval from the Animal Welfare Body of the University of Parma and were authorized by the Italian Ministry of Health.

3.2 APPARATUS AND BEHAVIORAL PARADIGM

During the VMT, each monkey was seated in a primate chair positioned in front of a custom-designed behavioral apparatus (Figure 20A), originally inspired by paradigms developed by Sakata and colleagues (Murata et al., 1996, 1997, 2000; Raos et al., 2006). The apparatus was horizontally divided into two sectors by a semi-reflective half-mirror. The upper sector housed a small black tube with an embedded white LED, which, when illuminated in complete darkness, projected a light spot onto the half-mirror. Due to optical reflection, this light appeared to the monkey as a fixation point aligned with the center of mass of the object positioned behind the mirror in the lower, non-visible sector. The lower compartment contained a motorized sliding platform that sequentially presented one of three different graspable objects through a 7 cm opening centered on the monkey's sagittal plane, and within reaching distance from its hand starting position. The object was always presented at the same fixed spatial location and distance from the hand starting position, such that object identity and the associated grip configuration, but not reach direction or movement extent, varied across trials. The objects consisted of: a ring, affording a hook grip involving insertion of the index finger into the ring; a small cone, requiring a lateral (side) grip achieved by opposing the thumb to the side of the index finger; and a large cone, affording a whole-hand prehension involving opposition of all fingers to the palm. These grip types were chosen based on their natural prevalence in macaque motor repertoire (Macfarlane & Graziano, 2009). Illumination of the lower sector was controlled by a strip of white LEDs, allowing visibility of the object only during specific task phases. Importantly, due to the optical setup, the fixation point remained perceptually aligned with the object even during its illumination. This optical configuration ensured that the gaze direction and spatial reference remained constant across light and dark conditions, minimizing potential visuospatial confounds.

Each trial began when the monkey placed its hand on a designated starting location. A variable intertrial interval ranging from 1 to 1.5 seconds preceded the onset of each new trial. The VMT comprised three randomized trial types (Figure 20B): grasping-in-the-light (light), grasping-in-the-dark (dark), and inaction trials (no-go condition). All trials required the animal to maintain its gaze on the fixation point.

Light trials: Following the appearance of the fixation point, the monkey had 1.2 seconds to initiate fixation. Successful fixation triggered a high-frequency auditory cue (1200 Hz

sine tone) signaling that a grasping trial was underway. After 0.8 seconds, the lower sector was illuminated, making the object visible. Following a variable delay period (0.8–1.2 s), cessation of the tone served as the go-signal, instructing the monkey to reach, grasp, and pull the object within 1.2 seconds, and to maintain the grip for at least 0.8 seconds. During grasping-in-the-light trials, full visual feedback was available throughout the movement.

Dark trials: These trials followed the same structure as grasping-in-the-light trials up to the go-signal. However, at the time of tone cessation, the light in the lower sector was turned off, requiring the monkey to execute the reaching and grasping movement in darkness. The fixation point remained visible throughout the trial, providing a spatial reference. Crucially, since grasping-in-the-light and grasping-in-the-dark trials were indistinguishable up to the go-signal, the preparatory processes were identical, isolating the effect of visual feedback on movement execution.

No-Go trials: These no-go trials matched the timing of go trials but were signaled by a low-frequency auditory cue (300 Hz sine tone) upon fixation. After the object was illuminated and subsequently extinguished (as in go trials), the monkey was required to withhold movement and maintain fixation for 1.2 seconds to receive a reward. No-Go trials allowed dissociation of neural activity related to action planning and visual processing from that related to actual motor output, and served as a perceptual-motor control condition minimizing working-memory demands.

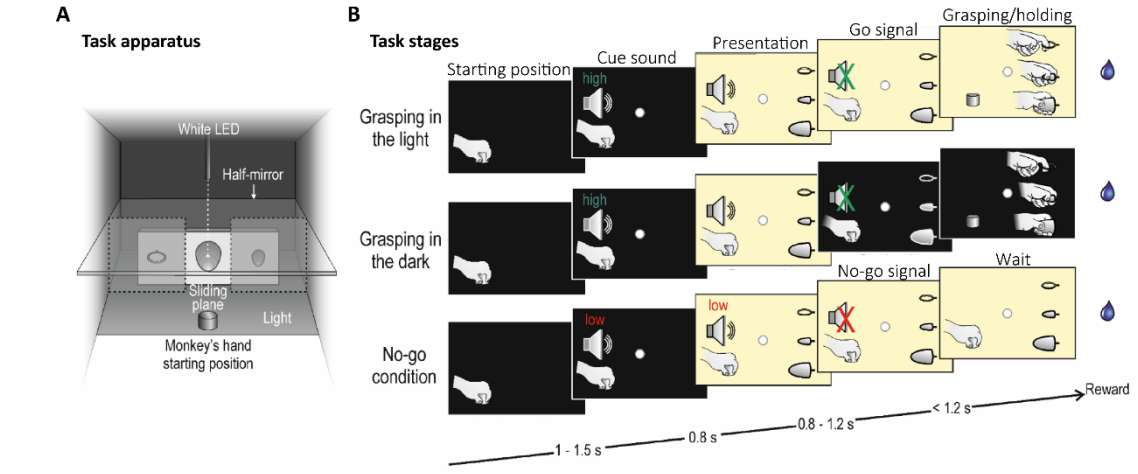

Figure 20. Apparatus and experimental design of VMT. (A) Experimental setup used for VMT execution. (B) Sequence of task phases for the grasping-in-the-light, grasping-in-the-dark conditions and object fixation. (Adapted from Bonini et al., 2014b).

To be considered valid, each trial required the animal to initiate and execute (or correctly withhold) the required movement within the specified temporal parameters. Trials were automatically aborted and excluded from analysis in the event of fixation break, incorrect movement execution, or failure to meet timing criteria, resulting in no reward delivery. Successful completion of a trial was consistently followed by administration of a liquid reward via a pressure-controlled delivery system (Crist Instruments, Hagerstown, MD), with equal reward volumes across all conditions. For each object and experimental condition, a total of 12 correctly executed trials were acquired.

3.3 RECORDING OF BEHAVIORAL EVENTS AND DEFINITION OF EPOCHS OF INTEREST

Behavioral monitoring during the task was performed using multiple contact-sensitive devices (Crist Instruments), which detected when the monkey's grounded hand made contact with the metallic surface of the start button or one of the target objects. An additional sensor was connected to a switch located behind each object, signaling the onset and sustained phase of object pulling. Each device provided a TTL signal, integrated into a LabView-based software platform responsible for real-time tracking of the animal's behavior. This software also controlled the generation and presentation of auditory and visual cues, managed reward delivery, and monitored behavioral errors such as fixation breaks.

Eye position was continuously recorded in parallel using a 50 Hz charge-coupled device (CCD) video camera (Ganz, F11CH4) equipped with an infrared filter and paired infrared light sources. The analog signals encoding horizontal and vertical eye positions were fed into a dedicated software system (Pupil) for calibration and preprocessing. The monkey was required to maintain gaze within a 5° radius around the fixation point throughout the task, minimizing potential confounds related to eye movements (Maranesi et al., 2013). Eye position data were monitored in real time by the same LabView software controlling the behavioral paradigm.

Digital output signals associated with task events, such as auditory and visual stimuli, object identity, reward delivery, and errors, were simultaneously recorded together with TTL signals from the contact devices by the Omniplex system (Plexon), synchronized with electrophysiological data acquisition. These behavioral event markers were

subsequently used to temporally align neuronal activity across trials and conditions, enabling the construction of peri-event time histograms and statistical data matrices.

Neural data analyses focused on five specific task epochs: *(1) Baseline*, defined as the 400 ms preceding object presentation, during which the monkey remained stationary with its hand on the start position while maintaining fixation. At this point, the trial type (go vs. no-go) was already signaled, allowing for the assessment of anticipatory neural modulations related to preparatory cognitive and motor processes in a stable behavioral context; *(2) Object presentation*, from 0 to 400 ms following the onset of object presentation; *(3) Premovement*, defined as the 400 ms preceding the go-signal (e.g., sound off); *(4) Movement*, from 0 to 400 ms after manipulum release onset; and *(5) Object pulling*, covering the 400 ms during the active phase of object pulling.

3.4 RECORDING TECHNIQUES AND SPIKE SORTING

Neuronal activity was recorded using linear multielectrode silicon probes arranged either as single-shaft arrays or in three-dimensional configurations. Two types of probes were used: 16-channel U-probes (Plexon) and 16-channel silicon probes manufactured by Atlas Neuroengineering (Herwik et al., 2009; Ruther et al., 2010). The U-probes had a diameter of 185 μm, with circular recording sites 15 μm in diameter, spaced 250 μm apart, and an impedance between 0.3 and 1 MΩ at 1 kHz. Atlas probes had a rectangular cross-section (140 μm × 100 μm), with 35 μm diameter recording sites, also spaced 250 μm apart, and an impedance ranging from 0.5 to 1.5 MΩ.

All recordings were performed transdurally using a manually controlled stereotaxic micromanipulator mounted on the recording chamber, with penetrations orthogonal to the cortical surface and an average insertion angle of ~40° relative to the sagittal plane. U-probes were inserted through a stainless-steel guide tube, which was first lowered to gently press on the dura, producing a dimpling of approximately 3–4 mm. The probe was then rapidly inserted through the guide tube so that about half of the recording sites entered the cortex, after which the tube was retracted to rest lightly on the dura, minimizing mechanical pulsations while maintaining optimal stability (Bonini et al., 2014b). Atlas probes, by contrast, were inserted using a dedicated vacuum-based insertion system (Bonini et al., 2014a). The probe was temporarily fixed to a custom insertion tool via a flexible polyimide cable and vacuum pump, allowing precise and stable advancement through the intact dura. The topmost recording site was left just outside the

cortex to serve as a reference, and the probe was then released to float within the tissue, ensuring mechanical decoupling from brain pulsations and long-term recording stability. This procedure typically required less than 10 minutes (Figure 21A).

Recordings were grounded either to the guide tube (U-probes) or the head-holding system (Atlas probes), and referenced to the most proximal recording site, placed subdurally but external to the cortex to reduce artifacts and maximize signal-to-noise ratio (Figure 21B). For acute recordings, neuronal activity was typically acquired after a stabilization period of approximately 30 minutes following insertion.

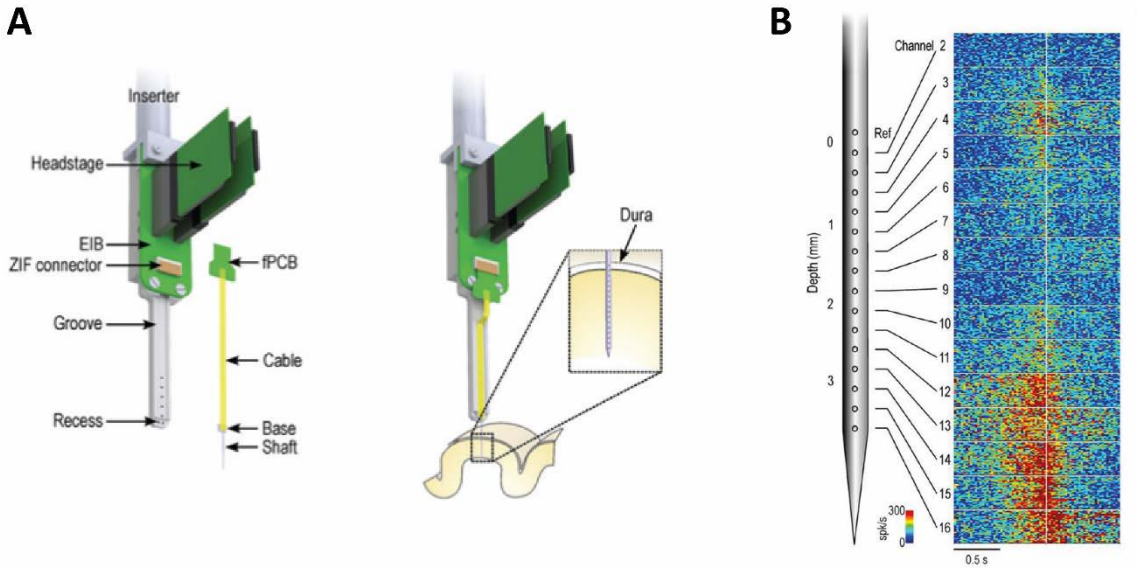

Figure 21. Atlas probe insertion system and example of multiunit activity in area F5. (A) Schematic reconstruction of the probe insertion system for Atlas probes. Left: Vacuum insertion tool carrying an electrode interface board (EIB) with two commercial headstages and a ZIF connector interfacing the flexible printed circuit board (fPCB) attached to the probe cable. The yellow ribbon cable is longer than the distance between inserter tip and connector, allowing slight retraction of the inserter after probe insertion to leave the probe floating. Right: Probe attached to the inserter with vacuum active, enabling insertion but not floating. Inset shows the topmost electrode (electrode 16), placed subdurally just outside the cortex as a reference. (Adapted from Bonini et al., 2014a). (B) Schematic of a linear multielectrode probe and example of multiunit activity simultaneously recorded from 15 channels during a representative F5 penetration. Activity is color-coded and aligned (white line) to object pulling onset in the visuomotor task (45 pooled trials). Stronger modulations were observed in deeper sites, consistent with recordings from the crown and posterior bank of the inferior arcuate sulcus. (Adapted from Bonini et al., 2014b).

The probes were implanted in various cortical regions (Figure 22A), either chronically or acutely, depending on the target area. Chronic implants were performed in the anterior intraparietal area (AIP; Lanzilotto et al., 2019; 2020; Maranesi et al., 2024) and the pre-supplementary motor area F6 (Albertini et al., 2020; Lanzilotto et al., 2016; Livi et al.,

2019), while acute recordings were carried out in premotor areas F5 (Bonini et al., 2014c; Ferroni et al., 2021) and F2 (Albertini et al., 2021). Implantation trajectories were guided by MRI reconstructions of individual brain anatomy to optimize targeting (Figure 22B).

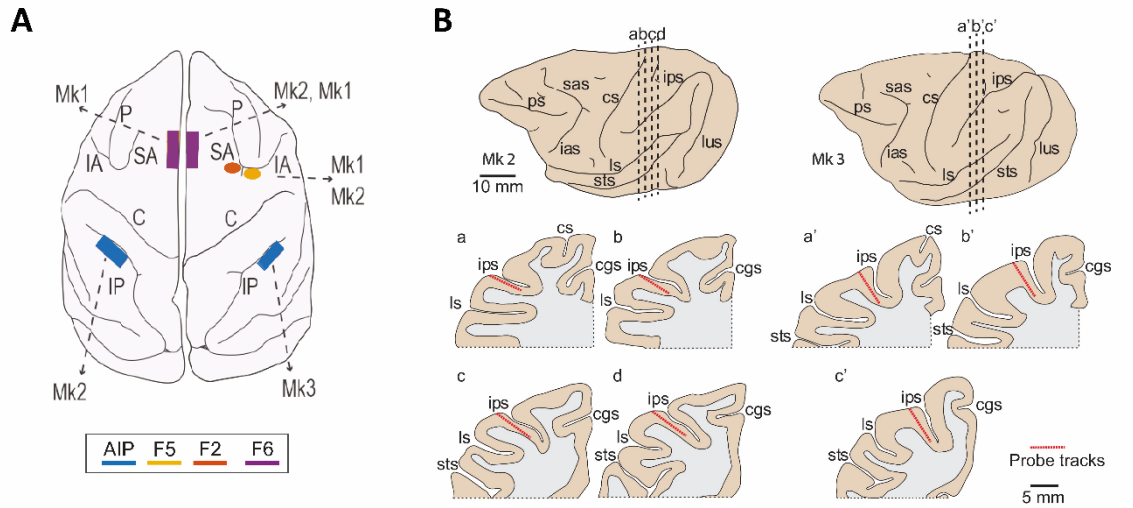

Figure 22. Cortical recording areas and example of probe trajectories in AIP. (A) Distribution of cortical recording sites across the three monkeys. (B) Example of reconstruction of chronically implanted probe trajectories in AIP along the intraparietal sulcus in monkeys Mk2 and Mk3. Dashed vertical lines indicate the entry points of each probe, whose paths are shown in the corresponding coronal sections below (a – d for Mk2; a′ – c′ for Mk3). Anatomical landmarks: Cgs, cingulate gyrus; cs, central sulcus; ias, inferior arcuate sulcus; ips, intraparietal sulcus; ls, lateral sulcus; lus, lunate sulcus; ps, principal sulcus; sas, superior arcuate sulcus; sts, superior temporal sulcus. (Adapted from Lanzilotto et al., 2019).

Postmortem histological reconstruction confirmed the localization of electrode penetrations (Lanzilotto et al., 2016) (Figure 23).

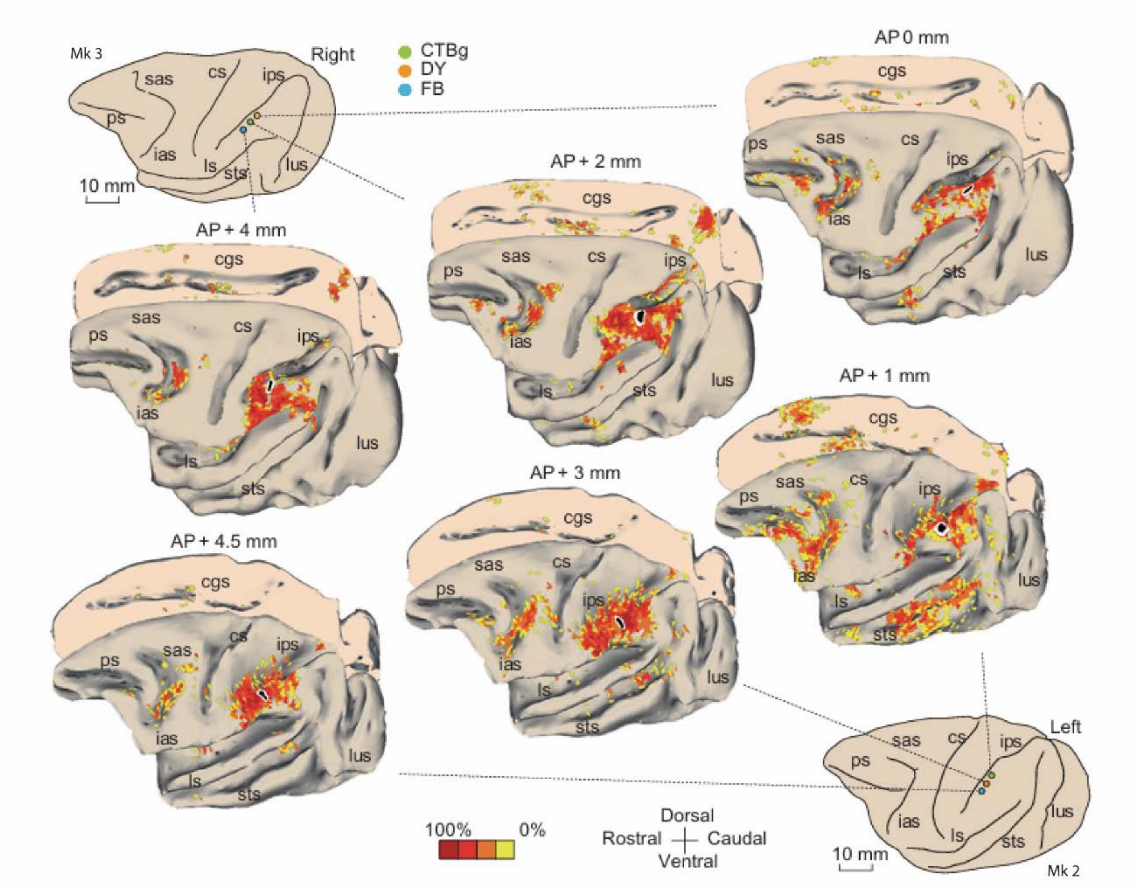

Figure 23. Example of retrograde labeling patterns in area AIP following tracer injections. Three-dimensional anatomical reconstructions illustrating the cortical distribution of retrogradely labeled cells after tracer injections at rostral (left), intermediate (center), and caudal (right) levels of area AIP in M3 (top) and Mk2 (bottom). These maps provide representative postmortem histological evidence supporting the localization of recording sites in AIP. For comparison, Mk3 data (right hemisphere) were mirrored to appear as left hemispheres; mesial surfaces are shown as right hemispheres. Color scale indicates relative density of labeled cells (600×600 μm² bins), expressed as a percentage of the peak labeling for each injection. Cgs, cingulate sulcus; other abbreviations as in Figure 22. (Adapted from Lanzilotto et al., 2019**)**

Signals from acute recordings were amplified and digitized at 40 kHz using a 16-channel Omniplex system (Plexon), while signals from chronic recordings were acquired at 30 kHz with the OpenEphys acquisition system using four 32-channel Intan amplifier boards.

Spike detection and sorting were performed offline using the MountainSort framework (Chung et al., 2017). Candidate spikes were extracted using a threshold of –3.0 standard deviations from the baseline noise. Clusters were classified based on the noise overlap metric, which quantifies the percentage of noise-like events within a cluster; units with a noise overlap below 0.1 were considered well-isolated single units.

To refine the quality of spike waveforms and eliminate outliers, a multi-step curation

procedure was applied. Spikes deviating more than ±3 standard deviations from the unit's average waveform were removed, typically eliminating about 10% of waveforms per unit. Waveforms were aligned to their negative peak within a 3-ms window and then spline-interpolated to a standardized length of 1,000 data points to allow for comparisons across probes and acquisition systems. Final validation of single-unit isolation was based on established criteria, including the presence of a clear refractory period (>1 ms), lack of cross-correlation with other units, and an inter-spike interval distribution consistent with single-neuron firing.

3.5 DATA ANALYSIS

All analyses were conducted using custom-developed scripts written in MATLAB R2024b, supplemented by MATLAB- and Python-based toolboxes.

3.5.1 Behavioral performance analysis

To assess behavioral performance across conditions, we conducted a three-way mixed-design ANOVA on reaction time (RT) and reaching–grasping time (RG), with Monkey as a between-subject factor and Object (ring, small, big) and Condition (light, dark) as within-subject factors. RT was defined as the interval between the go cue (SoundOff) and the onset of movement (MovOn, corresponding to the release of the resting manipulandum), whereas RG time corresponded to the movement duration from MovOn to object contact. The analysis was restricted to correct trials and was based on mean RT and RG values computed for each monkey, object, and condition across recording sessions. Prior to analysis, data distributions were inspected for normality and potential outliers. All values were expressed in seconds. Statistical analyses were performed in MATLAB R2024b using the *fitrm* and *ranova* functions. Main effects and interactions were examined for each dependent variable, and Greenhouse–Geisser–corrected *p*-values were reported when necessary. Interindividual variability was examined to verify that the direction of behavioral effects was consistent across monkeys. This analysis was designed to determine whether the absence of visual feedback (dark condition) influenced movement initiation and execution times, and to ensure that any differences observed in neural dynamics could not be attributed to behavioral variability across subjects.

3.5.2 Cross- decoding analysis

To jointly assess the role of each cortical area examined during grasping actions in light and dark conditions, and to investigate the neural encoding of observed objects throughout the different phases of the VMT across both modes, we employed a population decoding framework. This analysis was limited to trials in which the monkey performed correctly.

The decoding approach was based on cross-decoding, relying on a generalization framework as described by Meyers (2013) and previously implemented in prior works (Lanzilotto et al., 2020; Livi et al., 2019). Specifically, a Poisson naïve Bayes classifier was trained on neural data from 11 labeled trials per object, recorded during one of four task epochs: baseline, premovement, reaching/grasping, and holding. The classifier was then tested either on a trial excluded from the training set within the same epoch or on a trial from a different epoch. This method was designed to evaluate the degree to which the classifier, trained to decode object identity in one epoch, could generalize to decode the same objects during a different epoch. Such cross-decoding allowed us to probe the stability of object tuning and to identify shared neural coding schemes across distinct task phases and conditions.

3.5.3 Cross-validation procedure

The algorithm followed a cross-validation pipeline with the following steps:

1) Data preprocessing: Data from each neuron and cortical region (135 neurons from AIP, 136 from F5, 67 from F2, and 213 from F6) were converted from spike raster format into binned firing rates. These bins averaged neural activity over 400 ms, matching the duration of the four task epochs under study. Large bins were chosen to reduce noise and enhance decoding accuracy. For each neuron, 12 trials per stimulus (three stimuli total) were randomly selected. Neural responses from all neurons in a given region were concatenated to form pseudo-population vectors (simulated population responses combining neurons recorded in separate sessions under identical stimulus conditions). For example, 135 AIP neurons yielded 36 data points (12 trials × 3 stimuli) in a 135-dimensional space. *2) Data splitting:* Pseudo-population vectors were partitioned into 12 splits, with each split containing one response vector per stimulus. *3) Normalization*: Prior to classification, z-score normalization was applied to both training and test datasets. The

mean and standard deviation for each neuron (feature) were calculated from the training set and used to normalize both datasets. This step prevented neurons with high firing rates from disproportionately influencing the classifier. *4) Training and testing:* The classifier was trained on 11 splits (33 training data points) and tested on the remaining split (3 test data points). *5) Cross-validation*: This leave-one-split-out process was repeated 12 times so each split served once as a test set. *6) Performance evaluation:* Classification accuracy was computed per split and then aggregated. *7) Repetition for robustness*: Steps 1–6 were repeated 50 times with different random pseudo-populations and splits to ensure robustness. Final decoding accuracy was obtained by averaging results across all repetitions; chance performance was 33.3% (three objects). Decoding results were visualized as line plots showing average classification accuracy within 400-ms bins for each task epoch. Additionally, cross-temporal decoding was visualized using matrices with 100-ms bins and 50-ms steps to assess dynamic versus static population coding across task epochs and cortical areas.

3.5.4 Sliding-window ANOVA for object selectivity

To assess potential confounding effects of condition- or phase-dependent variations in neuronal selectivity, we quantified the proportion of object-selective neurons over time using a sliding-window ANOVA (SWA). This analysis was conducted to verify whether differences in cross-epoch generalization could be attributed to changes in the strength or timing of single-neuron selectivity rather than to genuine population-level mechanisms.

For each recording site and condition (light and dark), neuronal activity was aligned to two task events: object presentation onset (Light on) and movement onset (Mov on). Firing rates were computed in 100-ms windows sliding in 50-ms steps, and a one-way ANOVA was applied to test the main effect of object across the three task objects ($p < 0.05$, uncorrected). Neurons showing a significant main effect in a given window were classified as object-selective for that time bin. The resulting time series expressed, for each cortical area, the percentage of object-selective neurons across the trial in both light and dark conditions.

This procedure allowed us to characterize the temporal evolution of object selectivity and to directly compare its magnitude and dynamics across visual conditions, ensuring that differences in cross-epoch decoding performance were not driven by variations in basic neuronal tuning strength.

3.5.5 Rank stability analysis

To investigate the temporal consistency of object preference for individual neurons and cortical regions during the light and dark conditions, we conducted a rank stability analysis. For each neuron, the “best” object, defined as the one eliciting the highest normalized neural response during the reaching/grasping epoch, was identified as a reference. We then tracked the rank of this preferred object across the entire trial in 100-ms bins with 50-ms overlap, from baseline through the pulling phase. The stability of object preference was visualized using a color scale: red indicating stable, yellow partially stable, and blue unstable preference. Bins without neural activity significantly different from baseline (assessed via sliding-window ANOVA, 100-ms bins with 50-ms steps, $p > 0.05$ uncorrected) were blanked out and colored white, indicating no significant modulation. This method enabled us to characterize the dynamics of object representation and to identify subpopulations of neurons that contributed differently to stable object coding, especially during grasping in the dark. Neurons were then sorted based on their rank stability and divided into three equally sized subpopulations: Stable, Mixed, and Unstable, to examine how different levels of temporal consistency contributed to object coding during grasping in the dark.

3.5.6 Waveforms analysis

To categorize putative cell types based on extracellular spike waveform features, we applied WaveMAP, an unbiased clustering method recently described by Lee et al. (2021, 2023). WaveMAP integrates (i) UMAP (Uniform Manifold Approximation and Projection), a nonlinear dimensionality reduction technique that preserves local and global data structure in a low-dimensional representation (McInnes et al., 2018), and (ii) Louvain clustering, a graph-based community detection algorithm that groups neurons based on waveform similarity (Blondel et al., 2008).

Before clustering, average waveforms were normalized to emphasize shape over amplitude, reducing confounds from amplitude variability due to electrode distance (Lee et al., 2023). This method effectively identifies distinct cell classes characterized by waveform shape, consistent with opto-response clusters reported in human hippocampal slices (Andrews et al., 2024).

For clustering, WaveMAP was provided with an $N \times M$ matrix, where $N = 551$ neurons

and M = 1000 data points corresponding to 3-ms interpolated waveforms centered on the spike peak (1 ms before to 2 ms after). Neurons from all four cortical regions were combined to enhance clustering performance; this approach allowed waveform clustering to be driven purely by shape similarity, independent of cortical origin, ensuring unbiased classification before regional comparisons.

In addition to waveform clustering, we computed the trough-to-peak latency (TTP) of each average waveform, defined as the temporal delay between the negative trough (aligned at sample 334) and the subsequent positive peak. TTP was converted to milliseconds assuming 334 samples ≈ 1 ms, yielding a precise estimate of spike width. For each cluster, the TTP of the mean waveform was extracted and used to order clusters along a physiologically interpretable axis from narrow- to broad-spiking.

Putative axonal recordings (clusters 9 and 10), characterized by a positive pre-depolarization peak, were excluded from all subsequent analyses to avoid contamination from non-somatic sources (Barthó et al., 2004). The remaining neurons were retained for cross-area comparisons and, in AIP, were further divided into Stable, Mixed, and Unstable subpopulations according to their functional classification. Each neuron retained its functional label when assigned to a given waveform cluster, allowing the direct comparison of cluster composition across stability-defined subpopulations.

Finally, to statistically assess differences in waveform composition across regions and subpopulations, we compared the observed distribution of neurons across WaveMAP clusters against the expected distribution under the null hypothesis of equal proportions. χ^2 tests were therefore computed using real observed and expected counts per cluster, both for fine-grained cluster assignments and for the coarse narrow/broad classification.

4 RESULTS

Neural activity was recorded from four cortical areas, AIP (n = 135), F5 (n = 136), F2 (n = 67), and F6 (n = 213), across five hemispheres in three macaque monkeys, yielding a total of 551 single neurons (Table 1), all tested in both visual and memory-guided grasping conditions.

	AIP	F5	F2	F6
Mk1	—	68	22	74
Mk2	26	68	45	139
Mk3	109	—	—	—
Tot	**135**	**136**	**67**	**213**

Table 1. Distribution of isolated single units across recorded areas and individual monkeys

Behavioral performance was assessed in terms of reaction time (RT) (Figure 24A) and reaching–grasping time (RG) (Figure 24B). We carried out separate three-way mixed-design ANOVAs, including *Monkey* as a between-subject factor and *Object* and *Condition* (light, dark) as within-subject repeated-measures factors, on both reaction and reaching–grasping times. This analysis was used to assess the effects of visual condition and object identity on movement timing, while accounting for interindividual variability. In contrast, reaction times were overall significantly faster in the dark compared with the light condition ($p = 0.00006$), and reaching–grasping times showed a similar pattern ($p = 0.00007$). Both measures also varied with object type (RT: $p = 0.047$; RG: $p = 0.013$). Despite interindividual variability, the direction of these behavioral effects was consistent across monkeys (Figure 24C). These results indicate that, although visual feedback modulated movement timing, grasping actions were accurately and consistently performed in both conditions, likely relying on memory-based representations when vision was unavailable. The consistency of behavioral trends across subjects provides a coherent baseline for interpreting subsequent area-specific neural dynamics.

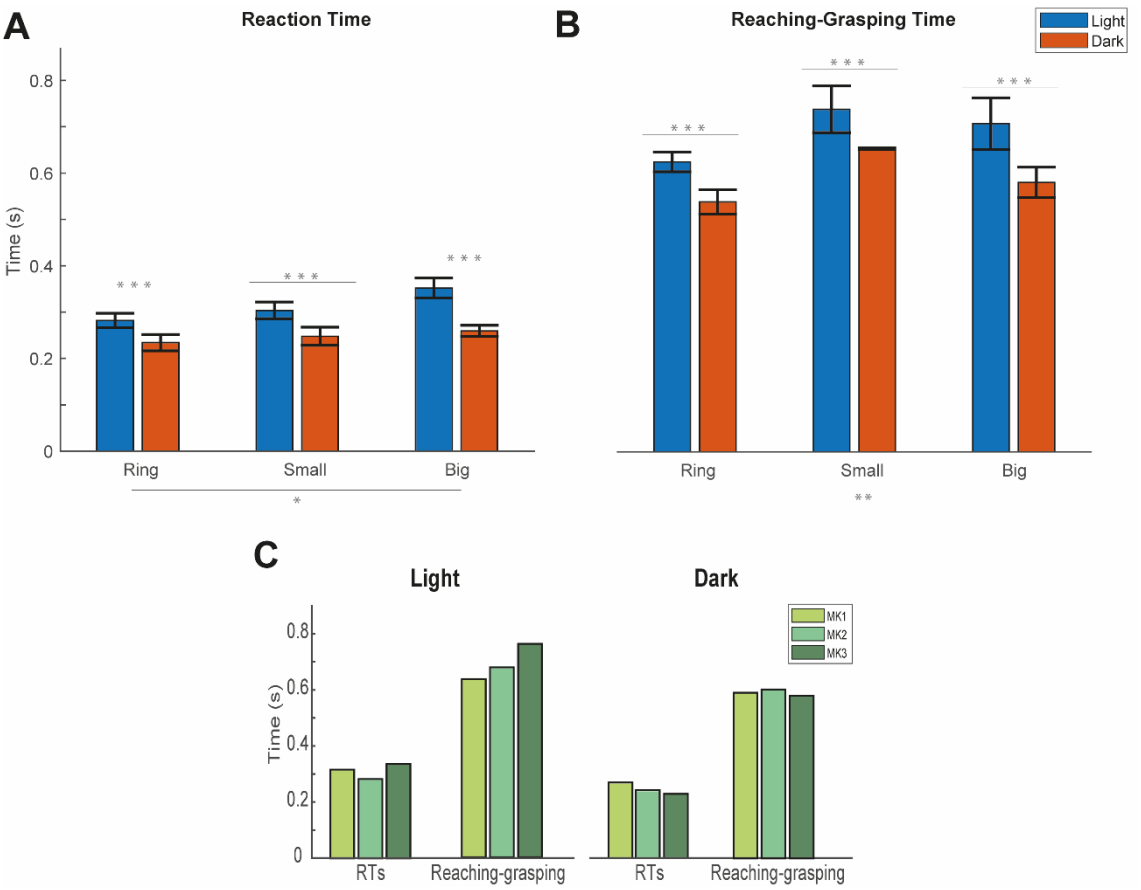

Figure 24. Behavioral performance in light and dark conditions. (A) Mean reaction times (RT) and (B) reaching–grasping times (RG) for each object (ring, small, big) under light and dark conditions. Bars represent mean ± standard error of the mean (SEM) across sessions, averaged across monkeys. Color code: light (blue), dark (orange). Asterisks indicate statistically significant effects as assessed by three-way mixed-design ANOVAs (*p < 0.05, **p < 0.01, ***p < 0.001). (C) Mean RT and RG values shown separately for each monkey, averaged across objects, illustrating interindividual variability while preserving the same overall behavioral trend across conditions. Color code for individual monkeys is indicated in the legend.

4.1 SENSORY- AND MEMORY-DRIVEN CODING OF OBJECTS: A COMPARISON OF PARIETO-FRONTAL AREAS

4.1.1 Cross-temporal generalization in light and dark go conditions

First, we investigated whether neurons in the recorded parieto-frontal areas maintained object-specific activity across different task epochs, and how this persistence differed between light and dark conditions. To this end, we performed a population cross-decoding analysis using a Bayesian classifier (Meyers, 2013), trained and tested across all combinations of task epochs (object presentation, premovement, movement, and pulling). This analysis tested whether the population code generalized across different task epochs, specifically whether object-related information was preserved over time. We then

compared this temporal generalization between light (Figure 25A–D) and dark (Figure 25E–H) conditions to determine how the availability of visual input influenced the stability of population coding.

In the light condition (Panels A–D), all areas showed clear within-epoch decoding, indicating robust object selectivity under visual guidance. When the classifier was trained on neural activity during the presentation phase (Panel A), decoding accuracy peaked for tests within the same epoch and partially generalized to the premovement and movement phases, particularly for AIP, F5, and F2. This pattern suggests that visual object information was preserved across the transition from perception to early motor planning. When training was performed on premovement activity (Panel B), decoding remained high when tested on movement, confirming temporal continuity between consecutive phases of the action. Training on the movement epoch (Panel C) produced a similar profile, with AIP and F5 showing the strongest generalization backward toward premovement, implying partial bidirectionality of the visual–motor code under full-vision conditions. However, when classifiers were trained on the pulling phase (Panel D), decoding accuracy dropped substantially across all areas, indicating a reorganization of neural activity following object contact and the emergence of feedback-related signals.

In the dark condition (Panels E–H), overall accuracy decreased, but the temporal organization of object coding changed markedly. When the classifier was trained on the presentation epoch (Panel E), AIP stood out for maintaining significant generalization to the movement phase, whereas decoding in F5, F2, and F6 rapidly declined. This indicates that AIP selectively maintained stronger and more consistent generalization from presentation to movement than F5, F2, and F6, thus preserving an object-specific code that bridged the visual and motor domains even in the absence of visual input. The same stability was evident when the classifier was trained on movement activity (Panel G) and tested backward on the presentation epoch, showing that the AIP code was shared between sensory and motor formats. In contrast, the premotor areas (Panels F and G) exhibited limited cross-epoch generalization, consistent with a stronger dependence on visual feedback for maintaining stable representations. Finally, during the pulling epoch (Panel H), decoding accuracy was low and comparable across all areas, reflecting a common influence of somatosensory feedback during object contact.

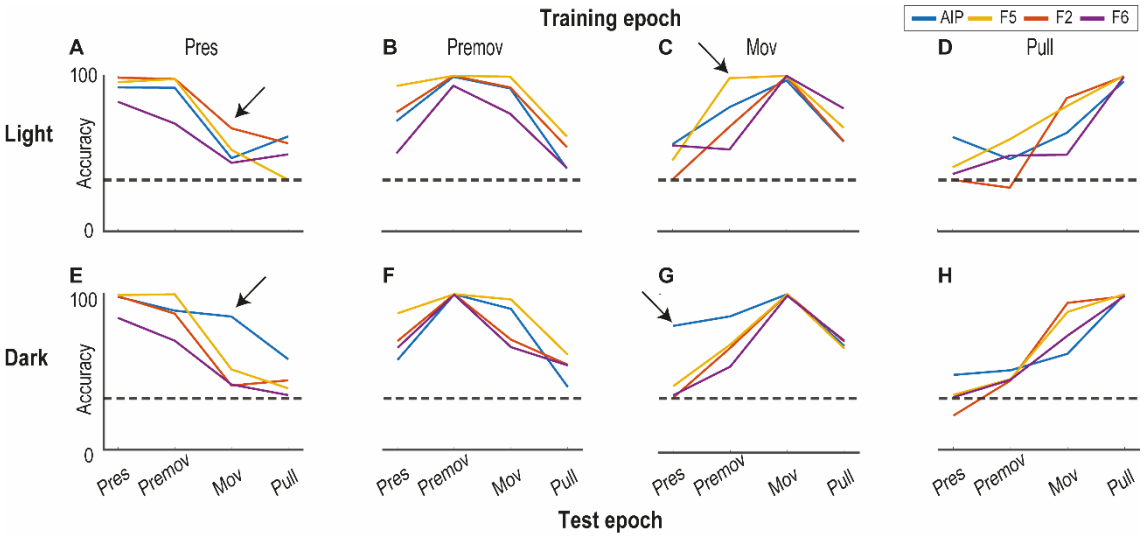

Figure 25. Cross-Decoding Accuracy Across Grasping Epochs in Light and Dark Conditions. Population cross-decoding analysis showing classification accuracy across training and test epochs of the grasping task for the visually guided (Panels A–D) and memory-guided (Panels E–H) conditions. Each panel corresponds to a specific training epoch: Presentation (A, E), Premovement (B, F), Movement (C, G), and Pulling (D, H). Test epochs are shown along the x-axis. Lines represent decoding accuracy for each cortical area, color-coded as indicated in the legend. Arrows indicate training–test epoch combinations relevant for evaluating the persistence and transfer of object-related representations across distinct task phases, as discussed in the text.

Taken together, the figure shows that, while in the light condition (Panels A–D) several parieto-frontal areas contributed to maintaining object-related information across consecutive task phases, in the dark condition (Panels E–H) this ability was largely confined to AIP. AIP uniquely preserved a stable population code linking object perception and movement execution when visual feedback was unavailable, highlighting its key role in sustaining object-specific representations when grasping movements rely on memory rather than visual guidance. In both conditions, decoding performance consistently declined during the pulling phase, reflecting the emergence of somatosensory feedback and the corresponding shift from internally maintained to feedback-driven representations at the time of object contact.

4.1.2 Cross-decoding analysis in the nogo condition

To assess whether the stable object coding observed in AIP during Go trials performed in the dark (Figure 25E–H) reflects visuomotor integration or instead sustained visual processing, we applied the same cross-decoding approach to NoGo trials (Figure 26), in which the monkeys fixated the object while refraining from movement execution. In this

condition, neural activity primarily reflects visual and attentional processing, allowing us to evaluate whether object-specific information remains stable over time in the absence of motor output. The analysis followed the same procedure used for the Go trials, employing four time windows of equal duration and aligned to comparable task epochs: Object presentation (Panel A), Early fixation (Panel B), Late fixation (Panel C), and Final fixation (Panel D). Each panel shows classification accuracy when the Bayesian classifier was trained on one epoch and tested across all others, as in the Go condition.

As shown in Panel A, decoding accuracy was highest during the object presentation phase and generalized modestly to Early fixation (Panel B), indicating consistent representation of object identity during the initial stages of visual processing. When training was performed on Early fixation (Panel B), decoding remained high within the same epoch but declined for later testing windows, suggesting reduced temporal stability as fixation was maintained. Training on the Late fixation phase (Panel C) produced a similar pattern, with strong within-epoch decoding but minimal cross-temporal generalization. In the Final fixation epoch (Panel D), decoding accuracy decreased further across all areas, reflecting the progressive attenuation of object-related activity over time. Across all panels, AIP (blue line) displayed slightly higher and more stable decoding accuracy than the premotor regions, with a flatter temporal profile. Compared to the Go condition, where AIP maintained robust generalization between presentation and movement epochs in the absence of visual input (Figure 25E,G), its stability here most likely reflects a purely visual persistence rather than a visuomotor transformation, as no motor planning or somatosensory feedback occurred.

Taken together, these results show that during NoGo trials, object representations were mainly confined to the early visual epochs and gradually decayed over time. AIP exhibited relatively sustained but visually driven coding, whereas premotor regions showed more transient activity. The absence of cross-epoch generalization comparable to that observed during memory-guided grasping (Figure 25E–H) confirms that AIP’s temporal stability in the dark reflects memory-driven visuomotor mechanisms rather than sustained visual processing.

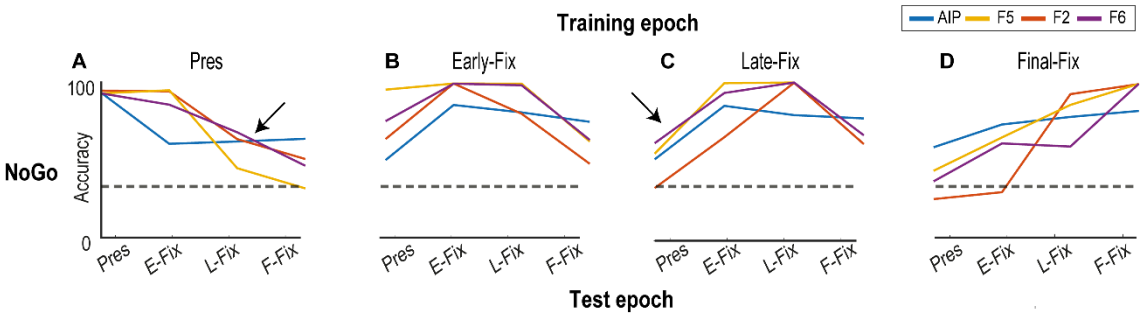

Figure 26. Cross-temporal decoding accuracy in the NoGo condition. Population cross-decoding analysis for NoGo trials, in which the monkeys maintained fixation on the object without executing a movement. Four time windows comparable to the epochs of the Go trials (Figure 25) were used for training and testing: Object presentation (Pres A), Early fixation (Early-Fix B), Late fixation (Late-Fix C), and Final fixation (Final-Fix D). Each panel corresponds to a specific training epoch, with test epochs shown along the x-axis. Lines represent decoding accuracy for each cortical area, color-coded as indicated in the legend. Arrows indicate training–test epoch combinations relevant for evaluating the temporal persistence of object-related representations across fixation phases, and for qualitative comparison with the corresponding decoding patterns observed in the Go condition, as discussed in the text. The figure shows that object-related information was primarily sustained during the early visual epochs, with AIP exhibiting greater temporal stability than premotor regions but lacking the visuomotor generalization observed in the Go condition.

4.1.3 Object selectivity across conditions

Could the stronger cross-epoch decoding observed in AIP during memory-guided grasping simply result from a higher neuronal object selectivity under dark conditions? To address this question, we quantified the percentage of object-selective neurons over time in both light and dark conditions using a sliding-window ANOVA (main effect: object). This analysis was performed separately for each area, aligning neuronal activity to both object presentation onset (Light on) and movement onset (Mov on).

As shown in Figure 27, the proportion of object-selective neurons increased shortly after object illumination in both conditions, peaking around movement onset. In AIP (Panel A), selectivity emerged rapidly after object presentation and remained relatively constant, with comparable time courses for the light (red) and dark (black) conditions. Notably, AIP showed overall lower selectivity levels compared to the premotor areas, indicating that the enhanced cross-temporal generalization observed under dark conditions (Figure 25E–H) cannot be explained by an increased proportion of tuned neurons. In F5 (Panel B), the proportion of selective neurons rose steeply following object illumination and peaked around movement onset, with almost overlapping curves across conditions. F6 (Panel C) exhibited a similar temporal profile, showing moderate and

sustained selectivity after light onset, again without condition-related differences. F2 (Panel D) displayed a transient increase in selectivity after object presentation, which declined after movement onset; as in the other regions, light and dark traces were largely superimposed.

Taken together, these results indicate that the proportion and temporal dynamics of object-selective neurons were largely consistent across the different perceptual conditions of the task. The enhanced temporal generalization of AIP during memory-guided grasping therefore cannot be attributed to stronger or more sustained single-neuron selectivity, but rather to population-level mechanisms supporting memory-based visuomotor transformations.

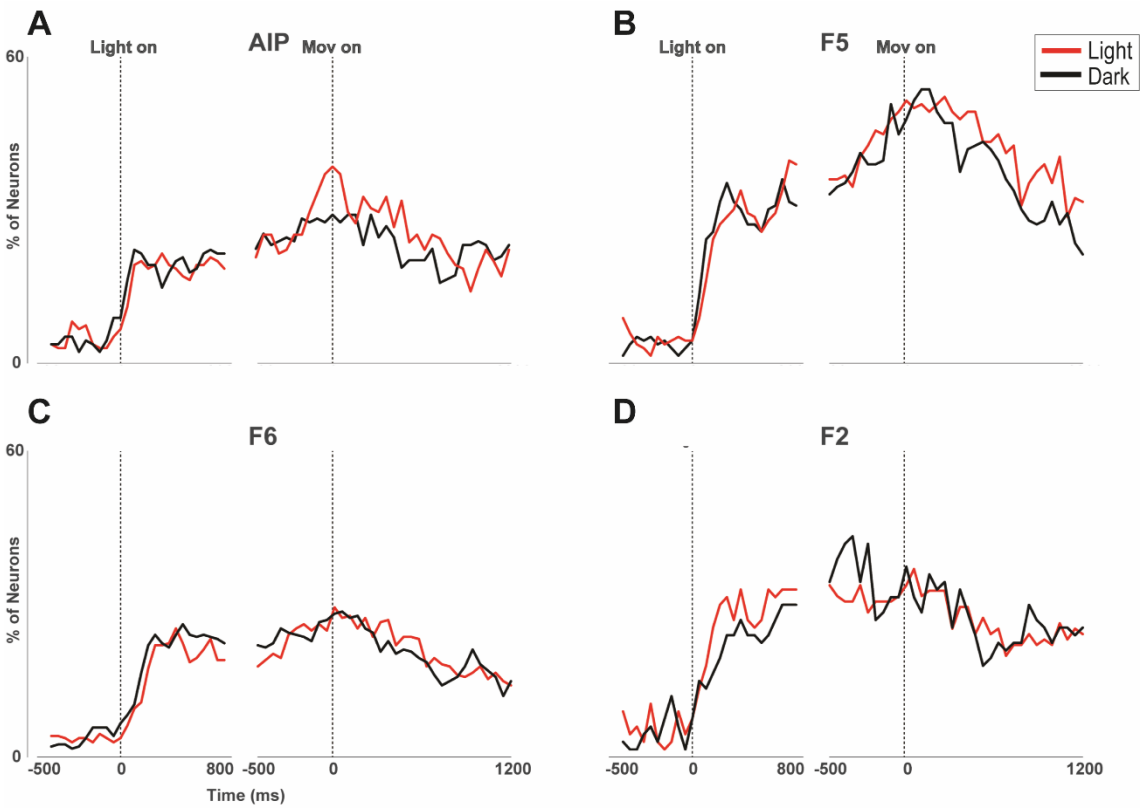

Figure 27. Object Selectivity Over Time Across Light and Dark Conditions. Percentage of object-selective neurons computed with a sliding-window ANOVA (main effect: object) for light (red) and dark (black) conditions. Neural activity is aligned to object presentation onset (Light on) and movement onset (Mov on). A: AIP; B: F5; C: F6; D: F2. The y-axis represents the percentage of selective neurons; the x-axis shows time (ms) relative to alignment points. No systematic differences in selectivity were observed between conditions, indicating that the stronger cross-epoch generalization of AIP in the dark condition (Figure 25) cannot be explained by an increase in the proportion of object-selective units.

4.1.4 Temporal dynamics of neural codes

To further characterize the temporal structure of object representations, we applied a time–time decoding analysis using the same Bayesian classifier framework. Decoding accuracy was computed over successive time bins across the entire task sequence, generating two-dimensional matrices in which training and testing times are plotted on the y- and x-axes, respectively (Figure 28). This approach allowed us to assess how object-specific information evolved over time within each area, distinguishing stable from rapidly changing population codes. In this context, differences across regions are interpreted based on the temporal structure of the decoding patterns, specifically the continuity and extent of high-accuracy regions relative to the diagonal, rather than on absolute accuracy values at individual time points.

In the Light condition (Panels A–D), all areas exhibited high decoding accuracy following object presentation, but the temporal profile of this accuracy differed across regions. F5 (Panel B) showed broad, square-like regions of high accuracy spanning presentation through movement, indicating sustained population coding within this interval. AIP (Panel A) and F2 (Panel C) also displayed extended regions of above-chance decoding, although with somewhat narrower cross-temporal generalization than F5. F6 (Panel D), by contrast, showed a narrow diagonal profile, suggesting a rapidly evolving, time-specific code. In the Dark condition (Panels E–H), overall decoding accuracy decreased across all regions, reflecting the loss of visual input. Nevertheless, distinct temporal profiles emerged across areas. F5 retained broad and temporally extended regions of high accuracy, indicating robust within-phase stability even in the absence of vision. AIP, by contrast, exhibited a more localized but clearly structured cluster linking the object and movement epochs, consistent with a temporally coherent population code that bridges perception and action phases. The continuity of this pattern across adjacent time bins indicates the preservation of a similar representational format over time, rather than isolated peaks of decoding performance confined to single time bins. Thus, while F5 maintained more sustained activity within single task periods, AIP preserved a cross-phase continuity of representation, reflecting its key role in supporting memory-guided visuomotor transformations when visual feedback is unavailable. F6 remained predominantly dynamic, and F2 showed intermediate temporal stability modulated by visual input.

Taken together, these results reveal complementary coding dynamics across the

grasping network. While F5 exhibits the most temporally sustained activity within continuous task phases, AIP uniquely preserves cross-phase consistency under memory-guided conditions, supporting the idea that its population code provides a stable link between perception and action when vision is unavailable. F6 maintains a flexible, time-specific coding profile, and F2 shows intermediate dynamics modulated by sensory context.

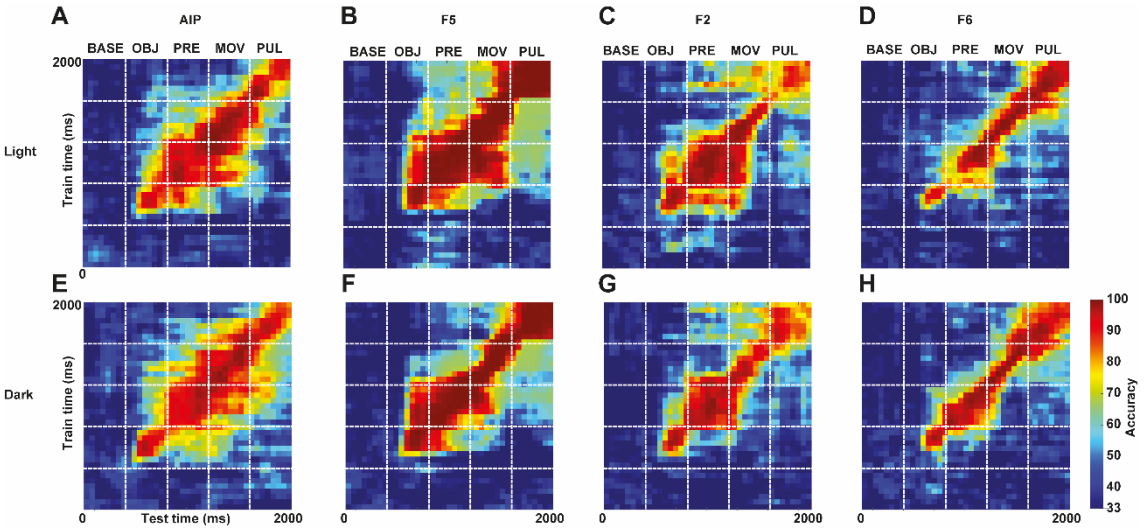

Figure 28. Temporal Evolution of Object Decoding Accuracy Across Light and Dark Condition. Time-resolved decoding matrices showing classification accuracy for light (Panels A–D) and dark (Panels E–H) conditions. Each panel corresponds to a cortical area: A,E: AIP; B,F: F5; C,G: F2; D,H: F6. Training time is shown on the y-axis, test time on the x-axis. Task epochs include Baseline (BASE), Object presentation (OBJ), Premovement (PRE), Movement (MOV), and Pulling (PUL). Decoding accuracy is represented by a color scale ranging from blue (low accuracy) to red (high accuracy). The temporal structure of decoding patterns (specifically the continuity and extent of high-accuracy regions relative to the diagonal) provides information about the stability or dynamism of population codes over time, with square-like distributions indicating stable representations and narrow diagonal patterns indicating rapidly evolving codes.

4.2 FUNCTIONALLY DISTINCT SUBPOPULATIONS SUSTAIN OBJECT TUNING STABILITY DURING MEMORY-DRIVEN GRASPING

To assess single-neuron contributions to population-level generalization (Fig. 25E–H), we applied a ranking-based analysis (Lanzilotto et al., 2019) and visualized object preference as rank plots (Fig. 29A). For each unit, the preferred object was defined in the Movement epoch from trial-averaged firing rates (three objects). Object selectivity across the trial was tested with a sliding-window one-way ANOVA (factor: object; α=0.05); only

significant bins were color-coded (rank 1 red, rank 2 yellow, rank 3 blue). We next quantified the temporal stability of object tuning, defined as the preservation of the same preferred object from the Presentation to the Movement epoch, as determined from the time course of significant bins. The preferred object identified during Movement was tracked backward in time to measure tuning persistence. Based on this criterion, neurons were ordered by the degree of tuning stability and divided into equal-sized Stable, Mixed, and Unstable subpopulations (orange/green/purple; color key in Fig. 29C). Representative units from each subpopulation and area are shown in Fig. 29B. Stable neurons (N1) maintain the same object preference from Presentation to movement onset; Mixed neurons (N2) preserve tuning only for part of that interval; Unstable neurons (N3) either change preference across epochs or lack selectivity in one epoch, precluding cross-epoch stability.

Training a Bayesian classifier on each subpopulation revealed that decoding accuracy increased with tuning stability across all areas (Stable > Mixed > Unstable in both training directions. Fig. 29C). Notably, Stable AIP neurons alone achieved accuracy comparable to the full AIP population (Fig. 29C vs. 25E–H), indicating that a stable subset can account for the population-level generalization observed in the absence of visual input. In contrast, Stable neurons in F5 and F2 exhibited lower cross-epoch accuracy, and F6 showed direction-dependent outcomes.

Training direction also varied by region: in AIP and F2, Movement→Presentation yielded higher accuracy than Presentation→Movement; F6 showed the opposite pattern; F5 was largely insensitive to training direction (Fig. 29C). When all subpopulations were considered together as the full population in each area (Fig. 25E–H), cross-epoch generalization was reduced or absent in F5, F2, and F6, but preserved in AIP. This pattern indicates that the presence of less-stable subpopulations attenuates the shared code in premotor regions, whereas in AIP the stable code remains robust when less-stable units are included.

In summary, single-neuron stability supports temporal generalization, yet stability alone does not fully account for the AIP-specific preservation of object representations. Despite similar proportions of stability-defined subpopulations across areas (Fig. 29A), only Stable AIP neurons both match full-population accuracy and remain unaffected by inclusion of less-stable subpopulations (Fig. 29C vs. 25E–H). We next asked whether the observed functional stability was associated with differences in discharge magnitude or

intrinsic physiology. To this end, additional physiological properties, expected to distinguish Stable AIP neurons from those in the other investigated regions, were examined in the following section.

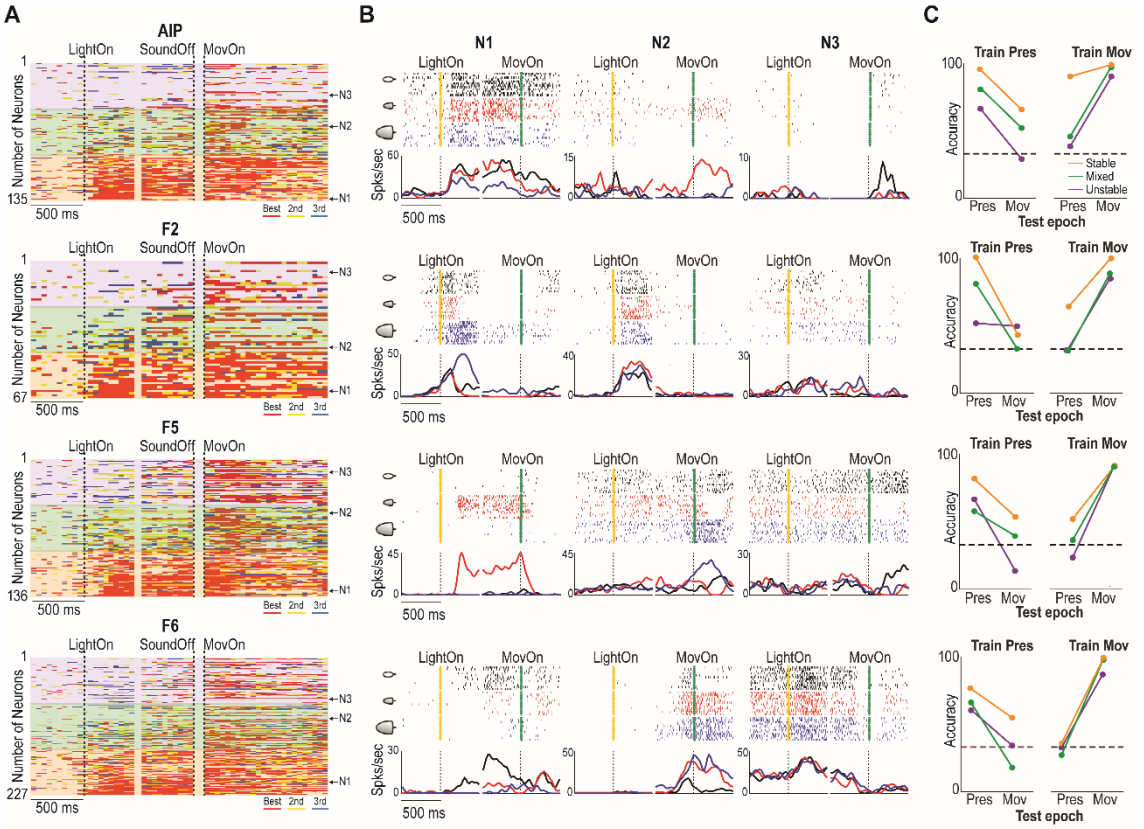

Figure 29. Ranking plots and cross-decoding analysis of functionally distinct subpopulations during memory-driven grasping. (A) Ranking plots for AIP, F2, F5, and F6 (top to bottom). Each time bin is color-coded to indicate the relative rank of the most preferred object over time. Non-selective bins (no significant modulation from baseline, one-way ANOVA, $p < 0.05$) are left blank (white). The color-coded bars on the right denote the three functionally distinct subpopulations classified by their temporal stability of object tuning (Stable, Mixed, Unstable). Labels N1–N3 indicate representative single neurons from each subpopulation corresponding to the examples shown in panel B. (B) Example discharge activity of representative neurons (N1–N3) aligned to object presentation and movement onset. Raster plots and peri-stimulus time histograms illustrate firing patterns for each object across trials. (C) Cross-epoch decoding analysis showing Bayesian classifier accuracy for each subpopulation across cortical areas. Classification performance is shown when the classifier was trained on one epoch and tested on the other, quantifying the generalization of object representations across task phases under the dark condition.

4.3 STABILITY IN BOTH TUNING AND DISCHARGE MAGNITUDE SUPPORT MEMORY-DRIVEN OBJECT CODING

To further clarify how stable neurons contribute to memory-based object coding, we examined the magnitude and temporal profile of their discharge activity. For each area, we averaged the normalized firing rate of neurons classified as *Stable* (Panel A), *Mixed*

(Panel B), and *Unstable* (Panel C; Figure 30).

In AIP, stable neurons showed the highest overall firing rates, with comparable response magnitude during the Presentation and Movement epochs. This indicates that object-related activity was not only consistent in tuning but also maintained in strength across the sensory-to-motor transition. F5, by contrast, displayed a clear increase in firing during movement, accompanied by greater variability between visual and motor phases, reflecting its lower coding stability. F2 and F6 showed weaker overall activity and smaller modulation across epochs, consistent with their limited contribution to cross-epoch generalization.

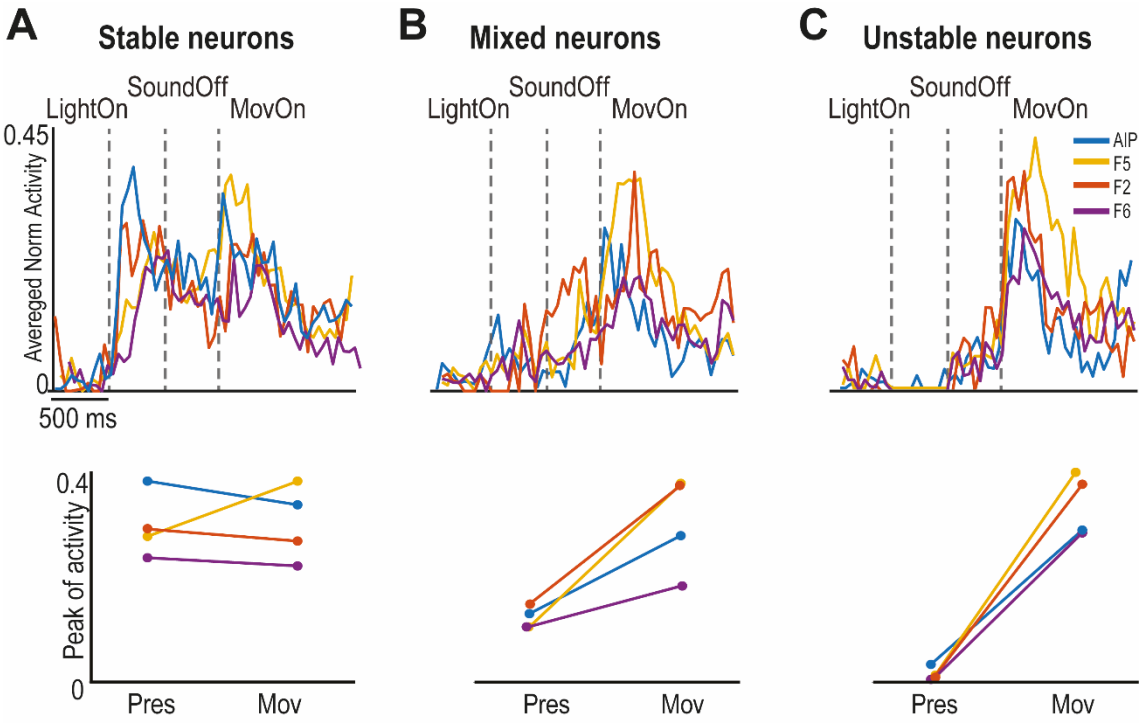

Figure 30. Normalized Firing Rate Across Neuronal Subpopulations and Task Epochs. (A) Stable, (B) Mixed, and (C) Unstable neurons. Average normalized activity over time across the investigated cortical areas (color-coded as indicated). The y-axis represents normalized firing rate; the x-axis shows time in milliseconds. Activity is aligned to object presentation (Light on), Go signal (Sound off), and movement onset (Mov on). Top panels show mean firing profiles; bottom panels display peak firing rates extracted from Presentation and Movement epochs.

We next asked whether these amplitude differences could enhance the distinctiveness of object representations within each area. To this aim, we assessed the *object-level dissimilarity* between Presentation and Movement epochs using confusion matrices computed from stable neurons (Figure 31). In AIP (Panel A), classifier predictions closely

matched true object identities, indicating that its stable neurons preserve object-specific activity patterns across the sensory–motor boundary. In F2 (Panel C), partial overlap between similar objects (e.g., small and big cones) suggested reduced discriminability. F5 (Panel B) and F6 (Panel D) exhibited systematic misclassifications toward single preferred objects (ring and small cone, respectively), implying that their motor activity was dominated by object-specific biases rather than sustained visual encoding.

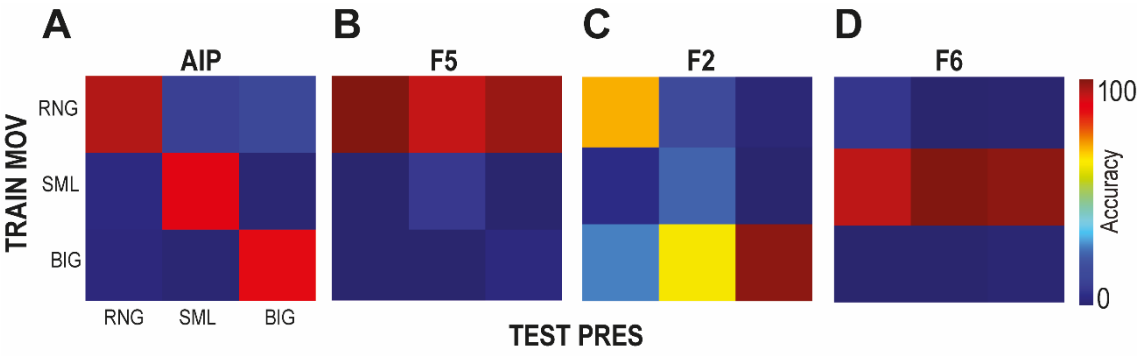

Figure 31. Object-Level Confusion Matrices Across Investigated Areas: Movement-to-Presentation Decoding. (A) AIP, (B) F5, (C) F2, (D) F6. Confusion matrices showing object-level classification accuracy for Stable neurons, obtained by training the classifier during the Movement epoch and testing during the Presentation epoch. Matrices were computed out-of-sample using a leave-one-split-out cross-validation procedure (see Cross-validation procedure, Methods 3.5.3). True object identity is shown on the y-axis and predicted identity on the x-axis. Diagonal values indicate correct classifications; off-diagonal entries represent misclassifications between objects.

Taken together, these findings show that AIP uniquely combines stable tuning and consistent discharge magnitude to preserve distinct object representations across visual and motor phases during memory-guided grasping. The combination of stable tuning and sustained discharge magnitude appears to underlie AIP's ability to maintain reliable object coding in the absence of visual feedback.

4.4 WAVEFORMS ANALYSIS

Given the functional distinctions observed across stability-defined subpopulations, we next examined whether these differences were also reflected in intrinsic physiological properties, potentially revealing distinct cellular classes underlying stable versus unstable coding. To this end, we analyzed extracellular spike waveforms using WaveMAP (Lee et al., 2021, 2023), an unsupervised clustering framework combining nonlinear

dimensionality reduction and graph-based community detection. This approach allowed neurons to be grouped based on waveform similarity while minimizing confounds related to signal amplitude. Across the full dataset (N = 551), WaveMAP (resolution = 1.4, n_neighbors = 14) identified ten distinct waveform clusters (Figure 32A-B), each characterized by a specific mean shape (Figure 32D). Cluster separability was quantified through post-hoc cross-validated classification (k-nearest neighbors in the UMAP space), which yielded a confusion matrix showing minimal overlap between groups (Figure 32C).

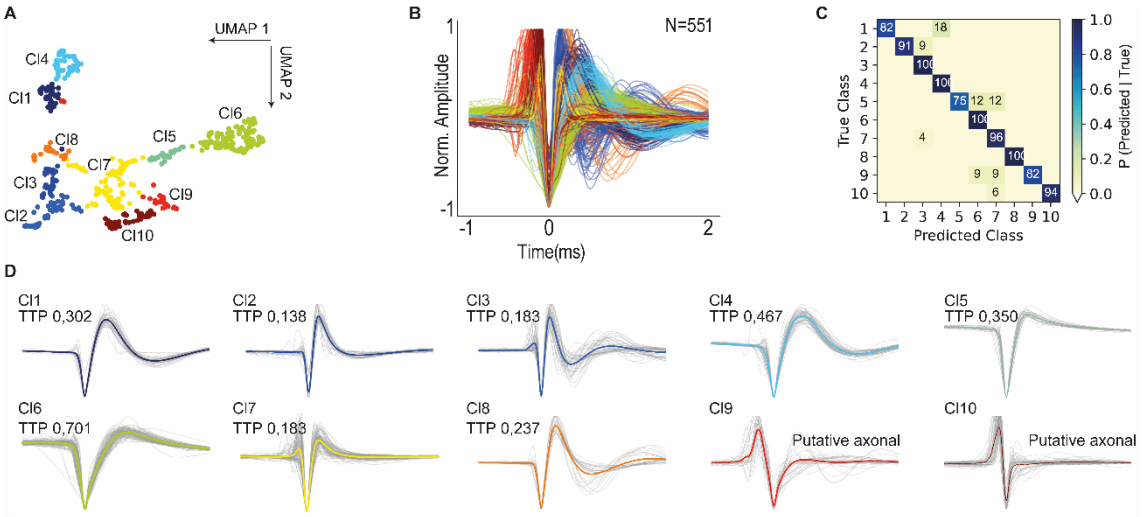

Figure 32. Unsupervised clustering of extracellular spike waveforms. (A) Low-dimensional embedding of the full dataset obtained via UMAP, where each point represents an individual neuron and colors indicate cluster membership. (B) Normalized spike waveforms (amplitude scaled to –1 to +1) for all neurons, aligned to the negative peak at 0 ms, with colors corresponding to cluster identity. (C) Confusion matrix illustrating the separability of clusters, with true labels on the y-axis and predicted labels on the x-axis; color intensity represents the conditional probability p (Predicted | True). (D) Composition of the ten identified clusters, showing individual waveforms in light gray and the cluster average in color, consistent with panels A and B.

Clusters were ordered according to the increasing trough-to-peak (TTP) duration of the mean waveform for each cluster, except for the last two clusters, which correspond to putative axonal recordings and were positioned at the end of the sequence due to their characteristic positive pre-negative deflection. Their relative distribution was then examined across the four cortical areas (Figure 33A). Significant differences emerged between regions (χ^2 test, $p < 0.05$), with AIP and F6 showing pronounced enrichments in specific clusters (AIP: 7, 5, 6; F6: 4, 6), while F5 and F2 were predominantly composed of clusters with shorter TTPs. Notably, F5 displayed peaks in clusters 3, 7, and 1, and F2 in clusters 3 and 7, indicating that each area exhibits a distinct composition of waveform-

defined neuronal subtypes.

Focusing on AIP subpopulations previously classified by functional stability, putative axonal waveforms (clusters 9 and 10, characterized by a positive pre-depolarization peak) were excluded to avoid confounds from non-somatic recordings (Barthó et al., 2004). The remaining neurons spanned clusters 2, 7, 1, 5, and 6. Comparisons across Stable, Mixed, and Unstable subpopulations revealed broadly similar distributions, with three notable exceptions: cluster 2 (TTP = 0.138 ms) was enriched in Unstable neurons, cluster 1 was absent in the Mixed group, and cluster 6 (TTP = 0.701 ms) showed reduced representation in Unstable neurons, suggesting a subtle shift toward narrower waveform profiles (Figure 33B). None of these differences reached statistical significance (χ^2 test, $p > 0.05$); however, their consistency across clusters and subpopulations suggests a potential association between waveform width and tuning stability, with broader spikes tending to characterize neurons exhibiting more stable object representations.

To obtain a coarser but interpretable distinction, neurons were classified as narrow- or broad-spiking based on a 0.3 ms TTP threshold, a conventional proxy for interneuron–pyramidal cell differentiation (McCormick et al., 1985; Mitchell et al., 2007). Given that clusters 3, 8, and 4 were not represented in AIP, only clusters 2, 7, and 1 were assigned to the narrow group, and clusters 5 and 6 to the broad group. Across the AIP population, 30.91% of neurons were narrow and 69.09% broad (Figure 33C). Notably, the proportion of broad-spiking neurons increased with functional stability: Unstable 58.82%, Mixed 68.42%, and Stable 78.95% (Figure 33C). Although these differences did not reach significance, and therefore cannot be interpreted as evidence of a causal relationship, the trend is consistent with the hypothesis that neurons displaying stable object tuning are more likely to belong to broad-spiking, excitatory-like populations.

Overall, waveform analysis reveals a gradual increase in the proportion of broad-spiking units with higher functional stability across AIP subpopulations, suggesting a subtle but systematic link between intrinsic electrophysiological properties and the persistence of object coding during memory-guided grasping.

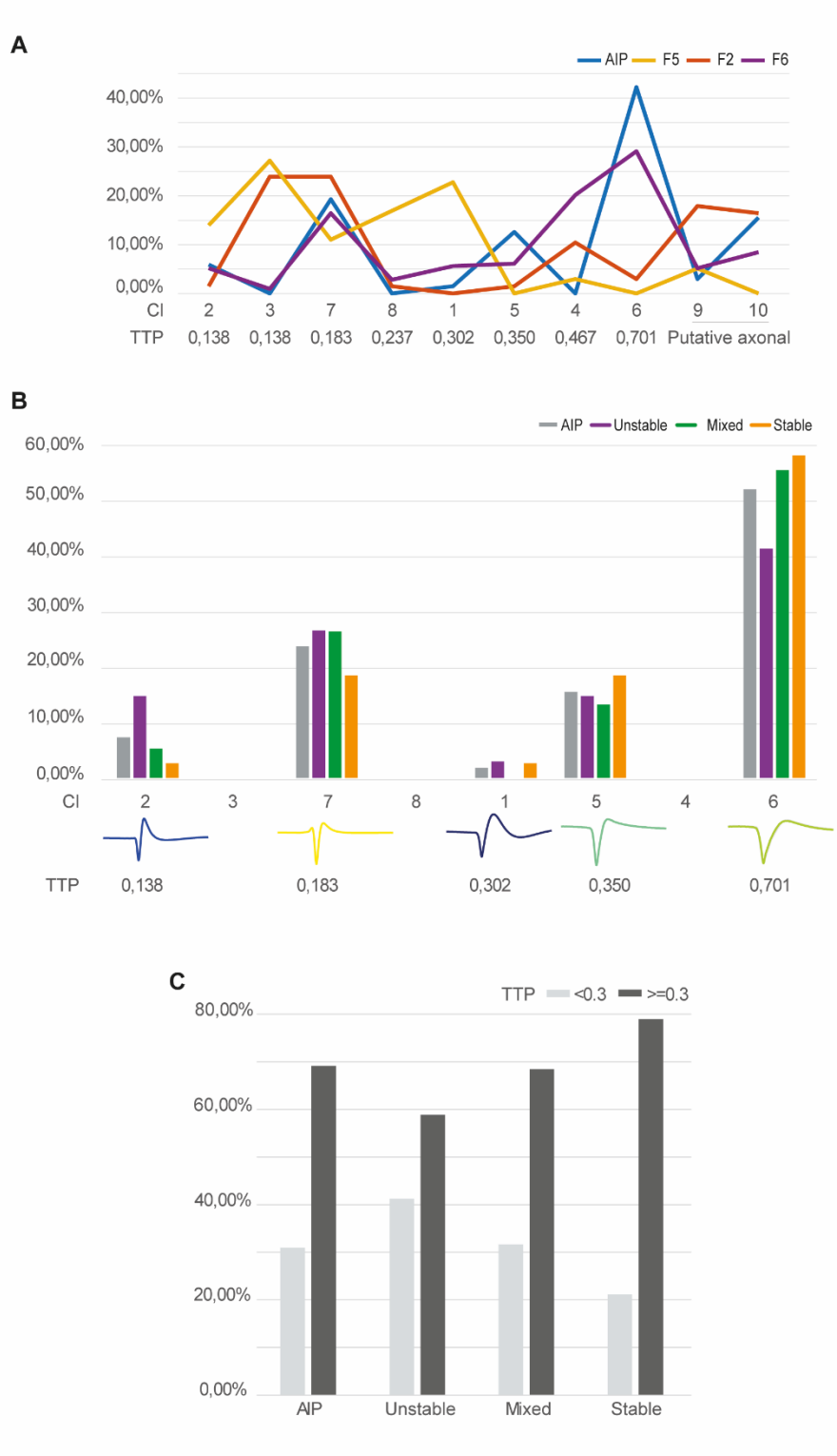

Figure 33. Distribution of waveform clusters across cortical areas and AIP subpopulations. (A) Percentage distribution of neurons (y-axis) across clusters (x-axis) for the four cortical areas, with cluster identity indicated by color. Time-to-peak (TTP) of the mean waveform for each cluster is reported. (B) Percentage distribution of neurons across clusters within the three AIP subpopulations, with the overall sample (gray) included for reference. Cluster colors are consistent with panel A, and mean waveforms along with their TTP are shown for each cluster. (C) Percentage of neurons in each AIP subpopulation classified as narrow- (TTP < 0.3 ms) or broad-spiking (TTP ≥ 0.3 ms), with cluster assignment indicated by color, highlighting the gradual increase of broad-spiking units with functional stability.

5 DISCUSSION

The present study investigated how multiple nodes of the parieto-frontal grasping network contribute to the maintenance of object-related information when visual feedback is absent. By integrating cross-temporal decoding, single-neuron stability analyses, and waveform-based classification, we identified a functional differentiation in the temporal organization of object coding across parietal and premotor regions. Specifically, AIP maintained object-selective activity across sensory–motor transitions, providing a memory-driven substrate that encodes object identity in the absence of visual input. In contrast, frontal areas (F5, F2, F6) exhibited transient, phase-dependent responses that dynamically transform this persistent parietal code into action-specific motor commands. Together, these complementary dynamics ensure the efficiency of grasping control across changing contextual situations.

5.1 BEHAVIORAL CONTROL AND NATURE OF SUSTAINED ACTIVITY

Behavioral data provide essential context for interpreting neural dynamics. Reaction and reaching and grasping times were significantly shorter in the dark, consistently across subjects, indicating efficient performance without vision and a shift toward more feedforward, ballistic execution with reduced online monitoring. This aligns with prior evidence in humans (Fitts, 1954; Desmurget et al., 1999; Saunders & Knill, 2003; Sarlegna & Miall, 2009) and in monkeys (Gaveau et al., 2014). The resulting acceleration reflects a temporally reweighted motor drive, with a steeper rate of force development and fewer visually mediated corrections (Maffiuletti et al., 2016; D'Emanuele et al., 2021). If light–dark differences reflected motor execution alone, such ballistic control would not be expected to diminish object information at the population level; at most, information would be confined to a narrower temporal window (Diedrichsen et al., 2010; Pruszynski & Scott, 2012). Instead, decoding is more accurate in light primarily in premotor hubs linked to online visuomotor monitoring and corrective processing, including dorsal premotor cortex in humans (Pisella et al., 2000; Tunik et al., 2005) and related regions in monkeys (Archambault et al., 2011), whereas AIP preserves cross-

epoch object coding in the dark.

Crucially, in No Go trials, with identical visual input but no movement preparation, object information declined rapidly after stimulus offset in all regions, including AIP. This indicates that visual stimulation or tonic attention alone is insufficient and rules out short-lived post-stimulus sensory carryover described in visual and frontoparietal systems in humans (Super et al., 2001; Harrison & Tong, 2009; Serences et al., 2009) and monkeys (Chelazzi et al., 1993; Miller et al., 1996). Most likely, sustained AIP activity during grasping in the dark, defined as stimulus-selective firing that outlasts the initial sensory response and bridges presentation to pre-movement and movement, reflects task-dependent retention of object information needed to guide actions in the absence visual feedback

5.2 STABLE OBJECT CODING IN AIP

Among all recorded regions, AIP was the only area exhibiting robust cross-epoch generalization of object coding between visual presentation and movement execution specifically in the dark condition. This finding indicates that, relative to F5, AIP retains more object-related information across the sensory–motor transition even when visual feedback is unavailable, thereby linking perceptual encoding and motor implementation under memory-driven conditions.

Previous studies have identified AIP as a core hub for transforming visual information about object features (such as shape, size, and orientation) into grasp-relevant motor parameters (Taira et al., 1990; Murata et al., 2000) and for dynamically interacting with premotor regions to support visuomotor transformations (Schaffelhofer et al., 2015). More recent work has implicated AIP in both visually guided and memory-driven grasping (Baumann et al., 2009; Schaffelhofer & Scherberger, 2016) and has shown that neurons in other parietal regions (V6A, PE, PEc) maintain reach- and grasp-related activity during delay periods without visual feedback (Breveglieri et al., 2016; Diomedi et al., 2024).

Building on this framework, the present results refine the picture of AIP’s contribution by demonstrating that its activity not only persists under memory-driven conditions but also generalizes across sensory and motor epochs better than in other areas

with similar – or even greater – object tuning during grasping in the light conditions, reflecting temporally stable object encoding at the population level regardless of the availability of sensory information. One may argue that this effect depends on a larger fraction of object-selective neurons in AIP, but the sliding-window ANOVA revealed comparable proportions and temporal profiles of object-selective neurons across light and dark conditions relative to the other areas, indicating that this enhanced cross-epoch generalization cannot be explained by differences in single-neuron selectivity. Moreover, the absence of such generalization under full vision suggests that the mechanism supporting stability is selectively engaged when visual feedback is unavailable, consistent with the recruitment of population-level dynamics that integrate information across neurons to preserve object identity throughout the sensory–motor transition.

5.3 FUNCTIONAL GRADIENT ALONG THE PARIETO-FRONTAL NETWORK

Comparing AIP tuning properties with those of frontal regions reveals a functional gradient within a distributed parieto-frontal circuit rather than a rigidly serial processing hierarchy. Across the network, the temporal structure of object-related activity differentiates stable from dynamic contributions to grasp control. AIP exhibited temporally persistent coding as revealed by the cross-decoding analyses linking Presentation and Movement epochs in the dark condition (Fig. 25E,G), with significant cross-epoch generalization between presentation and movement, under memory-guided conditions, providing continuity of object identity across phases. Crucially, cross-temporal generalization was bidirectional, from presentation to movement and vice versa, indicating that AIP's representation interacts with, rather than simply precedes, motor-related activity. This reciprocity argues against a purely feed-forward organization and instead supports recurrent exchange between parietal and frontal nodes.

In contrast, F5 displayed reliable premovement coding and strong generalization between adjacent epochs (Premovement↔Movement), with a slightly later onset than AIP but limited carryover from Presentation, particularly in the dark. This pattern suggests a consistency of object-related activity that is primarily confined to motor-related phases, rather than a persistent visual–motor bridge. Accordingly, the F5 decoding profile aligns with prior accounts of F5 as a hub for goal-directed action specification and

interfacing with downstream motor commands (Rizzolatti & Luppino, 2001; Bonini et al., 2014b; Ferroni et al., 2021). Area F2 showed intermediate behavior, reflecting its anatomical and functional role in integrating visuospatial and proprioceptive inputs to coordinate limb kinematics (Matelli et al., 1985; Davare et al., 2008), whereas F6 exhibited rapid, phase-specific transitions aligned with its involvement in internally generated action sequencing and higher-order control (Lanzilotto et al., 2016; Albertini et al., 2020). These distinctions reflect a temporal and computational gradient across reciprocally connected nodes of the grasping network (Borra et al., 2008; Gerbella et al., 2011). Parietal area AIP may therefore contribute temporally stable representations that ensure the continuity of object information across perceptual contexts, while premotor and supplementary motor areas implement more rapidly evolving transformations that enable flexible adaptation to task demands.

Such an organization reconciles two complementary coding demands evident in our data: cross-epoch stability, corresponding to the preservation of object information across presentation and movement phases, and adaptability, corresponding to the context-dependent updating of neural representations across task epochs, within a recurrent visuomotor architecture (Cisek & Kalaska, 2005). Overall, the observed dynamics are consistent with the view that these areas act as interacting components of a distributed loop, in which bidirectional exchanges balance persistent object coding with context-specific transformations.

5.4 SINGLE-NEURON AND POPULATION MECHANISMS OF STABILITY

The results of our stability analysis assessing how much the neuronal preference for a given object remain stable across time or switch to another, revealed that only a subset of neurons maintained consistent object preference across sensory and motor epochs. In AIP, this subset alone achieved cross-epoch classification accuracy (Presentation↔Movement) comparable to that of the full AIP population in the dark (Fig. 29C vs. 25E–H), suggsting that persistent population codes depend primarily on a core ensemble of stable neurons. These neurons also preserved comparable firing-rate magnitude during sensory and motor phases, suggesting continuity of object-related activity across the sensory–motor

transition.

When less-stable neurons were included, decoding performance decreased markedly in premotor regions but remained largely unaffected in AIP. This pattern suggests that AIP's population code integrates contributions from neurons with different tuning stability, allowing the overall representation to remain relatively robust despite unit-level variability. Such robustness likely reflects local recurrent mechanisms supporting the sustained discharge of interconnected neuronal clusters. Computational and electrophysiological models have shown that persistent activity can emerge from recurrent excitatory–inhibitory loops that maintain depolarization within local networks (Compte et al., 2000; Wang, 2001). Within these circuits, stable population-level activity results from the dynamic balance of excitation and inhibition rather than from sustained firing of individual neurons (Constantinidis & Wang, 2004). The relative stability of population coding in AIP, even in the presence of neurons with variable tuning, therefore suggests that these unstable or mixed units may contribute actively to maintaining the network state. Neurons with fluctuating discharge or mixed selectivity can transiently modulate local excitation or inhibition, thereby stabilizing the collective attractor dynamics through balanced feedback interactions (Lim & Goldman, 2013).

Under this framework, stable putative pyramidal neurons would anchor the core object representation, while more dynamic local populations help maintain temporal coherence and prevent drift of the ensemble code. Consistent with this view, waveform-based classification in AIP showed a monotonic increase in the proportion of broad spiking units across the stability-defined subpopulations (Unstable 58.82%, Mixed 68.42%, Stable 78.95%; Fig. 33C). Although this pattern did not reach statistical significance, it is compatible with a greater prevalence of broad spiking, putative excitatory neurons among the most stable units. This observation is compatible with the interpretation that putative pyramidal-like excitatory neurons provide structural support for persistence through recurrent excitation (McCormick et al., 1985), with stabilization contributed by more dynamic local populations, including interneurons and broadly tuned cells (Lemon et al., 2021). The interplay between stable and unstable/mixed subpopulations may provide a biologically grounded account of object-coding stability in AIP during grasping in the dark, a pattern not equivalently expressed under full vision, and is consistent with a context-dependent reconfiguration of the ensemble.

5.5 TRANSITION FROM SENSORY- TO MEMORY-DRIVEN STATES

What triggers and sustains the reconfiguration of AIP subpopulations from a sensory- to a memory-driven state? In the present task, the visual and memory-guided conditions shared identical sensory stimulation and motor structure up to the go cue; the critical manipulation was the extinction of object illumination at the go cue in the dark condition, such that the reach–to–grasp was executed without visual feedback. Accordingly, the emergence of memory-based coding in AIP cannot be explained by differences in the initial visual input; rather, it reflects context-dependent modulation within the network, operationally defined by the presence versus absence of visual feedback during movement execution. Under these conditions, AIP activity is likely reconfigured through the interaction between local recurrent dynamics and long-range top-down inputs. During visually guided grasping, AIP operates under dominant bottom-up visual drive from occipito-parietal pathways encoding object features and affordances, as shown for AIP in macaques (Murata et al., 2000), where neurons first represent the visual properties of the object (e.g., shape, size, orientation) and subsequently transform these features into affordance-based codes specifying how the object can be grasped or manipulated, thereby bridging perceptual and action-related representations. In parallel, studies in the dorsomedial stream demonstrate analogous visuomotor computations in area V6A, supporting the general principle that parietal cortex can transform visual information into grasp-related signals (Fattori et al., 2010). After object illumination is extinguished at the go cue, bottom-up visual drive to AIP from occipito-parietal pathways is no longer available, and the network reconfigures to sustain object-related activity internally. Frontal feedback signals, originating from premotor and prefrontal nodes, are likely to maintain AIP activity through recurrent excitation among local pyramidal neurons and interneurons.

Evidence from premotor–parietal interactions indicates that ventral premotor cortex (area F5) exerts modulatory influences on AIP activity during action preparation and object grasping (Schaffelhofer et al., 2015). This functional relationship is consistent with anatomical and tract-tracing studies demonstrating strong reciprocal AIP–F5 connectivity (Rizzolatti & Luppino, 2001; Borra et al., 2008) and further supported by recent detailed characterizations of these fronto-parietal pathways (Lanzilotto et al., 2019). In parallel, fronto–parietal coupling has been implicated in the maintenance of internal representations during delays and context-dependent behavior; preparatory signals in

premotor cortex provide a plausible source of top-down input to parietal regions during memory-guided actions (Hoshi & Tanji, 2006), and prefrontal dynamics support flexible cognitive control during rule- or context-dependent behavior (Brunamonti et al., 2016; Constantinidis et al., 2018). Taken together, these observations suggest that the transition to a memory-driven configuration in AIP reflects a shift in the relative contribution of sensory and frontal inputs, with visual drive prevailing under full vision and internally driven, top–down activity emerging when visual information is no longer available. Transient input from higher-order frontal areas at movement initiation may help stabilize AIP activity, supporting the maintenance of object-specific representations during grasp execution in the dark. Consistent with this interpretation, recordings along the AIP–F5 circuit show that representational format and information flow adapt to task context and demands during grasp, indicating flexible integration of sensory and cognitive inputs within AIP (Baumann et al., 2009; Schaffelhofer & Scherberger, 2016). Analogously, neurons in other parietal regions such as V6A flexibly encode object- and action-related variables during reach-to-grasp behavior, underscoring a broader parietal capability for context-dependent sensorimotor integration (Galletti et al., 2022). Thus, the memory-driven configuration described here should not be viewed as a residual or decaying trace, but as an actively maintained network state that preserves task-relevant object information when sensory feedback is unavailable.

Although we did not directly measure inter-areal coupling, this hypothesis aligns with established models of fronto-parietal working memory based on recurrent dynamics and reverberation (Fuster, 2001; Wang, 2001; Cisek & Kalaska, 2010) and is coherent with causal evidence at the circuit level indicating that perturbing fronto-parietal interactions impairs the planning and control of visually guided and memory-guided actions, as shown by parietal inactivation affecting inferotemporal activations during three-dimensional object vision (Van Dromme et al., 2016) and by muscimol injections in AIP disrupting hand preshaping during grasp (Gallese et al., 1994). Future work employing simultaneous multi-area recordings or causal perturbations (e.g., reversible inactivation or targeted stimulation) will be essential to determine whether frontal feedback indeed drives this state transition in AIP.

5.6 CONCEPTUAL IMPLICATIONS

The ability of AIP to maintain coherent object representations across sensory and motor epochs exemplifies a fundamental organizational principle: the coexistence of stable internal states within distributed neural dynamics. Under natural conditions, visual information is not continuously available, yet effective action requires maintaining an internal model of the environment that bridges sensory gaps. The dynamics observed in AIP suggest that the brain achieves this by stabilizing relational population codes that remain accessible to flexible frontal transformations during behavior. This principle parallels mechanisms established in other cortical systems, including persistent activity in prefrontal working-memory networks (Funahashi et al., 1989; Wang, 2001; Constantinidis & Goldman-Rakic, 2002) and attractor-like dynamics in the hippocampus supporting spatial coding (Wills et al., 2005), alongside sequence-based reactivation that supports memory consolidation and planning (Battaglia et al., 2011). Extending this framework to sensorimotor control highlights a shared computational logic between memory and action: the preservation of task-relevant information within continuously evolving population trajectories (Cisek & Kalaska, 2010; Murray et al., 2017).

5.7 METHODOLOGICAL CONSIDERATIONS

Several methodological factors constrain the interpretation of these results. Recordings from different cortical regions were obtained in separate sessions, precluding direct assessment of inter-areal coupling. Nonetheless, the use of identical behavioral protocols, task structure, and analytical pipelines across subjects mitigates this limitation and ensures functional rather than procedural comparability.

The combination of chronic (AIP, F6) and acute (F5, F2) recordings may have introduced a sampling bias among neuron types, in which acute recordings may favor the acquisition of larger pyramidal cells whereas chronic recordings may provide a more balanced mix including smaller inhibitory interneurons (Harris et al., 2016). However, with respect to waveforms, we provide descriptive cross-area summaries and restrict interpretation to within-area contrasts in AIP (stability-defined subpopulations). Moreover, waveform normalization and the exclusion of putative axonal units, together with cross-validated clustering, were applied as standard controls for amplitude-related

variability and classification robustness.

The classification of neurons into narrow- and broad-spiking categories was based on conventional trough-to-peak thresholds and should therefore be regarded as indicative rather than categorical. Despite these constraints, the convergence of independent analyses (population decoding, stability ranking, and waveform clustering) supports the robustness and coherence of the present conclusions.

An additional consideration concerns the potential laminar distribution of waveform-defined neuronal categories. In acute recording sessions, electrode penetrations can span different depths within the cortex; however, the premotor cortex is poorly laminated compared to primary sensory cortices (Belmalih et al., 2009), and recordings were obtained both on cortical banks and within sulci, precluding a systematic longitudinal sampling across cortical layers. As a result, electrode depth cannot be reliably mapped onto specific laminar compartments, and any depth-based analysis would lack clear anatomical interpretability. Accordingly, the present data do not allow a meaningful assessment of layer-specific contributions to waveform or functional categories.

5.8 FUNCTIONAL ROLE AND TRANSLATIONAL PERSPECTIVE

Understanding how cortical networks maintain object representations despite the absence of visual feedback constrains the neural principles underlying adaptive motor control. In grasp control, the dynamics observed in AIP, persistent, object-specific population activity, may instantiate a predictive mechanism that supports the continuation of movement when visual or proprioceptive feedback is delayed or unavailable. By retaining estimates of object features and expected hand–object configurations, this activity provides a stable reference that keeps motor commands coherent and appropriately adjusted even when external information is incomplete. In this sense, local stabilization in AIP exemplifies how the sensorimotor system compensates for intermittent input while preserving coordination under uncertainty.

These principles have direct translational relevance. Neuroprosthetic systems that decode motor intentions from cortical activity already leverage parietal and premotor signals to reconstruct intended movements and to restore functional reaching and grasping in paralysis (Ajiboye et al., 2017; Liu & Schieber, 2020; Mazzoni &

Chiappalone, 2023). However, many interfaces still rely on continuous feedback or require periodic recalibration to maintain stable control, underscoring the need for mechanisms that preserve task representations when inputs fluctuate (Dadarlat & O'Doherty, 2023). Incorporating AIP-inspired elements, specifically recurrent architectures that maintain object-centered representations during feedback loss, could enhance stability and continuity of control. Embedding predictive modules that preserve information about object geometry and anticipated interaction forces may enable smoother, more autonomous grasping when sensory input is degraded.

Comparable challenges arise in robotics, where reliable manipulation must be achieved under uncertain sensory conditions. Bio-inspired approaches increasingly adopt internal sensorimotor models for grasping with partial information, from learning-based pipelines to control schemes that explicitly stabilize hand–object interaction (Xie et al., 2023; Ruiz Garate et al., 2018; Bernotat et al., 2023). Yet many systems still depend on externally timed transitions or rigid state machines, lacking self-sustained activity comparable to biological circuits. Implementing recurrent, context-sensitive mechanisms analogous to those inferred in AIP could help robotic agents maintain predictive representations of object geometry and contact dynamics, improving adaptability when feedback is delayed or interrupted (Zhao et al., 2024).

Therefore, clarifying how parieto-frontal circuits stabilize object representations across sensory contexts refines our understanding of memory-based action and provides a neural framework for designing adaptive control strategies in neuroprosthetic and robotic systems.

6 CONCLUSIONS

This study shows that, within the investigated nodes of the macaque extended grasping network, AIP uniquely preserves object-specific representations across sensory and motor phases when visual feedback is unavailable. Whereas premotor regions express phase-locked, transient codes related to movement, AIP maintains a temporally stable representation that bridges perception and action. The convergence of multiple analytical approaches, including population decoding, single-neuron stability, and waveform-based classification, indicates that this stability emerges from the coordinated interaction of distinct neuronal subpopulations and from the ability of local circuits to reconfigure their functional state in the absence of sensory input. Frontal areas, in turn, implement flexible transformations that adapt these persistent parietal signals to the current behavioral context. Together, these results support a distributed, dynamically reconfigurable (recurrent) organization in which parietal stability and frontal flexibility act as complementary components of a unified visuomotor network, ensuring coherent grasp control across changing sensory conditions.

Beyond their immediate contribution to advancing our understanding of the principles underlying visuomotor organization, the present findings provide empirically grounded constraints for models of memory-guided action and offer cautious insights for translational efforts in neuroprosthetics and robotics. They indicate that parieto-frontal circuits can maintain, and flexibly transform, internal object representations when sensory information is lacking, outlining neural principles for more adaptive and predictive control systems.

More broadly, this work shows how the brain maintains coherent action by preserving internal representations that keep perception and execution aligned, even when the external world, quite literally, goes out of sight.

REFERENCES

Albertini, D., Gerbella, M., Lanzilotto, M., Livi, A., Maranesi, M., Ferroni, C. G., & Bonini, L. (2020). Connectional gradients underlie functional transitions in monkey pre-supplementary motor area. *Progress in Neurobiology, 184*, 101699. https://doi.org/10.1016/j.pneurobio.2019.101699

Albertini, D., Lanzilotto, M., Maranesi, M., & Bonini, L. (2021). Largely shared neural codes for biological and nonbiological observed movements but not for executed actions in monkey premotor areas. *Journal of Neurophysiology, 126*(3), 906–912. https://doi.org/10.1152/jn.00296.2021

Andersen, R. A., Snyder, L. H., Bradley, D. C., & Xing, J. (1997). Multimodal representation of space in the posterior parietal cortex and its use in planning movements. *Annual Review of Neuroscience, 20*, 303–330. https://doi.org/10.1146/annurev.neuro.20.1.303

Andersen, R. A., & Buneo, C. A. (2002). Intentional maps in posterior parietal cortex. *Annual Review of Neuroscience, 25*, 189–220. https://doi.org/10.1146/annurev.neuro.25.112701.142922

Andersen, R. A., & Cui, H. (2009). Intention, action planning, and decision making in parietal-frontal circuits. *Neuron, 63*(5), 568–583. https://doi.org/10.1016/j.neuron.2009.08.028

Archambault, P. S., Caminiti, R., & Battaglia-Mayer, A. (2011). Online control of hand trajectory and evolution of motor intention in the parietofrontal system. *Journal of Neuroscience, 31*(2), 742–752. https://doi.org/10.1523/JNEUROSCI.2623-10.2011

Aron, A. R., Robbins, T. W., & Poldrack, R. A. (2014). Inhibition and the right inferior frontal cortex: One decade on. *Trends in Cognitive Sciences, 18*(4), 177–185. https://doi.org/10.1016/j.tics.2013.12.003

Balasubramaniam, R., Haegens, S., Jazayeri, M., Merchant, H., Sternad, D., & Song, J. H. (2021). Neural encoding and representation of time for sensorimotor control and learning. *Journal of Neuroscience, 41*(5), 866–872. https://doi.org/10.1523/JNEUROSCI.1652-20.2020

Banks, A. P., & Gamblin, D. M. (2022). Successful everyday decision making: Combining attributes and associates. *Judgment and Decision Making, 17*(6), 1255–1286.

https://doi.org/10.1017/S1930297500009414

Barbosa, J., Stein, H., & Lundqvist, M. (2020). Interplay between persistent activity and activity-silent dynamics in the prefrontal cortex. *Nature Neuroscience, 23*(8), 1050–1059. https://doi.org/10.1038/s41593-020-0656-8

Barthó, P., Hirase, H., Monconduit, L., Zugaro, M., Harris, K. D., & Buzsáki, G. (2004). *Characterization of neocortical principal cells and interneurons by network interactions and extracellular features*. Journal of Neurophysiology, 92(1), 600–608. https://doi.org/10.1152/jn.01170.2003

Barz, F., Livi, A., Lanzilotto, M., Maranesi, M., Bonini, L., Paul, O., & Ruther, P. (2017). Versatile, modular 3D microelectrode arrays for neuronal ensemble recordings: From design to fabrication, assembly, and functional validation in non-human primates. *Journal of Neural Engineering*, *14*(3), 036010. https://doi.org/10.1088/1741-2552/aa5a90

Batista, A. P., & Andersen, R. A. (2001). The parietal reach region codes the next planned movement in a sequential reach task. *Journal of Neurophysiology*, 85(2), 539–544. https://doi.org/10.1152/jn.2001.85.2.539

Battaglia-Mayer, A., Caminiti, R., & Lacquaniti, F. (2001). The parietal cortex and the control of reaching movements. *Cerebral Cortex, 11*(5), 442–454. https://doi.org/10.1093/cercor/11.5.442

Battaglia-Mayer, A., Ferraina, S., Genovesio, A., Marconi, B., Squatrito, S., Molinari, M., Lacquaniti, F., & Caminiti, R. (2001). Eye-hand coordination during reaching. II. An analysis of the relationships between visuomanual signals in parietal cortex and parieto-frontal association projections. *Cerebral Cortex, 11*(6), 528–544. https://doi.org/10.1093/cercor/11.6.528

Baumann, M. A., Fluet, M. C., & Scherberger, H. (2009). Context-specific grasp movement representation in the macaque anterior intraparietal area. *Journal of Neuroscience, 29*(20), 6436-6448. https://doi.org/10.1523/JNEUROSCI.5479-08.2009

Begliomini, C., Wall, M. B., Smith, A. T., & Castiello, U. (2007). Differential cortical activity for precision and whole-hand visually guided grasping in humans. *European Journal of Neuroscience, 25*(4), 1245–1252. https://doi.org/10.1111/j.1460-9568.2007.05365.x

Belmalih, A., Borra, E., Contini, M., Gerbella, M., Rozzi, S., & Luppino, G. (2009).

Multimodal architectonic subdivision of the rostral part (area F5) of the macaque ventral premotor cortex. *Journal of Comparative Neurology*, 512(2), 183–217. https://doi.org/10.1002/cne.21892

Bencivenga, F., Tullo, M. G., Maltempo, T., von Gal, A., Serra, C., Pitzalis, S., & Galati, G. (2022). Effector-selective modulation of the effective connectivity within frontoparietal circuits during visuomotor tasks. *Cerebral Cortex*, 1–22. https://doi.org/10.1093/cercor/bhac223

Berger, M., Agha, N. S., & Gail, A. (2020). Wireless recording from unrestrained monkeys reveals motor goal encoding beyond immediate reach in frontoparietal cortex. *eLife, 9,* e51322. https://doi.org/10.7554/eLife.51322

Bernier, P. M., & Grafton, S. T. (2010). Human posterior parietal cortex flexibly determines reference frames for reaching based on sensory context. *Neuron, 68*(4), 776–788. https://doi.org/10.1016/j.neuron.2010.11.002

Bernstein, N. A. (2020). *Bernstein's construction of movements: The original text and commentaries* (M. L. Latash, Ed.). Routledge. https://doi.org/10.4324/9780367816797

Beste, C., Ness, V., Lukas, C., Hoffmann, R., Stüwe, S., Falkenstein, M., & Saft, C. (2012). Mechanisms mediating parallel action monitoring in fronto-striatal circuits. *NeuroImage, 62*(1), 137–146. https://doi.org/10.1016/j.neuroimage.2012.05.019

Blondel, V. D., Guillaume, J. L., Lambiotte, R., & Lefebvre, E. (2008). Fast unfolding of communities in large networks. *Journal of Statistical Mechanics: Theory and Experiment, 2008*(10), P10008. https://doi.org/10.1088/1742-5468/2008/10/P10008

Boen, R., Raud, L., & Huster, R. J. (2022). Inhibitory control and the structural parcellation of the right inferior frontal gyrus. *Frontiers in Human Neuroscience, 16,* 787079. https://doi.org/10.3389/fnhum.2022.787079

Boettcher, S. E. P., Gresch, D., Nobre, A. C., & van Ede, F. (2021). Output planning at the input stage in visual working memory. *Science Advances, 7*(13), eabe8212. https://doi.org/10.1126/sciadv.abe8212

Bonini, L., Ugolotti Serventi, F., Bruni, S., Maranesi, M., Bimbi, M., Simone, L., Rozzi, S., Ferrari, P. F., & Fogassi, L. (2012). Selectivity for grip type and action goal in macaque inferior parietal and ventral premotor grasping neurons. *Journal of Neurophysiology, 108*(6), 1607–1619. https://doi.org/10.1152/jn.01158.2011

Bonini, L., Maranesi, M., Livi, A., Bruni, S., Fogassi, L., Holzhammer, T., Paul, O., & Ruther, P. (2014a). Application of floating silicon-based linear multielectrode arrays for acute recording of single neuron activity in awake behaving monkeys. Biomedizinische Technik. Biomedical Engineering, 59, 273–281.

Bonini, L., Maranesi, M., Livi, A., Fogassi, L., & Rizzolatti, G. (2014b). Space-dependent representation of objects and other's action in monkey ventral premotor grasping neurons. *Journal of Neuroscience, 34*(11), 4108–4119. https://doi.org/10.1523/JNEUROSCI.4187-13.2014

Bonini, L., Maranesi, M., Livi, A., Fogassi, L., & Rizzolatti, G. (2014c). Ventral premotor neurons encoding representations of action during self and others' inaction. *Current Biology, 24*(14), 1611–1614. https://doi.org/10.1016/j.cub.2014.05.047

Borra, E., Belmalih, A., Calzavara, R., Gerbella, M., Murata, A., Rozzi, S., & Luppino, G. (2008). Cortical connections of the macaque anterior intraparietal (AIP) area. *Cerebral Cortex*, 18(5), 1094–1111. https://doi.org/10.1093/cercor/bhm146

Borra, E., & Luppino, G. (2017). Functional anatomy of the macaque temporo-parieto-frontal connectivity. *Cortex, 97*, 306–326. https://doi.org/10.1016/j.cortex.2016.12.007

Breveglieri, R., Bosco, A., Galletti, C., Passarelli, L., & Fattori, P. (2016). Neural activity in the medial parietal area V6A while grasping with or without visual feedback. *Scientific Reports, 6*, 28893. https://doi.org/10.1038/srep28893

Brunamonti, E., Mione, V., Di Bello, F., Pani, P., Genovesio, A., & Ferraina, S. (2016). Neuronal modulation in the prefrontal cortex in a transitive inference task: Evidence of neuronal correlates of mental schema management. *Journal of Neuroscience, 36*(4), 1223–1236. https://doi.org/10.1523/JNEUROSCI.1473-15.2016

Buchwald, D., & Scherberger, H. (2021). Visually and tactually guided grasps lead to different neuronal activity in non-human primates. *Frontiers in Neuroscience, 15*, 679910. https://doi.org/10.3389/fnins.2021.679910

Bufacchi, R. J., & Iannetti, G. D. (2018). An action field theory of peripersonal space. *Trends in Cognitive Sciences*, 22(12), 1076–1090. https://doi.org/10.1016/j.tics.2018.09.004

Buneo, C. A., & Andersen, R. A. (2006). The posterior parietal cortex: Sensorimotor interface for the planning and online control of visually guided movements.

Neuropsychologia, *44*(13), 2594–2606. https://doi.org/10.1016/j.neuropsychologia.2005.10.011

Bunge, S. A., Ochsner, K. N., Desmond, J. E., & Gabrieli, J. D. (2004). Prefrontal regions involved in keeping rules in working memory: A functional MRI investigation of verbal set-shifting. *Cognitive, Affective, & Behavioral Neuroscience, 4*(4), 335–347. https://doi.org/10.3758/CABN.4.4.334

Cai, W., Ryali, S., Chen, T., Li, C.-S. R., & Menon, V. (2014). Dissociable roles of right inferior frontal cortex and anterior insula in inhibitory control: Evidence from intrinsic and task-related functional parcellation, connectivity, and response profile analyses across multiple datasets. *Journal of Neuroscience, 34*(44), 14652–14667. https://doi.org/10.1523/JNEUROSCI.3048-14.2014

Caminiti, R., Innocenti, G. M., & Battaglia-Mayer, A. (2015). Organization and evolution of parieto-frontal processing streams in macaque monkeys and humans. *Neuroscience & Biobehavioral Reviews, 56*, 73–96. https://doi.org/10.1016/j.neubiorev.2015.06.014

Cerri, G., Shimazu, H., Maier, M. A., & Lemon, R. N. (2003). Facilitation from ventral premotor cortex of primary motor cortex outputs to macaque hand muscles. *Journal of Neurophysiology, 90*(2), 832–842. https://doi.org/10.1152/jn.01026.2002

Chelazzi, L., Miller, E. K., Duncan, J., & Desimone, R. (1993). A neural basis for visual search in inferior temporal cortex. *Nature, 363*(6427), 345–347. https://doi.org/10.1038/363345a0

Churchland, M. M., Cunningham, J. P., Kaufman, M. T., Foster, J. D., Nuyujukian, P., Ryu, S. I., & Shenoy, K. V. (2012). Neural population dynamics during reaching. *Nature, 487*(7405), 51–56. https://doi.org/10.1038/nature11129

Cisek, P., & Kalaska, J. F. (2005). Neural correlates of reaching decisions in dorsal premotor cortex: Specification of multiple direction choices and final selection of action. *Neuron, 45*(5), 801–814. https://doi.org/10.1016/j.neuron.2005.01.027

Cisek, P. (2007). Cortical mechanisms of action selection: The affordance competition hypothesis. *Philosophical Transactions of the Royal Society B: Biological Sciences, 362*(1485), 1585–1599. https://doi.org/10.1098/rstb.2007.2054

Cisek, P., & Kalaska, J. F. (2010). Neural mechanisms for interacting with a world full of action choices. *Annual Review of Neuroscience, 33*, 269–298.

https://doi.org/10.1146/annurev-neuro-051508-135409

Clark, A. (2013). Whatever next? Predictive brains, situated agents, and the future of cognitive science. *Behavioral and Brain Sciences, 36*(3), 181–204. https://doi.org/10.1017/S0140525X12000477

Colby, C. L., Duhamel, J. R., & Goldberg, M. E. (1996). Visual, presaccadic, and cognitive activation of single neurons in monkey lateral intraparietal area. *Journal of Neurophysiology*, 76(5), 2841–2852. https://doi.org/10.1152/jn.1996.76.5.2841

Constantinidis, C., Funahashi, S., Lee, D., Murray, J. D., Qi, X.-L., Wang, M., & Arnsten, A. F. T. (2018). Persistent spiking activity underlies working memory. *Journal of Neuroscience, 38*(32), 7020–7028. https://doi.org/10.1523/JNEUROSCI.2486-17.2018

Constantinidis, C., & Wang, X.-J. (2004). A neural circuit basis for spatial working memory. *Neuroscientist, 10*(6), 553–565. https://doi.org/10.1177/1073858404268742

Compte, A., Brunel, N., Goldman-Rakic, P. S., & Wang, X.-J. (2000). Synaptic mechanisms and network dynamics underlying spatial working memory in a cortical network model. *Cerebral Cortex, 10*(9), 910–923. https://doi.org/10.1093/cercor/10.9.910

Crammond, D. J., & Kalaska, J. F. (2000). Prior information in motor and premotor cortex: Activity during the delay period and effect on pre-movement activity. *Journal of Neurophysiology, 84*(2), 986–1005. https://doi.org/10.1152/jn.2000.84.2.986

Cui, H., & Andersen, R. A. (2011). Different representations of potential and selected motor plans by distinct parietal areas. *Journal of Neuroscience, 31*(49), 18130–18136. https://doi.org/10.1523/JNEUROSCI.6247-10.2011

Curtis, C. E., & D'Esposito, M. (2003). Persistent activity in the prefrontal cortex during working memory. *Trends in Cognitive Sciences, 7*(9), 415–423. https://doi.org/10.1016/S1364-6613(03)00197-9

D'Emanuele, S., Maffiuletti, N. A., Tarperi, C., Rainoldi, A., Schena, F., & Boccia, G. (2021). Rate of force development as an indicator of neuromuscular fatigue: A scoping review. *Frontiers in Human Neuroscience, 15*, 701916. https://doi.org/10.3389/fnhum.2021.701916

Dadarlat, M. C., Canfield, R. A., & Orsborn, A. L. (2023). Neural plasticity in sensorimotor brain–machine interfaces. Annual Review of Biomedical Engineering, 25,

51–76. https://doi.org/10.1146/annurev-bioeng-110220-110833

Davare, M., Andres, M., Cosnard, G., Thonnard, J.-L., & Olivier, E. (2006). Dissociating the role of ventral and dorsal premotor cortex in precision grasping. *Journal of Neuroscience, 26*(8), 2260–2268. https://doi.org/10.1523/JNEUROSCI.3386-05.2006

Davare M, Lemon R, Olivier E. Selective modulation of interactions between ventral premotor cortex and primary motor cortex during precision grasping in humans. J Physiol. 2008 Jun 1;586(11):2735-42. doi: 10.1113/jphysiol.2008.152603. Epub 2008 Apr 10. PMID: 18403420

D.lgs. 26/2014 (Italian law on animal research). (2014). Legislative Decree No. 26 of 4 March 2014 on the protection of animals used for scientific purposes. *Gazzetta Ufficiale, Serie Generale, 61,* 1–89.

Desmurget, M., Epstein, C. M., Turner, R. S., Prablanc, C., Alexander, G. E., & Grafton, S. T. (1999). Role of the posterior parietal cortex in updating reaching movements to a visual target. *Nature Neuroscience, 2*(6), 563–567. https://doi.org/10.1038/9219

Diedrichsen, J., Shadmehr, R., & Ivry, R. B. (2010). The coordination of movement: Optimal feedback control and beyond. *Trends in Cognitive Sciences, 14*(1), 31–39. https://doi.org/10.1016/j.tics.2009.11.004

Diomedi, S., Vaccari, F. E., Gamberini, M., De Vitis, M., Filippini, M., & Fattori, P. (2024). Neurophysiological recordings from parietal areas of the macaque brain during an instructed-delay reaching task. *European Journal of Neuroscience, 59*(7), 1429–1445. https://doi.org/10.1111/ejn.16592

Dum, R. P., & Strick, P. L. (1991). The origin of corticospinal projections from the premotor areas in the frontal lobe. *Journal of Neuroscience, 11*(3), 667–689. https://doi.org/10.1523/JNEUROSCI.11-03-00667.1991

European Directive 2010/63/EU. (2010). Directive 2010/63/EU of the European Parliament and of the Council of 22 September 2010 on the protection of animals used for scientific purposes. *Official Journal of the European Union, L276,* 33–79. https://eur-lex.europa.eu/legal-content/EN/TXT/?uri=CELEX%3A32010L0063

Fattori, P., Raos, V., Breveglieri, R., Bosco, A., Marzocchi, N., & Galletti, C. (2010). The dorsomedial pathway is not just for reaching: Grasping neurons in the medial parieto-occipital cortex of the macaque monkey. *Journal of Neuroscience, 30*(1), 342–349.

https://doi.org/10.1523/JNEUROSCI.3800-09.2010

Ferroni, C. G., Maranesi, M., Livi, A., Lanzilotto, M., & Bonini, L. (2017). Comparative performance of linear multielectrode probes and single-tip electrodes for intracortical microstimulation and single-neuron recording in macaque monkey. *Frontiers in Systems Neuroscience, 11*, 84.

Ferroni, C. G., Albertini, D., Lanzilotto, M., Livi, A., Maranesi, M., & Bonini, L. (2021). Local and system mechanisms for action execution and observation in parietal and premotor cortices. *Current Biology, 31*(13), 2819–2830.e4. https://doi.org/10.1016/j.cub.2021.04.034

Filimon, F., Nelson, J. D., & Hagler, D. J. (2007). Human cortical representations for reaching: Mirror neurons for actions with the hand. *Journal of Neuroscience, 27*(4), 1070–1081. https://doi.org/10.1523/JNEUROSCI.3803-06.2007

Fitts, P. M. (1954). The information capacity of the human motor system in controlling the amplitude of movement. *Journal of Experimental Psychology, 47*(6), 381–391. https://doi.org/10.1037/h0055392

Fluet, M. C., Baumann, M. A., & Scherberger, H. (2010). Context-specific grasp movement representation in macaque ventral premotor cortex. *Journal of Neuroscience, 30*(45), 15175–15184. https://doi.org/10.1523/JNEUROSCI.3343-10.2010

Friston, K. (2010). The free-energy principle: A unified brain theory? *Nature Reviews Neuroscience, 11*(2), 127–138. https://doi.org/10.1038/nrn2787

Fritsch, G., & Hitzig, E. (1870). Ueber die elektrische Erregbarkeit des Grosshirns. *Archiv für Anatomie, Physiologie und wissenschaftliche Medicin (Neue Folge)*, 300–332.

Fuster, J. M. (2001). The prefrontal cortex—An update: Time is of the essence. *Neuron, 30*(2), 319–333. https://doi.org/10.1016/S0896-6273(01)00285-9

Fuster, J. M. (2008). *The prefrontal cortex* (4th ed.). Academic Press.

Galletti, C., Gamberini, M., & Fattori, P. (2022). The posterior parietal area V6A: An attentionally-modulated visuomotor region involved in the control of reach-to-grasp action. *Neuroscience & Biobehavioral Reviews, 141*, 104823. https://doi.org/10.1016/j.neubiorev.2022.104823

Gallese, V., Murata, A., Kaseda, M., Niki, N., & Sakata, H. (1994). Deficit of hand preshaping after muscimol injection in monkey parietal cortex. *NeuroReport, 5*(12),

1525–1529. https://doi.org/10.1097/00001756-199407000-00029

Gallivan, J. P., McLean, D. A., Valyear, K. F., & Culham, J. C. (2011). Decoding action intentions from preparatory brain activity in human parieto-frontal networks. *Journal of Neuroscience, 31*(26), 9599–9610. https://doi.org/10.1523/JNEUROSCI.0080-11.2011

Gallivan, J. P., McLean, D. A., Flanagan, J. R., & Culham, J. C. (2013). Where one hand meets the other: Limb-specific and action-dependent movement plans decoded from preparatory brain activity in single human frontoparietal brain areas. *Journal of Neuroscience, 33*(5), 1991–2008. https://doi.org/10.1523/JNEUROSCI.0541-12.2013

Gallivan, J. P., Johnsrude, I. S., & Flanagan, J. R. (2016). Planning ahead: Object-directed sequential actions decoded from human frontoparietal and occipitotemporal networks. *Cerebral Cortex, 26*(2), 708–730. https://doi.org/10.1093/cercor/bhu302

Gaveau, V., Prablanc, C., Laurent, D., Rossetti, Y., & Priot, A.-E. (2014). Visuo-manual coordination during rapid online control of reaching movements. *Psychological Research, 78*(4), 443–456. https://doi.org/10.1007/s00426-013-0502-2

Gazzaley, A. (2011). Influence of early attentional modulation on working memory. *Neuropsychologia, 49*(6), 1410–1424. https://doi.org/10.1016/j.neuropsychologia.2010.12.022

Gerbella M, Belmalih A, Borra E, Rozzi S, Luppino G. Cortical connections of the anterior (F5a) subdivision of the macaque ventral premotor area F5. Brain Struct Funct. 2011 Mar;216(1):43-65. doi: 10.1007/s00429-010-0293-6

Gerbella, M., Rozzi, S., & Rizzolatti, G. (2017). The extended object-grasping network. *Experimental Brain Research, 235*(10), 2903–2916. https://doi.org/10.1007/s00221-017-5007-3

Gibson, J. J. (1950). *The perception of the visual world.* Riverside Press.

Gibson, J. J. (1979). *The ecological approach to visual perception.* Houghton Mifflin.

Goodale, M. A., Jakobson, L. S., & Keillor, J. M. (1994). Differences in the visual control of pantomimed and natural grasping movements. *Neuropsychologia, 32*(10), 1159–1178. https://doi.org/10.1016/0028-3932(94)90100-7

Graybiel, A. M. (2008). Habits, rituals, and the evaluative brain. *Annual Review of Neuroscience, 31*, 359–387. https://doi.org/10.1146/annurev.neuro.29.051605.112851

Graziano, M. S. A., & Cooke, D. F. (2006). Parieto-frontal interactions, personal space,

and defensive behavior. *Neuropsychologia*, *44*(6), 845–859. https://doi.org/10.1016/j.neuropsychologia.2005.09.009

Grol, M. J., Majdandžić, J., Stephan, K. E., Verhagen, L., Dijkerman, H. C., Bekkering, H., & Toni, I. (2007). Parieto-frontal connectivity during visually guided grasping. *Journal of Neuroscience*, 27(44), 11877–11887. https://doi.org/10.1523/JNEUROSCI.3923-07.2007

Haggard, P. (2008). Human volition: Towards a neuroscience of will. *Nature Reviews Neuroscience, 9*(12), 934–946. https://doi.org/10.1038/nrn2497

Harris, K. D., Quiroga, R. Q., Freeman, J., & Smith, S. L. (2016). Improving data quality in neuronal population recordings. *Nature Neuroscience*, 19(9), 1165–1174. https://doi.org/10.1038/nn.4365

Harrison, S. A., & Tong, F. (2009). Decoding reveals the contents of visual working memory in early visual areas. *Nature, 458*(7238), 632–635. https://doi.org/10.1038/nature07832

Herwik, S., Kisban, S., Aarts, A. A. A., Seidl, K., Girardeau, G., Benchenane, K., Zugaro, M. B., Wiener, S. I., Paul, O., Neves, H. P., & Ruther, P. (2009). Fabrication technology for silicon-based microprobe arrays used in acute and sub-chronic neural recording. *Journal of Micromechanics and Microengineering, 19*, 074008. https://doi.org/10.1088/0960-1317/19/7/074008

Hoshi, E., & Tanji, J. (2004). Differential roles of neuronal activity in the supplementary and presupplementary motor areas: From information retrieval to motor planning and execution. *Journal of Neurophysiology, 92*(6), 3482–3499. https://doi.org/10.1152/jn.00547.2004

Hoshi, E., & Tanji, J. (2006). Differential involvement of neurons in the dorsal and ventral premotor cortex during processing of visual signals for action planning. *Journal of Neurophysiology, 95*(6), 3596–3616. https://doi.org/10.1152/jn.01126.2005

Hesse, C., & Franz, V. H. (2009). Memory mechanisms in grasping. *Neuropsychologia, 47*(6), 1532–1545. https://doi.org/10.1016/j.neuropsychologia.2008.08.012

Hogendoorn, H., & Burkitt, A. N. (2019). Predictive coding with neural transmission delays: A real-time temporal alignment hypothesis. *eNeuro, 6*(2), ENEURO.0412-18.2019. https://doi.org/10.1523/ENEURO.0412-18.2019

Hu, Y., Eagleson, R., & Goodale, M. A. (1999). The effects of delay on the kinematics of grasping. *Experimental Brain Research, 126*(1), 109–116. https://doi.org/10.1007/s002210050720

Hubel, D. H., & Wiesel, T. N. (1968). Receptive fields and functional architecture of monkey striate cortex. *The Journal of Physiology, 195*(1), 215–243. https://doi.org/10.1113/jphysiol.1968.sp008455

Innocenti, G. M., Caminiti, R., Rouiller, E. M., Knott, G., Dyrby, T. B., Descoteaux, M., & Thiran, J.-P. (2019). Diversity of cortico-descending projections: Histological and diffusion MRI characterization in the monkey. *Cerebral Cortex, 29*(2), 788–801. https://doi.org/10.1093/cercor/bhx363

Intveld, R. W., Dann, B., Michaels, J. A., & Scherberger, H. (2018). Neural coding of intended and executed grasp force in macaque areas AIP, F5, and M1. *Scientific Reports, 8*(1), 17985. https://doi.org/10.1038/s41598-018-35488-z

Jeannerod, M. (1997). *The cognitive neuroscience of action.* Wiley-Blackwell.

Johnson, P. B., Ferraina, S., Bianchi, L., & Caminiti, R. (1996). Cortical networks for visual reaching: Physiological and anatomical organization of frontal and parietal lobe arm regions. *Cerebral Cortex, 6*(2), 102–119. https://doi.org/10.1093/cercor/6.2.102

Kandel, E. R., Schwartz, J. H., Jessell, T. M., Siegelbaum, S. A., & Hudspeth, A. J. (2013). *Principles of neural science* (5th ed.). McGraw-Hill.

Lanzilotto, M., Livi, A., Maranesi, M., Gerbella, M., Barz, F., Ruther, P., Fogassi, L., Rizzolatti, G., & Bonini, L. (2016). Extending the cortical grasping network: Pre-supplementary motor neuron activity during vision and grasping of objects. *Cerebral Cortex, 26*(12), 4435–4449. https://doi.org/10.1093/cercor/bhw315

Lanzilotto, M., Ferroni, C. G., Livi, A., Gerbella, M., Maranesi, M., Borra, E., Passarelli, L., Gamberini, M., Fogassi, L., Bonini, L., & Orban, G. A. (2019). Anterior intraparietal area: A hub in the observed manipulative action network. *Cerebral Cortex, 29*, 1816–1833.

Lanzilotto, M., Maranesi, M., Livi, A., Ferroni, C. G., Orban, G. A., & Bonini, L. (2020). Stable readout of observed actions from format-dependent activity of monkey's anterior intraparietal neurons. *Proceedings of the National Academy of Sciences, 117*, 16596–16605.

Lara, A. H., & Wallis, J. D. (2015). The role of prefrontal cortex in working memory: A mini review. *Frontiers in Systems Neuroscience, 9*, 173. https://doi.org/10.3389/fnsys.2015.00173

Lee, E. K., Balasubramanian, H., Tsolias, A., Anakwe, S. U., Medalla, M., Shenoy, K. V., & Chandrasekaran, C. (2021). Non-linear dimensionality reduction on extracellular waveforms reveals cell type diversity in premotor cortex. *eLife, 10*, e67490. https://doi.org/10.7554/eLife.67490

Lemon, R. N., Baker, S. N., & Kraskov, A. (2021). Classification of cortical neurons by spike shape and the identification of pyramidal neurons. *Cerebral Cortex, 31*(11), 5131–5138. https://doi.org/10.1093/cercor/bhab147

Lim, S., & Goldman, M. S. (2013). Balanced cortical microcircuitry for maintaining information in working memory. *Nature Neuroscience, 16*(9), 1306–1314. https://doi.org/10.1038/nn.3492

Livi, A., Lanzilotto, M., Maranesi, M., Fogassi, L., Rizzolatti, G., & Bonini, L. (2019). Agent-based representations of objects and actions in the monkey pre-supplementary motor area. *Proceedings of the National Academy of Sciences of the United States of America*, *116*, 2691–2700.

Luppino, G., Matelli, M., Camarda, R., & Rizzolatti, G. (1993). Corticocortical connections of area F3 (SMA-proper) and area F6 (pre-SMA) in the macaque monkey. *Journal of Comparative Neurology, 338*(1), 114–140. https://doi.org/10.1002/cne.903380109

Luppino, G., Murata, A., Govoni, P., & Rizzolatti, G. (1999). Largely segregated parietofrontal connections linking rostral intraparietal cortex (areas AIP and VIP) and the ventral premotor cortex (areas F5 and F4). *Experimental Brain Research, 128*, 181–187. https://doi.org/10.1007/s002210050833

Luppino, G., & Rizzolatti, G. (2000). The organization of the frontal motor cortex. *News in Physiological Sciences, 15*, 219–224. https://doi.org/10.1152/physiologyonline.2000.15.5.219

Macfarlane, N. B., & Graziano, M. S. (2009). Diversity of grip in *Macaca mulatta*. *Experimental Brain Research, 197*, 255–268. https://doi.org/10.1007/s00221-009-1909-z

Maffiuletti, N. A., Aagaard, P., Blazevich, A. J., Folland, J., Tillin, N., & Duchateau, J. (2016). Rate of force development: Physiological and methodological considerations. *European Journal of Applied Physiology, 116*(6), 1091–1116. https://doi.org/10.1007/s00421-016-3346-6

Maimon, G., & Assad, J. A. (2006). A cognitive signal for the proactive timing of action in macaque LIP. *Nature Neuroscience, 9*(7), 948–955. https://doi.org/10.1038/nn1716

Maranesi, M., Ugolotti Serventi, F., Bruni, S., Bimbi, M., Fogassi, L., & Bonini, L. (2013). Monkey gaze behaviour during action observation and its relationship to mirror neuron activity. *European Journal of Neuroscience, 38*(12), 3721–3730. https://doi.org/10.1111/ejn.12376

Maranesi, M., Lanzilotto, M., Arcuri, E., & Bonini, L. (2024). Mixed selectivity in monkey anterior intraparietal area during visual and motor processes. *Progress in Neurobiology, 236,* 102611. https://doi.org/10.1016/j.pneurobio.2024.102611

Marconi, B., Genovesio, A., Battaglia-Mayer, A., Ferraina, S., Squatrito, S., Molinari, M., Lacquaniti, F., & Caminiti, R. (2001). Eye-hand coordination during reaching. I. Anatomical relationships between parietal and frontal cortex. *Cerebral Cortex, 11*(6), 513–527. https://doi.org/10.1093/cercor/11.6.513

Marzocchi, N., Breveglieri, R., Galletti, C., & Fattori, P. (2008). Reaching activity in parietal area V6A of the macaque: Eye influence on hand direction and wrist orientation. *European Journal of Neuroscience, 27*(3), 775–789. https://doi.org/10.1111/j.1460-9568.2008.06021.x

Matelli M, Luppino G, Rizzolatti G. Patterns of cytochrome oxidase activity in the frontal agranular cortex of the macaque monkey. Behav Brain Res. 1985 Nov-Dec;18(2):125-36. doi: 10.1016/0166-4328(85)90068-3.

Mazzaglia, P., Verbelen, T., Çatal, O., & Dhoedt, B. (2022). The free energy principle for perception and action: A deep learning perspective. *Entropy, 24*(2), 301. https://doi.org/10.3390/e24020301

McCormick, D. A., Connors, B. W., Lighthall, J. W., & Prince, D. A. (1985). *Comparative electrophysiology of pyramidal and sparsely spiny stellate neurons of the neocortex*. Journal of Neurophysiology, *54*(4), 782–806. https://doi.org/10.1152/jn.1985.54.4.782

McInnes, L., Healy, J., & Melville, J. (2018). UMAP: Uniform manifold approximation

and projection. *Journal of Open Source Software, 3*(29), 861. https://doi.org/10.21105/joss.00861

Meyers, E. M. (2013). The neural decoding toolbox. *Frontiers in Neuroinformatics, 7*, 8. https://doi.org/10.3389/fninf.2013.00008

Miall, R. C., Weir, D. J., Wolpert, D. M., & Stein, J. F. (1993). Is the cerebellum a Smith predictor? *Journal of Motor Behavior, 25*(3), 203–216. https://doi.org/10.1080/00222895.1993.9942050

Michaels, J. A., & Scherberger, H. (2018). Population coding of grasp and laterality-related information in the macaque fronto-parietal network. *Scientific Reports, 8*(1), 1710. https://doi.org/10.1038/s41598-018-20051-7

Miller, E. K., & Cohen, J. D. (2001). An integrative theory of prefrontal cortex function. *Annual Review of Neuroscience, 24*, 167–202. https://doi.org/10.1146/annurev.neuro.24.1.167

Miller, E. K., Erickson, C. A., & Desimone, R. (1996). Neural mechanisms of visual working memory in prefrontal cortex of the macaque. *Journal of Neuroscience, 16*(16), 5154–5167. https://doi.org/10.1523/JNEUROSCI.16-16-05154.1996

Mitchell, J. F., Sundberg, K. A., & Reynolds, J. H. (2007). *Differential attention-dependent response modulation across cell classes in macaque visual area V4*. Neuron, 55(1), 131–141. https://doi.org/10.1016/j.neuron.2007.06.018

Monaco, S., Chen, Y., Medendorp, W. P., Crawford, J. D., Fiehler, K., & Henriques, D. Y. (2014). Functional magnetic resonance imaging adaptation reveals the cortical networks for processing grasp-relevant object properties. *Cerebral Cortex, 24*(6), 1540–1554. https://doi.org/10.1093/cercor/bht006

Moreno, A., de Lafuente, V., & Merchant, H. (2025). Time-varying encoding of grasping type and force in the primate motor cortex. *eNeuro, 12*(4), ENEURO.0010-25.2025. https://doi.org/10.1523/ENEURO.0010-25.2025

Mulcahy, G., Atwood, B., & Kuznetsov, A. (2020). Basal ganglia role in learning rewarded actions and executing previously learned choices: Healthy and diseased states. *PLOS ONE, 15*(2), e0228081. https://doi.org/10.1371/journal.pone.0228081

Murata, A., Gallese, V., Kaseda, M., & Sakata, H. (1996). Parietal neurons related to memory-guided hand manipulation. *Journal of Neurophysiology, 75*(5), 2180–2186.

https://doi.org/10.1152/jn.1996.75.5.2180

Murata, A., Fadiga, L., Fogassi, L., Gallese, V., Raos, V., & Rizzolatti, G. (1997). Object representation in the ventral premotor cortex (area F5) of the monkey. *Journal of Neurophysiology, 78*(4), 2226–2230. https://doi.org/10.1152/jn.1997.78.4.2226

Murata, A., Gallese, V., Luppino, G., Kaseda, M., & Sakata, H. (2000). Selectivity for the shape, size, and orientation of objects for grasping in neurons of monkey parietal area AIP. *Journal of Neurophysiology, 83*(5), 2580–2601. https://doi.org/10.1152/jn.2000.83.5.2580

Nachev, P., Kennard, C., & Husain, M. (2008). Functional role of the supplementary and pre-supplementary motor areas. *Nature Reviews Neuroscience, 9*(11), 856–869. https://doi.org/10.1038/nrn2478

Nelissen, K., Fiave, P. A., & Vanduffel, W. (2018). Decoding grasping movements from the parieto-frontal reaching circuit in the nonhuman primate. *Cerebral Cortex, 28*(4), 1245–1259. https://doi.org/10.1093/cercor/bhx037

Orban, G. A., Sepe, A., & Bonini, L. (2021). Parietal maps of visual signals for bodily action planning. *Brain Structure and Function, 226*(9), 2967–2988. https://doi.org/10.1007/s00429-021-02378-6

Park, J., Coddington, L. T., & Dudman, J. T. (2020). Basal ganglia circuits for action specification. *Annual Review of Neuroscience, 43*, 485–507. https://doi.org/10.1146/annurev-neuro-070918-050452

Parr, T., Pezzulo, G., & Friston, K. J. (2022). *Active inference: The free energy principle in mind, brain, and behavior*. The MIT Press. https://doi.org/10.7551/mitpress/12441.001.0001

Pasquereau, B., Nadjar, A., Arkadir, D., Bezard, E., Goillandeau, M., Bioulac, B., Gross, C. E., & Boraud, T. (2007). Shaping of motor responses by incentive values through the basal ganglia. *Journal of Neuroscience, 27*(5), 1176–1183. https://doi.org/10.1523/JNEUROSCI.3745-06.2007

Passingham, R. E., Bengtsson, S. L., & Lau, H. C. (2010). Medial frontal cortex: From self-generated action to reflection on one's own performance. *Trends in Cognitive Sciences, 14*(1), 16–21. https://doi.org/10.1016/j.tics.2009.11.001

Pesaran, B., Nelson, M. J., & Andersen, R. A. (2008). Free choice activates a decision

circuit between frontal and parietal cortex. *Nature, 453*(7193), 406–409. https://doi.org/10.1038/nature06849

Petrides, M. (2005). Lateral prefrontal cortex: Architectonic and functional organization. *Philosophical Transactions of the Royal Society B: Biological Sciences, 360*(1456), 781–795. https://doi.org/10.1098/rstb.2005.1631

Petzschner, F. H., & Krüger, M. (2012). How to reach: Movement planning in the posterior parietal cortex. *Journal of Neuroscience, 32*(14), 4703–4704. https://doi.org/10.1523/JNEUROSCI.0566-12.2012

Pezzulo, G., & Cisek, P. (2016). Navigating the affordance landscape: Feedback control as a process model of behavior and cognition. *Trends in Cognitive Sciences, 20*(6), 414–424. https://doi.org/10.1016/j.tics.2016.03.013

Picard, N., & Strick, P. L. (2001). Imaging the premotor areas. *Current Opinion in Neurobiology, 11*(6), 663–672. https://doi.org/10.1016/S0959-4388(01)00266-5

Pisella, L., Gréa, H., Tilikete, C., Vighetto, A., Desmurget, M., Rode, G., Boisson, D., & Rossetti, Y. (2000). An “automatic pilot” for the hand in human posterior parietal cortex: Toward reinterpreting optic ataxia. *Nature Neuroscience*, *3*(7), 629–636. https://doi.org/10.1038/76673

Pruszynski, J. A., & Scott, S. H. (2012). Optimal feedback control and the long-latency stretch response. *Experimental Brain Research, 218*(3), 341–359. https://doi.org/10.1007/s00221-012-3041-8

Raos, V., Umiltà, M. A., Murata, A., Fogassi, L., & Gallese, V. (2006). Functional properties of grasping-related neurons in the ventral premotor area F5 of the macaque monkey. *Journal of Neurophysiology, 95*(2), 709–729. https://doi.org/10.1152/jn.00463.2005

Redgrave, P., Prescott, T. J., & Gurney, K. (1999). The basal ganglia: A vertebrate solution to the selection problem? *Neuroscience, 89*(4), 1009–1023. https://doi.org/10.1016/S0306-4522(98)00319-4

Rice, N. J., Tunik, E., Cross, E. S., & Grafton, S. T. (2006). On-line grasp control is mediated by the contralateral anterior intraparietal sulcus. *Cerebral Cortex, 16*(9), 1451–1460. https://doi.org/10.1093/cercor/bhj086

Rizzolatti, G., Luppino, G., & Matelli, M. (1998). The organization of the cortical motor

system: New concepts. *Electroencephalography and Clinical Neurophysiology, 106*(5), 283–296. https://doi.org/10.1016/S0013-4694(98)00036-7

Rizzolatti, G., & Luppino, G. (2001). The cortical motor system. *Neuron, 31*(6), 889–901. https://doi.org/10.1016/S0896-6273(01)00423-8

Rolls, E. T., Cheng, W., & Feng, J. (2023). The orbitofrontal cortex and its role in the processing of reward and decision making. *Nature Reviews Neuroscience, 24*(1), 1–14. https://doi.org/10.1038/s41583-022-00659-7

Romo, R., Hernández, A., & Zainos, A. (2004). Neuronal correlates of a perceptual decision in ventral premotor cortex. *Neuron, 41*(1), 165–173. https://doi.org/10.1016/S0896-6273(03)00817-1

Ruiz Garate, V., Pozzi, M., Prattichizzo, D., & Ajoudani, A. (2018). A bio-inspired grasp stiffness control for robotic hands. *Frontiers in Robotics and AI*, 5, 89. https://doi.org/10.3389/frobt.2018.00089

Sakata, H., Taira, M., Kusunoki, M., Murata, A., Tsutsui, K., Tanaka, Y., Shein, W. N., & Miyashita, Y. (1999). Neural representation of three-dimensional features of manipulation objects with stereopsis. *Experimental Brain Research, 128*(1–2), 160–169. https://doi.org/10.1007/s002210050831

Sakai, K., & Passingham, R. E. (2006). Prefrontal set activity predicts rule-specific neural processing during subsequent cognitive performance. *Journal of Neuroscience*, 26(4), 1211–1218. https://doi.org/10.1523/JNEUROSCI.3887-05.2006

Sarlegna, F. R., & Miall, R. C. (2009). In human reaching, vision and proprioception contribute differentially to online control (see also Sarlegna & Sainburg, 2009, for planning). *Current Opinion in Neurobiology, 19*(6), 748–754. https://doi.org/10.1016/j.conb.2009.09.009

Saunders, J. A., & Knill, D. C. (2003). Humans use continuous visual feedback from the hand to control fast reaching movements. *Experimental Brain Research, 152*(3), 341–352. https://doi.org/10.1007/s00221-003-1525-2

Schaffelhofer, S., Agudelo-Toro, A., & Scherberger, H. (2015). Decoding a wide range of hand configurations from macaque motor, premotor, and parietal cortices. *Journal of Neuroscience, 35*(3), 1068–1081. https://doi.org/10.1523/JNEUROSCI.3594-14.2015

Schaffelhofer, S., & Scherberger, H. (2016). Object vision to hand action in macaque

parietal, premotor, and motor cortices. *eLife*, *5*, e15278. https://doi.org/10.7554/eLife.15278

Scherberger, H., & Andersen, R. A. (2007). Target selection signals for arm reaching in the posterior parietal cortex. *Journal of Neuroscience*, *27*(8), 2001–2012. https://doi.org/10.1523/JNEUROSCI.4274-06.2007

Serences, J. T., Ester, E. F., Vogel, E. K., & Awh, E. (2009). Stimulus-specific delay activity in human primary visual cortex. *Psychological Science*, *20*(2), 207–214. https://doi.org/10.1111/j.1467-9280.2009.02276.x

Shadlen, M. N., & Newsome, W. T. (2001). Neural basis of a perceptual decision in the parietal cortex (area LIP) of the rhesus monkey. *Journal of Neurophysiology*, *86*(4), 1916–1936. https://doi.org/10.1152/jn.2001.86.4.1916

Shadmehr, R., Smith, M. A., & Krakauer, J. W. (2010). Error correction, sensory prediction, and adaptation in motor control. *Annual Review of Neuroscience*, *33*, 89–108. https://doi.org/10.1146/annurev-neuro-060909-153135

Sherrington, C. S. (1906). *The integrative action of the nervous system*. New Haven, CT: Yale University Press.

Shima, K., & Tanji, J. (2000). Neuronal activity in the supplementary and presupplementary motor areas for sequential movements. *Journal of Neurophysiology*, 84(4), 2148–2160. https://doi.org/10.1152/jn.2000.84.4.2148

Snyder, L. H., Batista, A. P., & Andersen, R. A. (1997). Coding of intention in the posterior parietal cortex. *Nature*, *386*(6621), 167–170. https://doi.org/10.1038/386167a0

Snyder, L. H., Batista, A. P., & Andersen, R. A. (2000). Intention-related activity in the posterior parietal cortex: A review. *Vision Research*, *40*(10–12), 1433–1441. https://doi.org/10.1016/s0042-6989(00)00052-3

Stentiford, R., & Cerminara, N. L. (2019). Timing rewarding movements. *Neuron*, *103*(3), 358–360. https://doi.org/10.1016/j.neuron.2019.07.024

Stokes, M. G. (2015). 'Activity-silent' working memory in prefrontal cortex: A dynamic coding framework. *Trends in Cognitive Sciences*, *19*(7), 394–405. https://doi.org/10.1016/j.tics.2015.05.004

Streng, M. L., Popa, L. S., & Ebner, T. J. (2022). Cerebellar representations of errors and internal models. *The Cerebellum*, *21*(5), 814–820. https://doi.org/10.1007/s12311-022-

01406-3

Supèr, H., Spekreijse, H., & Lamme, V. A. F. (2001). Two distinct modes of sensory processing observed in monkey primary visual cortex (V1). *Nature Neuroscience, 4*(3), 304–310. https://doi.org/10.1038/85170

Taira, M., Mine, S., Georgopoulos, A. P., Murata, A., & Sakata, H. (1990). Parietal cortex neurons of the monkey related to the visual guidance of hand movement. *Experimental Brain Research, 83*(1), 29–36. https://doi.org/10.1007/BF00232190

Takakusaki, K., Saitoh, K., Harada, H., & Kashiwayanagi, M. (2004). Role of basal ganglia-brainstem pathways in the control of motor behaviors. *Neuroscience Research, 50*(2), 137–151. https://doi.org/10.1016/j.neures.2004.06.015

Thoenissen, D., Zilles, K., & Toni, I. (2002). Differential involvement of parietal and precentral regions in movement preparation and motor intention. *Journal of Neuroscience, 22*(20), 9024–9034. https://doi.org/10.1523/JNEUROSCI.22-20-09024.2002

Thura, D., & Cisek, P. (2017). The basal ganglia do not select reach targets but control the urgency of commitment. *Neuron, 95*(5), 1160–1170.e5. https://doi.org/10.1016/j.neuron.2017.07.039

Tung, C., Lord, S. R., Pelicioni, P. H. S., Sturnieks, D. L., & Menant, J. C. C. (2023). Prefrontal and motor planning cortical activity during stepping tasks is related to task complexity but not concern about falling in older people: A fNIRS study. *Brain Sciences, 13*(12), 1675. https://doi.org/10.3390/brainsci13121675

Tunik, E., Frey, S. H., & Grafton, S. T. (2005). Virtual lesions of the anterior intraparietal area disrupt goal-dependent online adjustments during object-directed grasping. *Nature Neuroscience, 8*(4), 505–511. https://doi.org/10.1038/nn1430

Van Dromme, I. C., Premereur, E., Verhoef, B.-E., Vanduffel, W., & Janssen, P. (2016). Posterior parietal cortex drives inferotemporal activations during three-dimensional object vision. *PLOS Biology, 14*(4), e1002445. https://doi.org/10.1371/journal.pbio.1002445

Vargas-Irwin, C. E., Franquemont, L., Black, M. J., & Donoghue, J. P. (2015). Linking objects to actions: Encoding of target object and grasping strategy in primate ventral premotor cortex. *Journal of Neuroscience, 35*(30), 10888–10897. https://doi.org/10.1523/JNEUROSCI.1574-15.2015

Wang, X.-J. (2001). Synaptic reverberation underlying mnemonic persistent activity. *Trends in Neurosciences, 24*(8), 455–463. https://doi.org/10.1016/S0166-2236(00)01868-3

Welniarz, Q., Worbe, Y., & Gallea, C. (2021). The forward model: A unifying theory for the role of the cerebellum in motor control and sense of agency. *Frontiers in Systems Neuroscience, 15*, Article 644059. https://doi.org/10.3389/fnsys.2021.644059

Westwood, D. A., & Goodale, M. A. (2003). Perceptual illusion and the real-time control of action. *Spatial Vision, 16*(3–4), 243–254. https://doi.org/10.1163/156856803322467518

Wise, S. P., Moody, S. L., Blomstrom, K. J., & Mitz, A. R. (1998). Changes in motor cortical activity during visuomotor adaptation. *Experimental Brain Research, 121*(3), 285–299. https://doi.org/10.1007/s002210050462

Wolpert, D. M., Miall, R. C., & Kawato, M. (1998). Internal models in the cerebellum. *Trends in Cognitive Sciences, 2*(9), 338–347. https://doi.org/10.1016/s1364-6613(98)01221-2

Xie, Z., Liang, X., & Roberto, C. (2023). Learning-based robotic grasping: A review. *Frontiers in Robotics and AI*, 10, 1038658. https://doi.org/10.3389/frobt.2023.1038658

Zhao, Z., Yu, H., Wu, H., & Zhang, X. (2024). Bio-inspired affordance learning for 6-DoF robotic grasping: A transformer-based global feature encoding approach. *Neural Networks*. https://doi.org/10.1016/j.neunet.2023.12.005